

DEVELOPMENT OF ANALYTICAL ASSAYS FOR DETECTION OF SMALL  
MOLECULES USING APTAZYMES

by

Jennifer Renee Willard Furchak

A dissertation submitted in partial fulfillment  
of the requirements for the degree of  
Doctor of Philosophy  
(Chemistry)  
in the University of Michigan  
2007

Doctoral Committee:

Professor Robert T. Kennedy, Co-Chair  
Associate Professor Nils G. Walter, Co-Chair  
Professor David R. Engelke  
Professor Mark E. Meyerhoff  
Professor Richard D. Sacks (Deceased)

© Jennifer Renee Willard Furchak  
All rights reserved  
2007

To Mom, Dad, Jamie, Ric, Davi, and Dave  
for your love, support, and encouragement

## ACKNOWLEDGEMENTS

I would like to thank my advisors, Dr. Robert T. Kennedy and Dr. Nils G. Walter, for their continued guidance, support, and encouragement throughout my time in graduate school. I am grateful to the other members of my committee including Dr. David R. Engelke, Dr. Richard D. Sacks, and Dr. Mark E. Meyerhoff for guiding my academic development and providing helpful suggestions and comments for my dissertation. I am also grateful to all the members of the Kennedy group and the Walter lab, both past and present, for their assistance, suggestions, and friendship over the years. Having two sets of helpful, friendly, and encouraging colleagues has been a wonderful blessing. In particular, the members of the affinity group including Dr. Rebecca J. Whelan, Dr. Emily E. Jameson, Dr. Jennifer M. Cunliffe, Dr. Peilin Yang, Mr. Rex Pei, and Mr. Colin Jennings have shared many insightful conversations about research and life and have tirelessly dressed in pink. I am especially thankful for Dr. Rebecca J. Whelan, who has been an inspiration and a very good friend. Mr. Zechariah D. Sandlin has been a tremendous resource for troubleshooting difficult research problems and a tremendous encouragement in difficult times. Mr. John Hoerter and Ms. Liz McDowell have offered many insightful thoughts on difficult research problems. The women with whom I have had the opportunity to share a lab space with over the last several years have been encouraging colleagues and friends in times of joy as well as in times of less

joy. They include Dr. Rebecca J. Whelan, Dr. Peilin Yang, Ms. Chamaree de Silva, and Ms. Qihui Ni.

I am grateful to the many friends who have offered support over the years. There are several in particular who have been absolutely indispensable throughout graduate school. I am especially grateful for Dr. Melissa Bobeck, Dr. Drew Bobeck, Dr. Amelia Fuller, and Dr. Brian Brennan, with whom I have shared chemistry and life. I am also grateful for Ms. Sarah Kissel (Brennan), who is the best and most supportive girlfriend a person could imagine.

My family has been amazingly supportive and encouraging throughout my time in graduate school, and I am forever grateful for their love. Mom and Dad have always believed in and inspired me. My brothers, Mr. Jamie Willard; Mr. Ric Willard; and Mr. Brother (Davi) Willard, and my sister-in-law, Ms. Beth Willard, have supported me in everything. My husband, Mr. Dave Furchak, has offered unconditional love and support from beginning to end. Thank you, Dave, for being such a wonderful friend.

Most of all, I am grateful to Jesus Christ, the God of all creation, for the interesting systems He has given me to study and for the way He always serves as my Provider.

## TABLE OF CONTENTS

DEDICATION .....	ii
ACKNOWLEDGEMENTS .....	iii
LIST OF FIGURES .....	viii
LIST OF APPENDICES.....	x
LIST OF ABBREVIATIONS.....	xi
ABSTRACT .....	xiii
CHAPTER 1. INTRODUCTION .....	1
Background .....	1
Aptamers and aptazymes .....	1
Detection of Transduced Signal.....	9
Dissertation Overview.....	15
CHAPTER 2. ASSAY FOR GLUCOSAMINE-6-PHOSPHATE USING A LIGAND-ACTIVATED RIBOZYME AND FRET OR CE-LIF DETECTION .....	17
Introduction .....	17
Experimental Section .....	21
Results and Discussion .....	26
Single-Turnover FRET Assay.....	26
Single-Turnover CE Assay .....	31

Multiple-Turnover FRET Assay .....	36
Multiple-Turnover CE Assay.....	41
Conclusions.....	42
CHAPTER 3. CHARACTERIZATION OF ENGINEERED APTAZYMES FOR USE IN DETECTION OF ATP AND CAMP .....	44
Introduction .....	44
Experimental Section .....	47
Results and Discussion .....	48
Design of trans-cleaving aptazymes .....	48
Cleavage of trans-cleaving aptazymes.....	50
Characterization of trans-cleaving aptazymes .....	51
Conclusions .....	58
CHAPTER 4. MULTIPLEXED DETECTION OF SMALL MOLECULES BY GEL ELECTROPHORESIS USING APTAZYMES.....	60
Introduction .....	60
Experimental Section .....	62
Results and Discussion .....	63
Design of trans-cleaving aptazymes .....	63
Multiplex of cAMP and ATP aptazymes.....	64
Multiplex of ATP and <i>glmS</i> aptazymes .....	67
Conclusions .....	70
CHAPTER 5. SUMMARY AND FUTURE DIRECTIONS.....	72
Summary.....	72

Assays for GlcN6P using the glmS ribozyme.....	72
Characterization of the ATP and cAMP aptazymes .....	75
Future Directions .....	78
Multiple-turnover cleavage reactions of the <i>glmS</i> ribozyme .....	78
Structure-function relationship of the cAMP and ATP aptazymes: trans versus cis.....	79
CGE multiplex assays.....	80
Application of assays to real samples.....	81
Design/select new aptazymes for interesting molecules .....	82
APPENDICES .....	84
REFERENCES .....	104



## LIST OF FIGURES

### Figure

1-1	FRET response to ribozyme cleavage.....	13
1-2	CE response to ribozyme cleavage .....	14
2-1	Schematic drawing of the high speed CE instrument used for kinetics studies. ....	25
2-2	The <i>glmS</i> ribozyme minimal structure and fluorophore labels.....	27
2-3	(A) 100 $\mu$ M GlcN6P detection by FRET measured in 50mM HEPES-KOH, pH 7.5, 200 mM KCl, 25 mM DTT, 50 mM MgCl <sub>2</sub> , 20 nM <i>glmS</i> ribozyme, 10 nM doubly labeled substrate, 37 °C. (B) Fit of donor fluorescence (single exponential association) for determination of cleavage rate.....	29
2-4	FRET calibration curve.....	31
2-5	500 $\mu$ M GlcN6P detection by CE measured in 50 mM HEPES-KOH, pH 7.5, 200 mM KCl, 25 mM DTT, 20 mM MgCl <sub>2</sub> , 500 nM singly labeled substrate, 1 $\mu$ M <i>glmS</i> ribozyme, 25 °C. ....	33
2-6	CE calibration .....	35
2-7	Comparison of three constructs of Fyn binding to Fluor-Fyn peptide.....	39
2-8	Multiple-turnover FRET with cycling .....	41
3-1	Design of trans-cleaving aptazymes .....	49
3-2	Cleavage activity of ATP, cAMP, and cGMP aptazymes with each of three substrates.....	51
3-3	Characterization of ATP and cAMP aptazymes .....	53
3-4	Calibration of ATP and cAMP aptazymes.....	54
3-5	Specificity of cAMP and ATP aptazymes .....	56
3-6	ATP aptazyme activation by ATP and AMP.....	58

4-1	Multiplexed detection of ATP and cAMP .....	65
4-2	Multiplexed detection of ATP and GlcN6P.....	68
4-3	Calibration curve for multiplexed assay of ATP (●) and GlcN6P (■). .....	70
A-1	SELEX.....	85
A-2	Progress of SELEX after five rounds of selection .....	95
A-3	Progress of SELEX after ten rounds of selection .....	96

## LIST OF APPENDICES

### Appendix

A	SELECTIVE EVOLUTION OF LIGANDS BY EXPONENTIAL ENRICHMENT (SELEX) .....	84
B	T7 HIS TAGGED RNA POLYMERASE PREPARATION.....	98

## LIST OF ABBREVIATIONS

Å	Angstrom
A	Adenosine
ADP	Adenosine diphosphate
AMP	Adenosine monophosphate
ATP	Adenosine triphosphate
<i>B. subtilis</i>	<i>Bacillus subtilis</i>
C	Cytidine
cAMP	Cyclic adenosine monophosphate
cCMP	Cyclic cytidine monophosphate
cDNA	Copy deoxyribonucleic acid
CE	Capillary electrophoresis
CGE	Capillary gel electrophoresis
CE-LIF	Capillary electrophoresis – laser induced fluorescence
cGMP	Cyclic guanosine monophosphate
cNMP	Cyclic nucleotide monophosphate
DNA	Deoxyribonucleic acid
DTT	Dithiothreitol
FITC	Fluorescein isothiocyanate
FMN	Flavin mononucleotide
FRET	Fluorescence Resonance Energy Transfer
Fru-6P	Fructose-6-phosphate
G	Guanosine

GlcN6P	Glucosamine-6-phosphate
HEPES-KOH	4-(2-hydroxyethyl)-1-piperazineethanesulfonic acid
HPLC	High Performance Liquid Chromatography
kD	kiloDalton
$K_d$	Dissociation constant
LDR	Linear dynamic range
LIF	Laser induced fluorescence
LOD	Limit of detection
MALDI-TOFMS	Matrix-assisted laser desorption/ionization – time of flight mass spectrometry
mRNA	Messenger ribonucleic acid
nmol	Nanomole
nL	Nanoliter
NTP	Nucleoside triphosphate
pI	Isoelectric point
$R^2$	Coefficient of determination of a linear regression
RNA	Ribonucleic acid
pmol	Picomole
PAGE	Polyacrylamide Gel Electrophoresis
PCR	Polymerase chain reaction
SELEX	Selective Evolution of Ligands by Exponential Enrichment
T	Deoxythymidine
$\mu$ L	Microliter
$\mu$ M	Micromolar
V	Volts
UV	Ultraviolet
W	Watts

## ABSTRACT

Advances in understanding the complexity of cellular mechanisms depend upon methods that can quantify affinity interactions between biological molecules. Additionally, fields such as chemical biology and drug discovery require methods for identifying molecules that can probe these affinity interactions. Aptazymes are RNA-based enzymes that catalyze chemical reactions in response to binding interactions with targets of interest, making them suitable for use in quantifying affinity interactions and screening for bioactive molecules. Much of the promise of aptazymes comes from the ability to design or select them for chosen target molecules, and remains unexplored as relatively few of the known aptamers have been appended to ribozymes to create aptazymes. The analytical potential, which arises from the unique and tunable ability of these molecules to translate effector binding into a detectable signal in the form of an RNA cleavage reaction, is also still in early stages of development.

We have developed glucosamine-6-phosphate (GlcN6P) sensitive assays that detect substrate cleavage by the naturally occurring GlcN6P-dependent *glmS* ribozyme via either fluorescence resonance energy transfer (FRET) or capillary electrophoresis with laser induced fluorescence (CE-LIF). We achieve a dynamic range extending from 0.5 to 500  $\mu\text{M}$  GlcN6P when turning over a single substrate. Signal amplification and 13-fold increased sensitivity are achieved under multiple-turnover reaction conditions.

We have analyzed aptazymes that are activated by ATP and cAMP for compatibility in multiplexed assays and developed a qualitative assay for these molecules

based on polyacrylamide gel electrophoresis (PAGE) with fluorescence detection. We also developed a multiplexed assay for simultaneous detection of GlcN6P and ATP using the *glmS* ribozyme and ATP aptazyme. This assay detects GlcN6P with a limit of detection (LOD) of 40 nM and ATP with an LOD of 1  $\mu$ M. Our assays demonstrate the potential of aptazymes, in conjunction with FRET, CE-LIF, and PAGE detection, to serve as recognition and transduction elements for assays of small molecules.

## CHAPTER 1

### INTRODUCTION

#### **Background**

Affinity interactions are abundant in nature and are useful for analytical applications. They have found use in elucidating interesting biological phenomena, detecting and quantifying relevant molecules, and show promise in areas such as pharmaceutical development. Toward these ends, various probing molecules have been used, including antibodies, peptides, small molecules, and nucleic acids in methods such as gel mobility shift assays, western blotting, and immunoassays.

The development of nucleic acid-based methods for the detection of biomolecules involves recognition and transduction elements and a method of detection. Aptamers and aptazymes have served in these roles with a variety of different detection systems. Of the two, aptamers have been more extensively studied, with the use of aptazymes as analytical agents a promising and relatively open area for research.

#### **Aptamers and aptazymes**

**Aptamers.** Aptamers are nucleic acids molecules that have been evolved to have non-natural binding interactions with targets of interest, making them suitable for application in quantifying affinity interactions and screening for bioactive molecules.<sup>1</sup> The sensitive and specific binding characteristics of aptamers make them useful



candidates for diagnostic, therapeutic, and analytical applications. Aptamers are obtained through Selective Evolution of Ligands by EXponential enrichment (SELEX), a combinatorial ligand discovery process that starts from large, synthetic libraries of random-sequence nucleic acid molecules to isolate ligands with high affinity and specificity for molecular targets.<sup>2-4</sup> In SELEX, an oligonucleotide library is exposed to the target of interest, and subsets of sequences that have affinity are partitioned from those sequences with little or no affinity. The process is iterative, typically involving ten to fifteen rounds of selection with increasing stringency and ending when a set of ligands with the desired binding characteristics is obtained. SELEX has been used to isolate molecules to a broad range of targets, from small molecules to large proteins.<sup>5</sup>

RNA base pairing and other sequence dependent intramolecular interactions vary among the library molecules, providing a large number of different tertiary structures in the population. Among these are commonly recognized motifs: hairpins, bulges within helices, pseudoknots, and G-quartets. Biological function, including binding affinity, is determined by the intramolecular interactions of each molecule.<sup>6</sup>

Affinities of aptamers for their target molecules can be quite high, with dissociation constants extending into the picomolar range.<sup>7,8</sup> These affinities rival or exceed the capabilities of antibodies, making aptamers good candidates for analytical assays. The evolution process enables control over kinetic and thermodynamic properties of the aptamer-target binding interaction.<sup>9</sup>

Aptamers have been demonstrated as viable replacements for antibodies in many immunological experiments. In fact, oligonucleotides provide significant advantages over antibodies in several regards.<sup>9</sup> Many of these are a result of the evolution process,

which allows the *in vitro* development of aptamers as opposed to the *in vivo* development of antibodies. The *in vitro* selection process confers the advantage of a wider range of target molecules by including those that would be toxic *in vivo* as well as those that would not induce an immune response. Due to the reliability of chemical synthesis of aptamers after they have been sequenced, less batch-to-batch variation is expected than is expected for antibodies, which are always produced from animals or cell culture. Aptamers are more stable for long-term storage than antibodies, and can be restored even after denaturation. Aptamers can be modified after selection to further optimize binding affinities or to add modified bases to prevent degradation if they will be introduced to biological samples. Further, no immunogenicity is expected from aptamers if they are introduced to the body. Finally, reporter molecules such as fluorescein and linkers such as biotin can often be easily attached to aptamers at precise locations without disrupting their activities.<sup>10</sup>

Aptamers also have some disadvantages when compared to antibodies, and researchers are currently working to improve these areas. Aptamers, especially RNA aptamers, may suffer from degradation in biological samples.<sup>11</sup> Non-natural bases have helped to reduce this problem.<sup>1</sup> The significant negative charge of nucleic acid molecules may make selection for binding to negatively charged targets difficult, though selection for binding to some such molecules has been successful.<sup>9</sup> While commercial production of antibodies is routine, there is no such process for obtaining aptamers. One company, SomaLogic (Boulder, CO), is developing aptamers for a variety of proteins to be used in array format for clinical biomarker detection.<sup>12</sup> They have informally offered to develop aptamers for any protein with which they are provided. While this

technology is still in development, research into the applicability of these molecules in analytical techniques is also being developed.

Aptamers have been developed for many targets and have been used in a number of diagnostic and therapeutic applications. Uses include affinity purification of proteins,<sup>13</sup> imaging,<sup>14</sup> therapeutics,<sup>15</sup> and specific detection and precise quantification of molecules.<sup>1, 9, 16, 17</sup> Aptamer affinity interactions have been monitored with a myriad of analytical instrumentation including flow cytometry,<sup>18</sup> affinity probe capillary electrophoresis,<sup>19</sup> capillary electrochromatography,<sup>20</sup> fluorescence resonance energy transfer (FRET),<sup>17</sup> and affinity chromatography.<sup>9, 13, 21, 22</sup>

**Aptazymes.** RNA is a widely studied biopolymer that is involved in cellular functions ranging from protein biosynthesis to catalysis of chemical reactions and regulation of gene expression by RNA interference and riboswitches.<sup>23-25</sup> Catalytic RNA's, or ribozymes, catalyze the cleavage or ligation of the RNA phosphodiester backbone.<sup>26</sup> While combinatorial chemistry methods have resulted in the *in vitro* development of aptamers,<sup>10</sup> further development by coupling aptamers with ribozymes has resulted in allosterically regulated ribozymes, or aptazymes, which catalyze cleavage reactions as the result of the binding of specific effector ligands.<sup>27</sup> To date, one naturally occurring aptazyme has also been identified, which is the *glmS* ribozyme.<sup>28</sup>

Some aptamers exhibit conformational changes as they bind their targets with high affinity, making them a natural choice for allosteric function. Aptazymes typically regulate catalytic function via conformational changes that are induced by the binding of effector molecules at sites distinct from their active sites. Interestingly, this is not true for the naturally occurring *glmS* ribozyme, as its effector acts as a cofactor rather than

inducing a conformational change.<sup>29</sup> An engineered aptazyme can be thought of as consisting of three domains: an effector binding center, a catalytic center, and a communication domain bridging the two. Aptazymes can be generated by SELEX by adding an additional selection step for catalytic function or they can be designed rationally, taking advantage of the modular nature of RNA by joining three domains, one with each of the above functions. That is, coupling a known aptamer to a known ribozyme via a communication domain. Typically some variation is introduced into the communication domain to select for sensitive and specific response to the effector. Much of the promise of these molecules comes from the power of this coupling, and remains unexplored as relatively few of the known aptamers have been appended to ribozymes to create aptazymes. The analytical potential, which arises from the unique and tunable ability of these molecules to translate effector binding into a detectable signal in the form of a cleavage reaction, is also still in early stages of development.

The hammerhead ribozyme has been used most extensively for aptazyme design. It is a naturally occurring self-cleaving ribozyme that is found as a part of some plant and animal pathogens. Its structure is relatively simple and well characterized. The hammerhead motif is a three stem junction with much of the core sequence conserved. It catalyzes cleavage of the nucleic acid backbone via transesterification chemistry that generates 5'-hydroxyl and 2',3'-cyclic phosphate termini.<sup>30</sup>

Different kinds of libraries can be used for allosteric selection. The random region is typically one or two domains of an otherwise rationally designed aptazyme (the communication or effector binding domains). Whichever design is used for the library, an ideal selection scheme involves both positive and negative selection steps in each

round of selection. The negative selection step involves incubation under selection conditions in the absence of effector. Species that catalyze aptazyme cleavage are removed. The positive selection step follows where molecules that catalyze cleavage in the presence of effector are retained, amplified, and put through another round of selection. In this way, the library is enriched for catalytic aptazymes over several rounds. Additional negative selection steps can be applied in order to remove aptazymes that are activated by molecules similar to the desired effector.<sup>1</sup>

In an aptazyme assay, the effector ligand can be detected by monitoring the cleavage reaction. Examples of *in vitro* selected or engineered aptazymes include aptazymes for theophylline,<sup>31-34</sup> ATP,<sup>31, 35</sup> cAMP,<sup>36-38</sup> cGMP,<sup>36-38</sup> cCMP,<sup>38</sup> FMN,<sup>31, 32, 34,</sup><sup>39</sup> doxycycline,<sup>40</sup> 3-methylxanthine,<sup>33</sup> pefloxacin,<sup>41</sup> cobalt ion,<sup>42</sup> oligonucleotides,<sup>43-46</sup> and various proteins.<sup>47-49</sup> Some of these have been shown to function as recognition and transduction elements for assays in complex chemical and biological samples.<sup>17, 27, 42, 50</sup>

***glmS* ribozyme.** The *glmS* ribozyme is a natural aptazyme that undergoes a self-cleavage reaction in the presence of glucosamine-6-phosphate (GlcN6P).<sup>28</sup> This ribozyme is located in an untranslated region upstream of the *glmS* mRNA in *B. subtilis*, where it serves to downregulate the *glmS* gene in response to the metabolic product of the GlmS enzyme, glutamine-fructose-6-phosphate amidotransferase, an intermediate in cell wall biosynthesis, by degrading the mRNA. The GlcN6P metabolite modulates the catalytic rate of this ribozyme and thus the availability of the *glmS* gene product. In many aptazymes, the ligand dependent cleavage rate is attributed to a conformational change that occurs upon ligand binding, but we and others have recently shown that this adaptive binding is not observed with the binding of GlcN6P.<sup>29, 51, 52</sup> Instead, GlcN6P

is thought to play a catalytic role in the cleavage reaction,<sup>29</sup> and the reaction has been demonstrated to be relatively specific for GlcN6P, showing no cleavage with many molecules structurally similar to GlcN6P and a substantially reduced rate of cleavage with a few molecules, like glucosamine.<sup>28, 29, 51, 53</sup> This specificity makes the *glmS* ribozyme promising for use in analytical assays.

As an analyte, GlcN6P is potentially interesting in at least two different systems. In bacteria, GlcN6P is a precursor in cell wall biosynthesis. Therefore, identification of compounds that could activate *glmS* ribozyme cleavage and potentially inhibit cell wall biosynthesis could be advantageous in drug discovery. The *glmS* ribozyme is highly conserved in genomes of some bacterial pathogens, like *Bacillus anthracis* and *Staphylococcus aureus*, making it a relevant detection target.<sup>54</sup> GlcN6P is involved in the hexosamine biosynthetic pathway, which is ubiquitous in all organisms, and whose major end products are essential sugar building blocks for biosynthesis of peptidoglycan in bacteria, chitin in fungi and glycoproteins in mammals.<sup>55</sup> The first and rate limiting step in this synthesis is the conversion of fructose-6-phosphate into GlcN6P. One to three percent of cellular glucose that is converted to fructose-6-phosphate (Fru-6P) enters this pathway, and increased flux into this pathway has been shown to result in impaired ability of insulin to stimulate glucose uptake.<sup>56</sup> Detailed characterization of this pathway could lead to insight into a mechanism of development of insulin resistance in cells.

Several methods have been developed for monitoring GlcN6P formation in this pathway. They include a colorimetric Morgan-Elson assay;<sup>57</sup> a radiometric assay with <sup>14</sup>C-fructose-6P as substrate and detection to 1 pmol;<sup>58</sup> an HPLC assay of o-

phthaldialdehyde derivatized GlcN6P, which can detect as little as 5 pmol;<sup>59</sup> and a matrix-assisted laser desorption/ionization time-of-flight mass spectrometry (MALDI-TOFMS) assay, which can detect into the low nmol range.<sup>60</sup> These all require multiple derivatization steps and/or radioactivity.

**cAMP, cGMP, and ATP aptazymes.** By rational design, coupling an RNA aptamer to the hammerhead ribozyme via a variable communication domain, the Breaker group built an aptazyme for ATP.<sup>32</sup> The ATP aptamer was selected separately, and has a  $K_d$  of 0.7  $\mu$ M. The aptamer also binds to adenosine and AMP with similar affinities.<sup>61</sup> While a rational design strategy for obtaining aptazymes is appealing, not all aptamers effectively induce conformational change and, thus, aptazyme cleavage upon binding.<sup>32</sup>

Using *in vitro* selection, the Breaker group developed aptazymes that respond to cAMP and cGMP.<sup>37</sup> This “allosteric selection” scheme applied selective pressure to a hammerhead ribozyme that was coupled to a 25 nucleotide random sequence domain via a known communication domain. In negative selection steps, the library was incubated in the absence of effector under reaction conditions and uncleaved precursors were isolated by PAGE and subjected to positive selection in the presence of the effector molecules. The cleaved 5' products were purified by PAGE and amplified. In later rounds of negative selection, the library was incubated with alternate cNMP's to remove any that had cross-reactivity. The cGMP aptazyme was further optimized for higher affinity binding by mutagenization and reselection.<sup>38</sup> The apparent dissociation constants for these aptazymes were determined by measuring the half maximal cleavage activity. For the cGMP aptazyme, the apparent  $K_d$  is 200  $\mu$ M. The apparent  $K_d$  for the cAMP aptazyme is 500  $\mu$ M.<sup>38</sup> These aptazymes are activated by a conformational

change caused by effector binding. The weak affinities are expected to prevent assays using these aptazymes from rivaling LOD's obtained in current assays.

Assays for ATP can be used to determine cell viability because it is the major source of metabolic energy. Detection of ATP is also used to study some of the many cellular processes in which it is involved, which include biosynthetic reactions and signal transduction pathways, where ATP is used as a substrate by kinases that phosphorylate proteins and lipids, as well as by adenylate cyclase, which uses ATP to produce the second messenger molecule cAMP. Detection of cAMP can be used to study signal transduction and enzyme activity.

Commercial kits are available for the detection of ATP, cAMP, and cGMP with detection limits that are in the pM range. Immunoassays for these molecules have traditionally involved radiochemical formats, but many are now fluorescence or bioluminescence based. With the current stage of development of aptazymes, it is not realistic to expect that they will offer similar LOD's. Perhaps the most interesting characteristic of an aptazyme system is the ability to design or develop aptazymes for a wide range of interesting analytes, which could include ones that are currently difficult to detect. For now, proof-of-principle assays are called for that demonstrate the potential of this interesting group of molecules in analyte detection.

### **Detection of Transduced Signal**

Analyte detection based on aptazymes has potential advantages over detection based on antibodies and protein enzymes, which have been the workhorses in molecular recognition for analytical assays. Many of the potential advantages of oligonucleotide



reagents, such as ease and reproducibility of manufacture, come from the ability to chemically synthesize nucleic acids.<sup>62</sup> Aptazymes also offer the advantage over aptamers of detection of even transient binding events. After aptazyme cleavage, the products of the catalyzed reaction remain, even if the target molecule rapidly dissociates.

Employing ribozymes in analytical assays requires the development of a reliable method for quantitatively detecting the cleavage reaction. Ideally a detection method uses a minimal amount of sample, is fast, can be run in parallel or in array formats, and does not require elaborate design of the reagents. Previous ribozyme assays have followed conversion of substrate into cleavage product by a variety of separation based and real-time methods. Polyacrylamide gel electrophoresis (PAGE) has been the most widely used technique for monitoring ribozyme cleavage. Use of PAGE involves removing aliquots from a cleavage reaction at various time points, stopping the reactions, and separating them in parallel on a gel, often with detection and quantification achieved by radiolabeling the RNA. The collection of these data is tedious, results in relatively poor temporal resolution, and typically involves hazardous radioisotopes. In some cases, HPLC separation has been employed, alleviating the need for radioisotopes, but it is neither a real-time nor high-throughput tool.<sup>63-65</sup> Capillary gel electrophoresis (CGE) has also been used to separate and detect ribozyme cleavage and has been applied in high throughput in a microchip-based assay.<sup>66, 67</sup> Some real-time methods have been used, primarily involving changes in fluorescence intensity,<sup>68, 69</sup> fluorescence polarization,<sup>70</sup> or fluorescence resonance energy transfer (FRET).<sup>71-73</sup> These methods provide precise determination of rate constants, but can suffer from sources of fluorescence change outside of bond cleavage and the possibility that cleavage is spectroscopically silent.

**Fluorescence resonance energy transfer (FRET).** Fluorescence resonance energy transfer, or Förster transfer, originates from the non-radiative transfer of energy between two fluorophores, a donor and an acceptor, by the coupling of transition dipoles through space. Excitation of the donor fluorophore results in transfer of energy to the acceptor rather than radiative emission. The acceptor then emits at its characteristic wavelength, and a unique excitation/emission spectrum is observed.<sup>74</sup> The rate of energy transfer,  $k_T$ , is strongly dependent on the distance,  $R$ , between the fluorophores. Thus, the energy transfer efficiency,  $E_T$ , is also dependent on distance, demonstrated by the following equations:

$$k_T = \frac{1}{\tau_D \cdot \left(\frac{R_0}{R}\right)^6} \quad (1-1)$$

$$E_T = \frac{R_0^6}{R^6 + R_0^6} \quad (1-2)$$

where  $\tau_D$  is the donor fluorescence lifetime in the absence of the acceptor and  $R_0$  is the Förster distance at which  $E_T$  is 50%.  $R_0$  is characteristic of the fluorophore pair used, dependent on their spectral overlap and the relative spatial orientation, and ranges from 20 to 90 Å. This range allows the measurement of fluorophore distances ranging from 10 to 100 Å, a relevant range for detecting ribozyme cleavage.<sup>71</sup> This real-time technique can be used to precisely determine the rate of a ribozyme cleavage reaction with a temporal resolution of seconds or better.

FRET has been widely used in the study of cleavage kinetics and global changes in RNA conformation.<sup>71-73,75</sup> By attaching a pair of fluorophores to different locations

on a nucleic acid molecule, relative distances between the labeled sites can be identified and monitored in real-time by steady-state FRET while conformational or catalytic changes occur. In a ribozyme designed for FRET, donor and acceptor fluorophores are positioned on the RNA so that they are relatively close before ribozyme cleavage, thus energy transfer is observed. After cleavage and dissociation of the cleavage product, the distance between the fluorophores increases. The resulting decrease in FRET ratio ( $I_{\text{acceptor}}/I_{\text{donor}}$ ) and increase in donor fluorophore emission ( $I_{\text{donor}}$ ) are monitored in real-time (Figure 1-1) to precisely determine the rate of a ribozyme cleavage reaction with a 1-s temporal resolution or better. Such temporal resolution allows observation of structural dynamics and precise determination of rate constants. Disadvantages of FRET include the requirement for two fluorophores, the addition of which is expensive and time consuming, and its sensitivity to quenching.

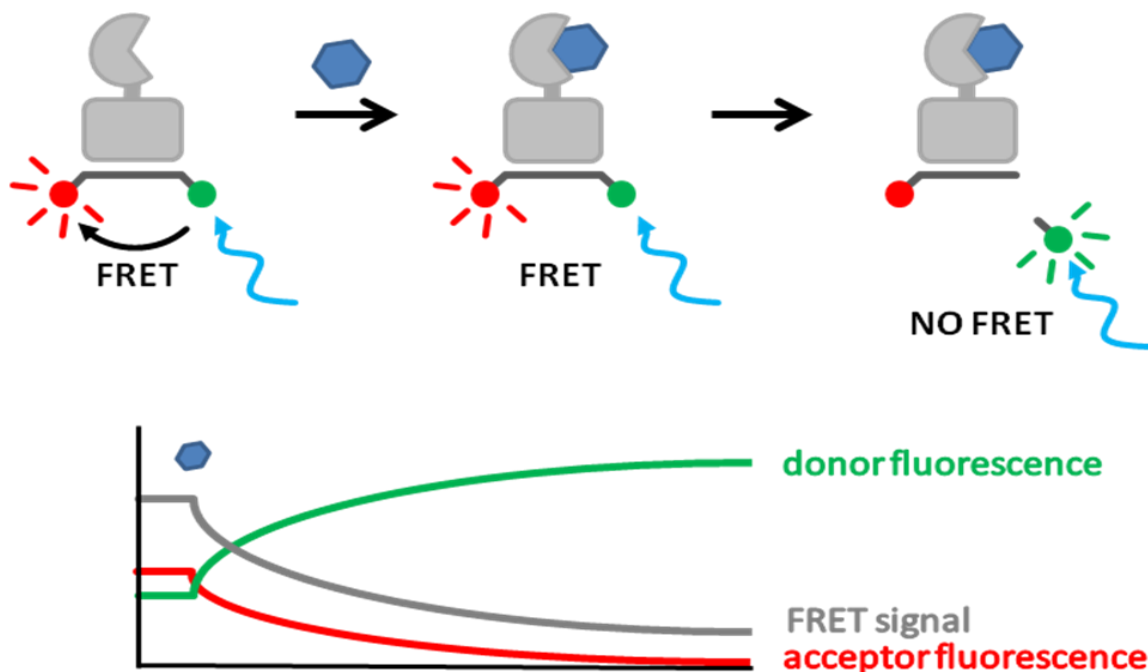


Figure 1-1: FRET response to ribozyme cleavage. Before analyte addition, energy from incident light is transferred from donor to acceptor fluorophore. After addition, analyte binds and the substrate is cleaved, releasing the cleavage product, resulting in an increase in donor fluorescence and decrease in acceptor fluorescence and FRET ratio.

**Capillary electrophoresis (CE).** Free-solution CE relies on differences in charge-to-size ratio of components to separate mixtures. It rapidly separates analytes on the basis of their electrophoretic mobility,  $\mu_e$ , in free solution in a narrow bore fused silica capillary with high efficiency due to the application of high electric fields (Figure 1-2). Analyte mobility is proportional to charge,  $q$ , and inversely proportional to hydrodynamic radius,  $r$ , and solvent viscosity,  $\eta$ , as expressed:

$$\mu_e = \frac{q}{6\pi\eta r} \quad (1-3)$$

The sum of the analyte mobility and the bulk, electroosmotic flow,  $\mu_{eof}$ , in the capillary determine the apparent mobility,  $\mu_{app}$ , of the analyte and the product of  $\mu_{app}$  and the applied electric field,  $E$ , determine analyte velocity,  $v$ , in the capillary:

$$v = \mu_{app}E = (\mu_e + \mu_{eof})E \quad (1-4)$$

Thus, even negatively charged nucleic acids can be separated with normal polarity, toward the negative electrode, when the electroosmotic flow is greater than the analyte mobility. In our assays, detection is achieved by laser-induced fluorescence (LIF), which offers increased sensitivity over UV detection.

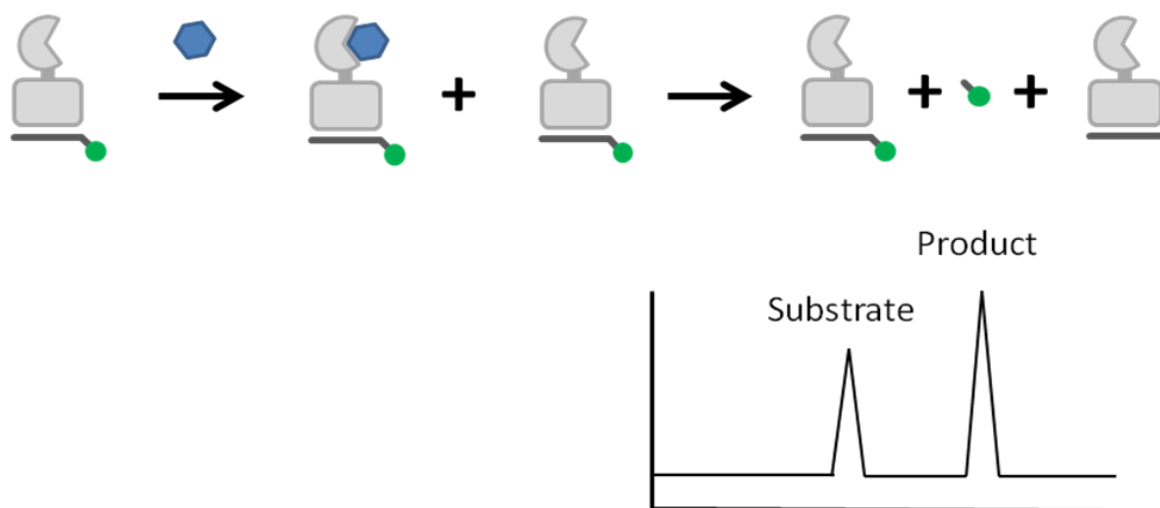


**Figure 1-2: CE response to ribozyme cleavage. After cleavage reaction, uncleaved substrate is separated from fluorescent cleavage product.**

Free-solution CE has been used on many biochemical systems, including those for which gel electrophoresis has been traditionally used for analysis, and has had application in separation of DNA and protein mixtures.<sup>20, 76, 77</sup> These have included studies of

aptamer-protein interactions by affinity probe CE, in which the aptamer was fluorescently labeled and mixed with protein. The aptamer-protein complex could then be separated from free aptamer, when the separation time is short enough to prevent dissociation.<sup>16, 19, 78-80</sup> CE has also been used to monitor enzyme reactions, in which substrate is converted into a product, as with an aptazyme cleavage reaction. Repeat injection of a sample over time allows for determination of kinetic properties of the system, as the increase in product formation (or substrate depletion) is monitored over time.<sup>81, 82</sup>

CGE separates molecules based on electrophoretic mobility in a capillary through a sieving matrix, in a capillary in which electroosmotic flow has been eliminated, typically by coating the inner walls. Capillary gel electrophoresis (CGE) is widely used for the separation of nucleic acid molecules, especially of DNA. It has been used to observe ribozyme cleavage, with separation achieved in hydroxyethyl cellulose in a capillary<sup>66</sup> and in linear polyacrylamide in a microchip, with overlapping, automated capillary injections.<sup>67</sup>

Free solution CE and CGE have many advantages over slab gel electrophoresis including higher resolution, higher sensitivity, shorter analysis time, better quantification, less reagent consumption, and ease of automation.

### **Dissertation Overview**

The overall objective of this work was to develop FRET and CE-LIF based assays for the detection and quantification of small molecules using aptazymes. First, an assay for GlcN6P was developed using the *glmS* ribozyme for recognition and transduction in single turnover reactions. Detection was achieved by FRET and CE-LIF. Both

methods were also used to monitor the cleavage reaction and obtain kinetic information. This assay was improved through the use of multiple turnover reaction conditions. Signal amplification was achieved at long times by holding the reaction at 50 °C, where the data suggest that the rate-limiting step is the binding of substrate to the ribozyme. The assay was further improved by cycling the temperature between a reaction temperature, 42 °C, at which the cleavage reaction is fast and seems to be limited by the off rate of the substrate from the ribozyme, and a dissociation temperature, 60 °C, at which substrate dissociation occurs. The potential for developing a multiplexed system in which two substrates can be simultaneously detected by two ribozymes was explored after characterizing two additional aptazymes, for ATP and cAMP. In a proof-of-principle, the ATP aptazyme was multiplexed with the *glmS* ribozyme to detect ATP and GlcN6P, with separation by gel electrophoresis. The ATP aptazyme is cross-activated by cAMP, so while a qualitative assay is possible, a quantitative, multiplexed assay of these two compounds is not achievable. These assays demonstrate the potential for aptazymes to serve as recognition and transduction elements in analytical assays. They also elucidate a need for further improvement in sensitivity and specificity of aptazymes for use in analytical assays.

## CHAPTER 2

### ASSAY FOR GLUCOSAMINE-6-PHOSPHATE USING A LIGAND-ACTIVATED RIBOZYME AND FRET OR CE-LIF DETECTION

#### Introduction

RNA is a widely studied biopolymer that is involved in a myriad of cellular functions ranging from protein biosynthesis to catalysis of chemical reactions and regulation of gene expression by RNA interference and riboswitches.<sup>23-25</sup> Catalytic RNAs, or ribozymes, catalyze the cleavage or ligation of the RNA phosphodiester backbone. Riboswitches are non-coding, 5' leader regions of mRNA that bind small molecules with high specificity and subsequent modulation of transcription, translation, or mRNA processing.<sup>83</sup> Combinatorial chemistry methods have resulted in the *in vitro* development of nucleic acid molecules that bind small molecules and proteins.<sup>10</sup> Further development has resulted in allosterically regulated ribozymes, or aptazymes, which catalyze cleavage reactions as the result of the binding of specific effector ligands.<sup>27</sup> Examples of *in vitro* selected or engineered aptazymes include aptazymes for theophylline,<sup>31-34</sup> ATP,<sup>31, 35</sup> cAMP,<sup>36-38</sup> cGMP,<sup>36-38</sup> cCMP,<sup>38</sup> FMN,<sup>31, 32, 34, 39</sup> doxycycline,<sup>40</sup> 3-methylxanthine,<sup>33</sup> pefloxacin,<sup>41</sup> cobalt ion,<sup>42</sup> oligonucleotides,<sup>43-46</sup> and various proteins.<sup>47-49</sup> To date, only one naturally occurring aptazyme has been identified, which is the *glmS* ribozyme, a catalytic riboswitch.<sup>28</sup>

The *glmS* ribozyme undergoes a self-cleavage reaction in the presence of glucosamine-6-phosphate (GlcN6P).<sup>28</sup> In many aptazymes, the ligand dependent



cleavage rate is attributed to a conformational change that occurs upon ligand binding, but it has been shown that this adaptive binding is not observed in the case of the *glmS* ribozyme. Instead, GlcN6P is thought to play a catalytic role in the cleavage reaction. The reaction has been demonstrated to be relatively specific for GlcN6P, showing no cleavage with many structurally similar molecules to GlcN6P and a substantially reduced rate of cleavage with a few molecules, like glucosamine.<sup>28, 29, 51, 53</sup> This specificity makes the *glmS* ribozyme promising as an model system for an analytical assay.

The specificity of the binding interactions and resultant signal transducing cleavage reactions of aptazymes make them appealing for use as analytical reagents. In an aptazyme assay, the effector ligand can be detected by monitoring the cleavage reaction. Indeed several assays that utilize aptazymes as a recognition element have been reported.<sup>17, 27, 42, 50</sup>

Analyte detection based on aptazymes has potential advantages over detection based on antibodies and protein enzymes, which have been the workhorses in molecular recognition for analytical assays. Many of the potential advantages of oligonucleotide reagents, such as ease and reproducibility of manufacture, come from the ability to chemically synthesize nucleic acids. In some cases, their affinities rival or exceed the capabilities of antibodies, while the evolution process enables control over kinetic and thermodynamic properties of the aptamer-target binding interaction. The *in vitro* selection process also confers the advantage of offering response to a wider range of target molecules by including those that would be toxic *in vivo* as well as those that would not induce an immune response. Due to the reliability of chemical synthesis of aptamers after they have been sequenced, less batch to batch variation is expected than is

expected for antibodies, which are produced *in vivo*. Aptamers are more stable for long-term storage than antibodies, and can be restored even after denaturation. Aptamers can be modified after selection to further optimize binding affinities or to add modified bases to prevent degradation if they will be introduced to biological sample. Further, no immunogenicity is expected from aptamers if they are introduced to the body. Finally, reporter molecules such as fluorescein and linkers such as biotin can often be easily attached to aptamers at precise locations without disrupting their activities.<sup>62</sup>

Employing ribozymes in analytical assays requires the development of a reliable method for quantitatively detecting the cleavage reaction. Ideally a detection method should use a minimal amount of sample, is fast, can be run in parallel or array formats, and does not require elaborate design of the reagents. Previous ribozyme assays have followed conversion of substrate into cleavage product by a variety of separation based and real-time methods. PAGE has been the most widely used technique for monitoring ribozyme cleavage. Use of PAGE involves removing aliquots from a cleavage reaction at various time points, stopping the reactions, and separating them in parallel on a gel, often with detection and quantification achieved by radiolabeling the RNA. The collection of these data is tedious, results in long analysis times, and typically involves hazardous radioisotopes. In some cases, HPLC has been employed, alleviating the need for radioisotopes, but it is neither real-time nor high throughput.<sup>63-65</sup> Capillary gel electrophoresis (CGE) has also been used to separate and detect ribozyme cleavage and has been applied in high throughput in a microchip-based assay.<sup>66, 67</sup> Some real-time methods have been used, primarily involving changes in fluorescence intensity,<sup>68, 69</sup> fluorescence polarization,<sup>70</sup> or fluorescence resonance energy transfer (FRET).<sup>71-73</sup>

These methods provide precise determination of rate constants, but can suffer from sources of fluorescence change outside of bond cleavage and the possibility that cleavage is spectroscopically silent. This paper describes the use of FRET and the first application of free-solution capillary electrophoresis (free-solution CE), that is gel-free nucleic acid separation, for monitoring ribozyme cleavage.

FRET is an effective method for observing ribozyme cleavage.<sup>71-73</sup> In a FRET-designed ribozyme, donor and acceptor fluorophores are positioned on the RNA so that they are relatively close before ribozyme cleavage, but separate after cleavage and dissociation of the cleavage product. The resulting decrease in FRET and increase donor fluorophore emission are monitored in real-time to precisely determine the rate of a ribozyme cleavage reaction with 1 second temporal resolution or better. This temporal resolution allows observation of structural dynamics and precise determination of rate constants. Some disadvantages of FRET include the requirement for two fluorophores, the addition of which is expensive and time consuming, and its sensitivity to quenching.

Capillary gel electrophoresis (CGE) is widely used for the separation of nucleic acid molecules, especially of DNA. It has been used to observe ribozyme cleavage, with separation achieved in hydroxyethyl cellulose in a capillary<sup>66</sup> and in linear polyacrylamide in a microchip, with overlapping, automated capillary injections.<sup>67</sup> Free-solution CE has been extensively used on biochemical systems, including those for which gel electrophoresis has been commonly used for separation, and has had application in separation of DNA and protein mixtures.<sup>20, 76, 77</sup> These have included studies of aptamer-protein interactions.<sup>16, 19, 78-80</sup> In this work, we demonstrate the utility of free-solution CE in the detecting ribozyme cleavage. Free-solution CE and CGE

have many advantages over slab gel electrophoresis including higher resolution, higher sensitivity, shorter analysis time, and better quantification.

As a model system, we explore use of the *glmS* ribozyme to detect GlcN6P. The specificity of the *glmS* ribozyme for GlcN6P and its modulated rate in response to GlcN6P make the ribozyme interesting for use in an assay for GlcN6P. The cis-cleaving *glmS* ribozyme has previously been investigated in a GlcN6P assay using fluorescence polarization.<sup>40</sup> A minimal, trans-cleaving *glmS* construct has previously been developed and demonstrated to be similar in activity to the naturally occurring cis-ribozyme.<sup>51</sup> A similar trans-cleaving ribozyme has been used in a FRET based assay.<sup>54,</sup>  
<sup>84</sup> In the trans model developed previously in the Walter lab, an external substrate is added to the *glmS* ribozyme and GlcN6P activated cleavage results in three RNA molecules: the cleavage product, a three nucleotide molecule; the cleaved substrate at eight nucleotides; and the unchanged ribozyme molecule, which is twenty three nucleotides in length.<sup>51</sup> The kinetics of this reaction were monitored by FRET and free-solution CE and each technique was used in development of an analytical assay. This work demonstrates the potential utility of coupling FRET or CE with ribozymes for the detection and quantification of small molecules.

## Experimental Section

**Chemicals.** Unless stated otherwise, all chemicals used in the experiments were purchased from Sigma-Aldrich Co. (St. Louis, MO). Tris-glycine buffer (10×) was purchased from Bio-Rad laboratories (Hercules, CA). All solutions were prepared with deionized water from an E-Pure water purification system (Barnstead International Co.,

Dubuque, IA). Rhodamine 110 was purchased from Molecular Probes (Eugene, OR). RNA was purchased from the Howard Hughes Medical Institute Biopolymer/Keck Foundation Biotechnology Resource RNA Laboratory at the Yale University School of Medicine (New Haven, CT).

**Preparation of RNA.** The substrate strand contained 2'-O-methyl protection groups and was deprotected as recommended by the manufacturer and purified as previously described.<sup>85, 86</sup> For FRET measurements, the substrate strand was modified on the 5' and 3' ends with fluorescein (donor) and tetramethylrhodamine (acceptor), respectively, as also previously described.<sup>73</sup> RNA concentrations were calculated from their absorption at 260 nm and corrected for the additional absorption of fluorescein and tetramethylrhodamine by using the relations  $A_{260}/A_{492} = 0.3$  and  $A_{260}/A_{554} = 0.49$ , respectively. The ribozyme strand was generated by run-off transcription from a double-stranded, PCR amplified template that encoded an upstream T7 promoter. Transcriptions were purified as previously described (Harris et al. 2004), and the RNA concentration was calculated as described above.

**FRET and CE cleavage kinetics reactions.** Single-turnover cleavage reactions to compare FRET and CE kinetics were performed under the following conditions: 50 mM HEPES-KOH, pH 7.5; 200 mM KCl; 25 mM DTT; and 20 mM MgCl<sub>2</sub>. Ribozyme and substrate concentrations were 20 nM and 10 nM, respectively for FRET experiments and 1000 nM and 500 nM, respectively, for CE experiments. The ribozyme and substrate strands were annealed at 70 °C for 2 min, then cooled to room temperature over 5 min before reacting at 25 °C. Cleavage was monitored as described below.

**FRET cleavage assay.** Single-turnover cleavage reactions were performed under the following conditions: 50 mM HEPES-KOH, pH 7.5; 200 mM KCl; 25 mM DTT; 50 mM MgCl<sub>2</sub>; 20 nM ribozyme and 10 nM substrate. The ribozyme and substrate strands were prepared as described above. The reaction took place at 37 °C unless otherwise noted. Steady-state FRET measurements of the glmS ribozyme doubly labeled with fluorescein and tetramethylrhodamine were performed on a AB2 spectrofluorometer. Fluorescein was excited at 490 nm (4 nm bandwidth), and fluorescence emission was recorded simultaneously at the fluorescein (520 nm, 8 nm bandwidth) and tetramethylrhodamine (585 nm, 8 nm bandwidth) wavelengths, by shifting the emission monochromator back and forth. A FRET ratio was calculated as F585/F520. Stock solutions (135 μL) for final concentrations as listed for the reactions above were annealed as described and transferred to a 150 μL cuvette kept at appropriate temperature by a circulating water bath. After 1 minute, GlcN6P was added to an appropriate final concentration in 15 μL to initiate the reaction and mixed manually in about 5 s.

**FRET multiple-turnover cleavage experiments.** Multiple-turnover cleavage experiments were prepared and monitored as the single-turnover assay above, except ribozyme and substrate strands were 10 nM and 100 nM, respectively. The reactions took place at the temperatures indicated in Results and Discussion. To cycle the temperature of the sample in the cuvette, two water baths were maintained at appropriate temperatures and their connecting hoses manually switched.

**High-speed CE cleavage assays.** Single-turnover CE experiments were performed under the same reaction conditions as the single-turnover FRET experiments,

except the ribozyme and substrate concentrations were 400 nM and 200 nM, respectively, and they contained 25 nM rhodamine 110 as an internal standard. Stock solutions were prepared, annealed as described above, and reactions started by adding 45  $\mu$ L stock solution to pre-aliquoted 5  $\mu$ L GlcN6P for appropriate final concentrations. They were incubated at 37 °C in a thermal cycler for 10 min or 30 s, as appropriate, then quenched with 10  $\mu$ L EDTA, pH 8 to a final concentration of 100 mM EDTA and stored on ice until analysis. Multiple-turnover samples were performed under the same conditions except with 20 nM ribozyme and 200 nM substrate. They were either incubated at 50 °C or cycled between 42 °C and 60 °C, as described in Results and Discussion.

A schematic drawing of the flow-gated high-speed CE-LIF instrument used for kinetics analysis is illustrated in Figure 2-1. An unmodified fused silica capillary (10  $\mu$ m inner diameter, 360  $\mu$ m outer diameter, total length = 7.5 cm, inlet to detector length = 3.8 cm) was used as the separation capillary. GlcN6P was delivered to a pressurized sample container containing reaction mixture at a flow rate of 5  $\mu$ l/s for 2 s by pressure. A 5  $\times$  2 mm microbar in the sample vial together with the stir plate underneath allowed the sample to be mixed immediately. After mixing, the sample was delivered to the flow gate at a rate of 0.8  $\mu$ l/s by pressure. Samples were then introduced onto the capillary by electrokinetic injection via a flow gate interface at 2 kV for 1 s and separated at 15 kV. The total delay time between addition of unlabeled peptide and the collection of the first electropherogram was 7 s, including sample delivery time, high voltage ramping time and injection time. Electropherograms were collected every 12.5 s. Tris-glycine-potassium buffer (25 mM tris(hydroxyamino)methane, 192 mM glycine, 5 mM K<sub>2</sub>HPO<sub>4</sub>) was continuously delivered to the flow gate at a rate of 1.5 ml/min by a

Series I HPLC pump (LabAlliance, Fisher Scientific, Pittsburgh, PA). For CE assays, the sample mixing system was not used, the separation capillary was 25  $\mu\text{m}$  inner diameter, 360  $\mu\text{m}$  outer diameter, total length = 7 cm, inlet to detector length = 3.5 cm, and samples were introduced onto the capillary by electrokinetic injection via a flow gate interface at 1 kV for 50 ms and separated at 12 kV in tris-glycine-potassium buffer.

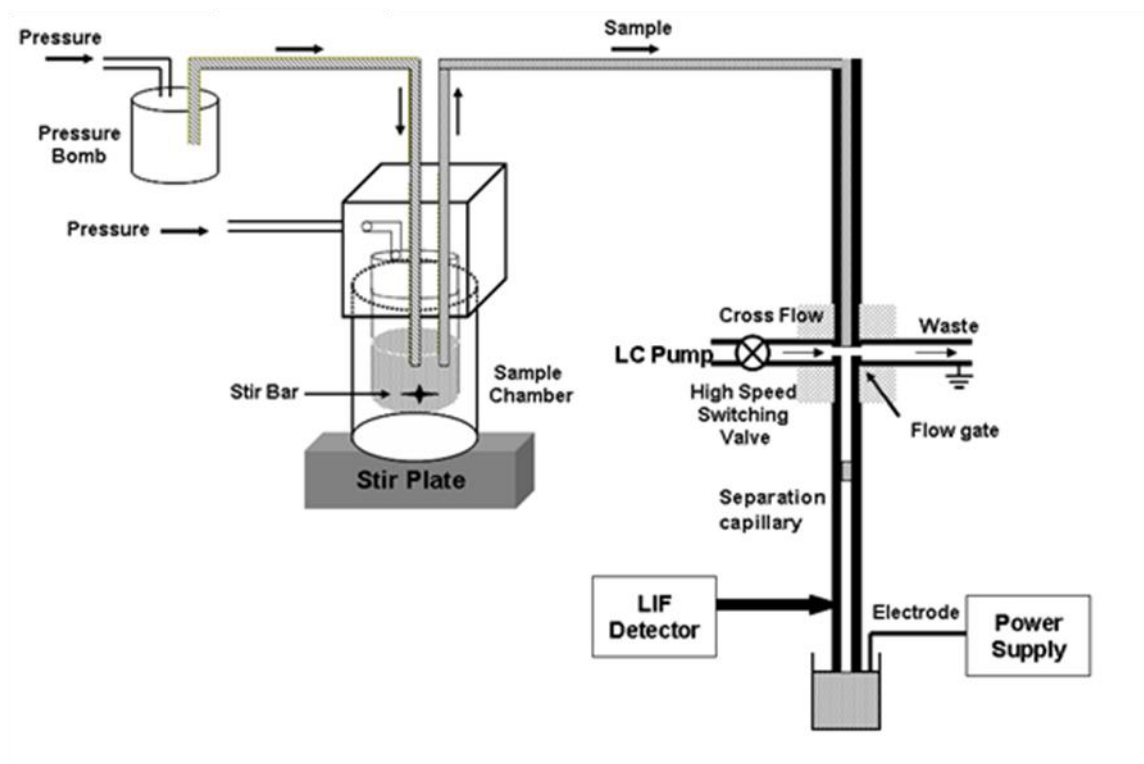


Figure 2-1. Schematic drawing of the high speed CE instrument used for kinetics studies. For the CE assays, the sample mixing system was not used. Figure adapted from source.<sup>87</sup>

The peak heights were obtained from the electropherograms using Cutter<sup>88</sup> and normalized complex peak height (product peak height divided by sum of peak heights of



product and substrate) was plotted versus time to extract  $k_{\text{obs}}$  by fitting the curve into one-component exponential decay function (kinetics) or against GlcN6P concentration for the assays.

## Results and Discussion

**Single-Turnover FRET Assay.** The cleavage reaction of a minimal, trans-cleaving *glmS* ribozyme (Figure 2-2) induced by GlcN6P was monitored by FRET, as has previously been demonstrated.<sup>51</sup> The substrate strand of the *glmS* ribozyme was labeled on the 5' end with fluorescein as the FRET donor and on the 3' end with rhodamine as acceptor fluorophore (Figure 2-2).

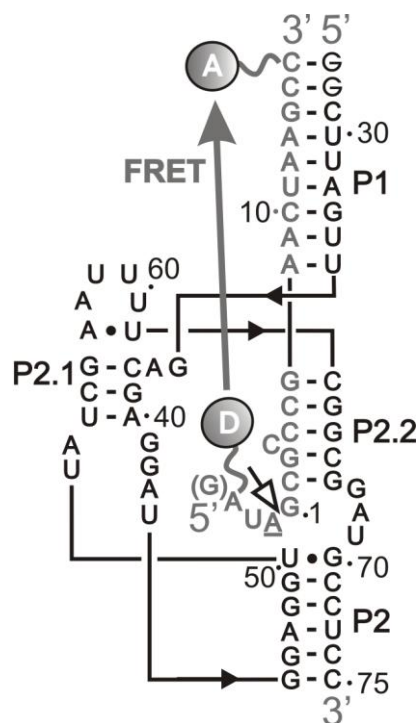


Figure 2-2. The *glmS* ribozyme minimal structure and fluorophore labels. The doubly labeled construct is used for FRET studies, while the substrate strand is labeled with only the donor fluorophore, fluorescein, for CE studies. The open arrow indicates the cleavage site.<sup>51</sup>

In the intact ribozyme-substrate complex, the fluorophores are sufficiently close (~52 Å) to allow efficient energy transfer from the excited donor to the acceptor, resulting in emission at the wavelength characteristic of the acceptor. After cleavage, the 5'-product dissociates from the ribozyme-substrate complex, so that the fluorescein emission increases and the FRET ratio decreases (Figure 2-3A). There is also a small increase in acceptor signal, which we attribute to donor signal detected in the acceptor channel. The cleavage rate was determined by fitting the FRET decrease as well as the donor fluorescence increase upon GlcN6P addition with single exponential decay and association curves, respectively. The measured rate constants were in good agreement, for example, at 250 μM GlcN6P, the measured rate constants were  $0.032 \pm 0.004 \text{ s}^{-1}$  and

$0.0294 \pm 0.0006 \text{ s}^{-1}$  for the FRET and donor fluorescence fits, respectively. In view of their similarity, for all further work the donor signal was used due to its higher signal to noise ratio (Figure 2-3B).

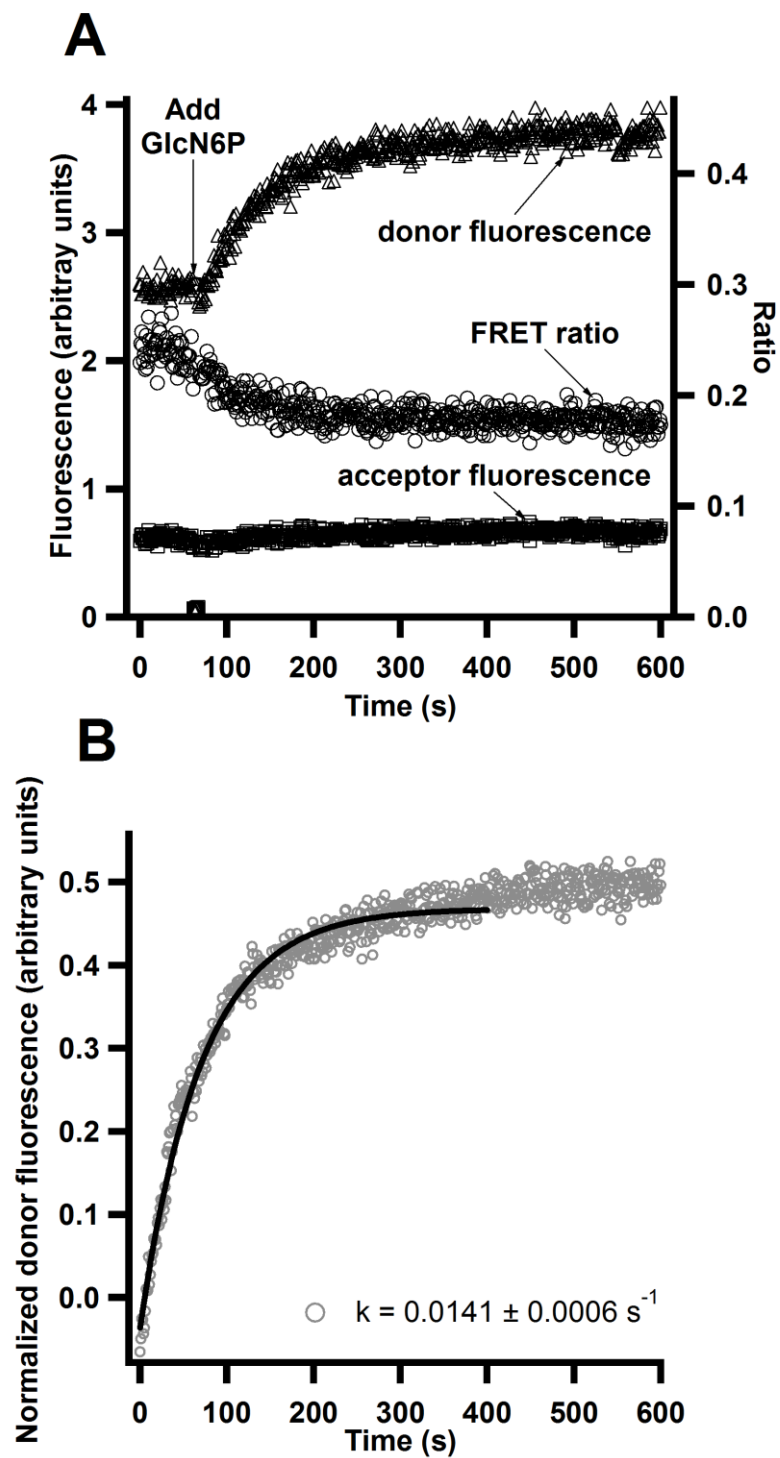


Figure 2-3. A. 100  $\mu\text{M}$  GlcN6P detection by FRET measured in 50 mM HEPES-KOH, pH 7.5, 200 mM KCl, 25 mM DTT, 50 mM  $\text{MgCl}_2$ , 20 nM glmS ribozyme, 10 nM doubly labeled substrate, 37  $^\circ\text{C}$ . B. Fit of donor fluorescence (single exponential association) for determination of cleavage rate.

Previous reports on using this aptazyme used 50 mM HEPES-KOH, pH 7.5; 200 mM KCl; and 10 mM MgCl<sub>2</sub> as the reaction buffer. As buffer conditions can have a significant effect on assay kinetics, we varied several parameters to ensure adequate cleavage rates for the assay. For this study, 50 mM HEPES-KOH, 200 mM KCl, and 25 mM DTT were used as the background electrolytes and 10 nM substrate was used. Other parameters were varied sequentially over the following ranges as follows: pH 7.5 or 8.5, MgCl<sub>2</sub> concentration from 10-50 mM, ribozyme concentration from 20-50 nM, and temperature from 25-60 °C. Within these limits, the best assay sensitivity was achieved with pH 7.5, 50 mM MgCl<sub>2</sub>, 20 nM *glmS* ribozyme, and reaction temperature at 37 °C. The ribozyme is inactive at 60 °C. These conditions were used for subsequent assays.

Cleavage rates were measured by FRET over a range of concentrations of GlcN6P. As shown by the calibration curves in Figure 2-4, the rate of cleavage increases linearly with GlcN6P up to 500 μM analyte with an R<sup>2</sup> value of 0.999. The limit of detection (LOD) is 0.8 μM, which was calculated as 3 times the standard deviation of the blank divided by the slope of the calibration curve. At high concentrations of GlcN6P, above the linear dynamic range, the rate of cleavage is very fast, leading to high standard deviations, at least in part as a result of the length of time required for analyte addition and mixing.

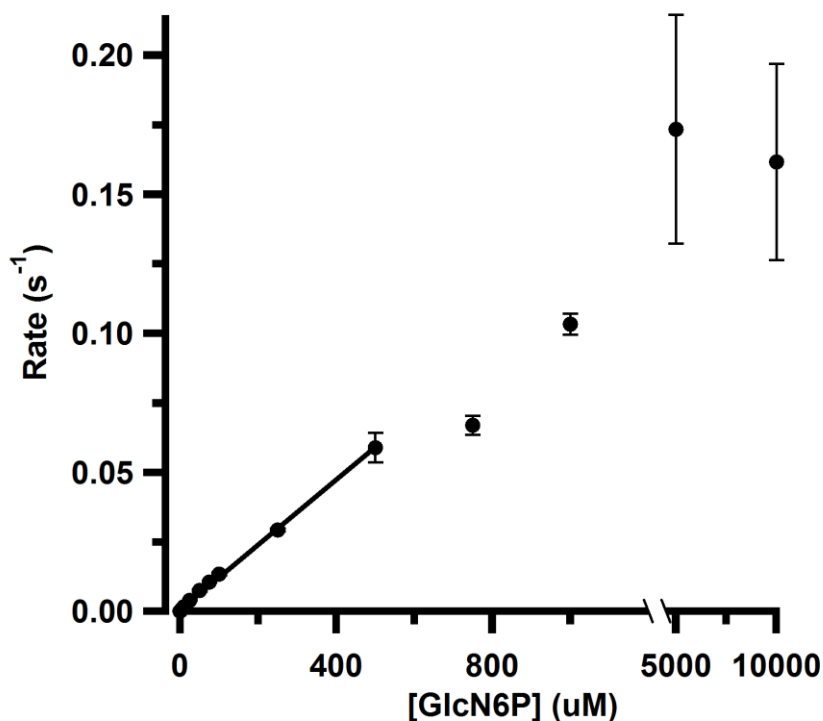


Figure 2-4. FRET calibration curve. Response is based on rate of cleavage reaction, which increases linearly up to 500  $\mu\text{M}$  with an  $R^2$  value of 0.999. The limit of detection is 0.8  $\mu\text{M}$ .

**Single-Turnover CE Assay.** We next used free-solution CE-LIF to monitor the single-turnover reaction of our *glmS* ribozyme with a 5' fluorescein labeled substrate. The reaction mixture was sampled every 12.5 seconds and analyzed by CE-LIF. The resulting electropherograms have three peaks: internal standard (rhodamine 110), ribozyme-substrate complex, and cleavage product (Figure 2-5A). The progress of the reaction was monitored by observing the decreasing height of the ribozyme-substrate complex peak as well as the increasing peak height of the cleavage product. For quantitative analysis, these two peak heights were normalized by dividing by their sum. The reaction rate constant was obtained by plotting the normalized peak heights versus

time and fitting the data with single exponential decay and association curves (Figure 2-5B). The reaction rate constant in the presence of 500  $\mu\text{M}$  GlcN6P was determined to be  $0.0052 \pm 0.0002 \text{ s}^{-1}$ , in good agreement with the rate of  $0.00603 \pm 0.00008 \text{ s}^{-1}$  determined by FRET for the same GlcN6P concentration. In response to 5 mM GlcN6P, the rate constant is measured to be  $0.029 \pm 0.001 \text{ s}^{-1}$  by CE and  $0.028 \pm 0.001 \text{ s}^{-1}$  by FRET. These results demonstrate that the rapid CE separation allows for kinetic monitoring of the ribozyme reaction.

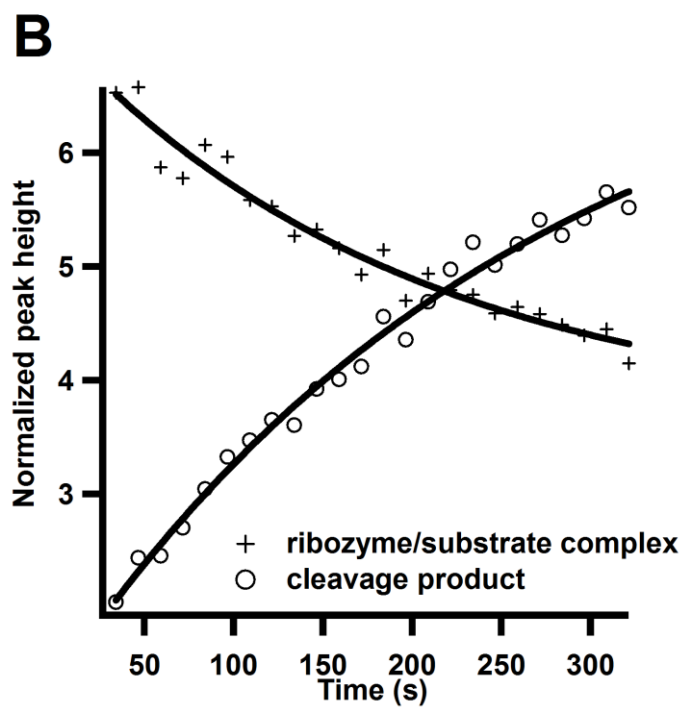
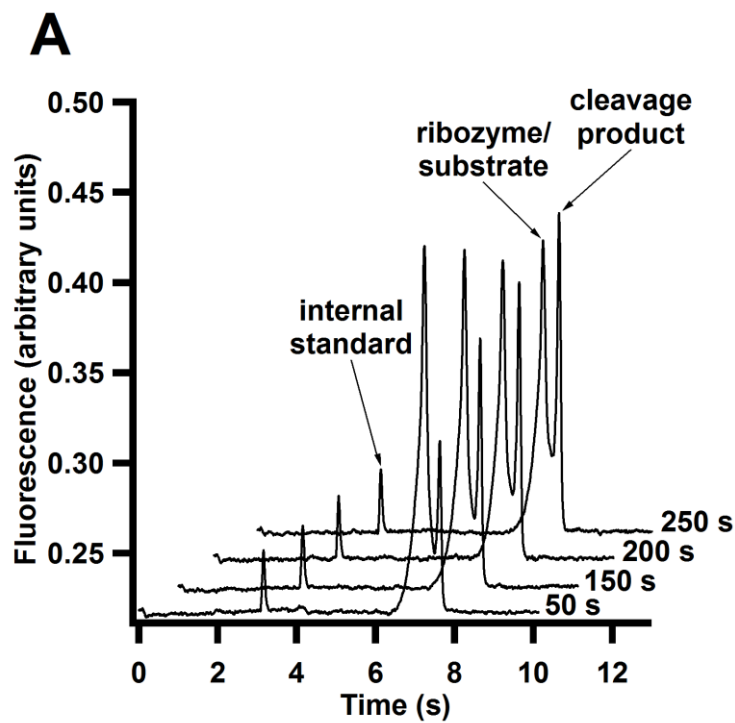


Figure 2-5. 500  $\mu\text{M}$  GlcN6P detection by CE measured in 50 mM HEPES-KOH, pH 7.5, 200 mM KCl, 25 mM DTT, 20 mM  $\text{MgCl}_2$ , 500 nM singly labeled substrate, 1  $\mu\text{M}$  glmS ribozyme, 25  $^\circ\text{C}$ . A. Electropherograms of ribozyme cleavage. B. Fit of ribozyme cleavage rate as measured by CE, which is in good agreement with rate determined by FRET.  $k = 0.0052 \pm 0.0002 \text{ s}^{-1}$ .



We next evaluated the use of CE-LIF as a readout for an GlcN6P assay by detecting the extent of reaction with a range of concentrations of GlcN6P using solution conditions optimized by FRET. For the CE assay, the cleavage reaction was started and ten minutes later the sample was injected into the CE for separation and detection. The separation was completed in less than ten seconds, eliminating the need to quench the cleavage reaction. Thus, the use of a separation step to the assay allowed normalization of a single time point measurement, simplifying the assay for GlcN6P. Normalizing the data in the same way as described for determining the rate of reaction by CE provided information about the fraction of substrate cleaved, from which a calibration was obtained. The linear dynamic range for this calibration extends from 0.5 to 10  $\mu\text{M}$  (Figure 2-6).

After a 10 min reaction at concentrations of GlcN6P over 10  $\mu\text{M}$ , the reaction has proceeded to completion. Therefore, to extend the dynamic range to GlcN6P concentrations above 10  $\mu\text{M}$ , the reaction mixture was injected at thirty seconds instead of ten minutes. At this reaction time, concentrations of GlcN6P below 10  $\mu\text{M}$  are indistinguishable due to the very small progression of the cleavage reaction, but concentrations greater than 10  $\mu\text{M}$  are easily distinguished, resulting in a linear dynamic range from 10 to 100  $\mu\text{M}$  (Figure 2-6). With the two calibrations, the LDR for our free-solution CE assay is 0.5 to 100  $\mu\text{M}$  GlcN6P, with an  $R^2$  of 0.998. The detection limit is 0.5  $\mu\text{M}$ . The single-turnover assays demonstrate the potential of the *glmS* ribozyme in an assay to detect GlcN6P as well as the utility of CE in monitoring the progress of a cleavage reaction.

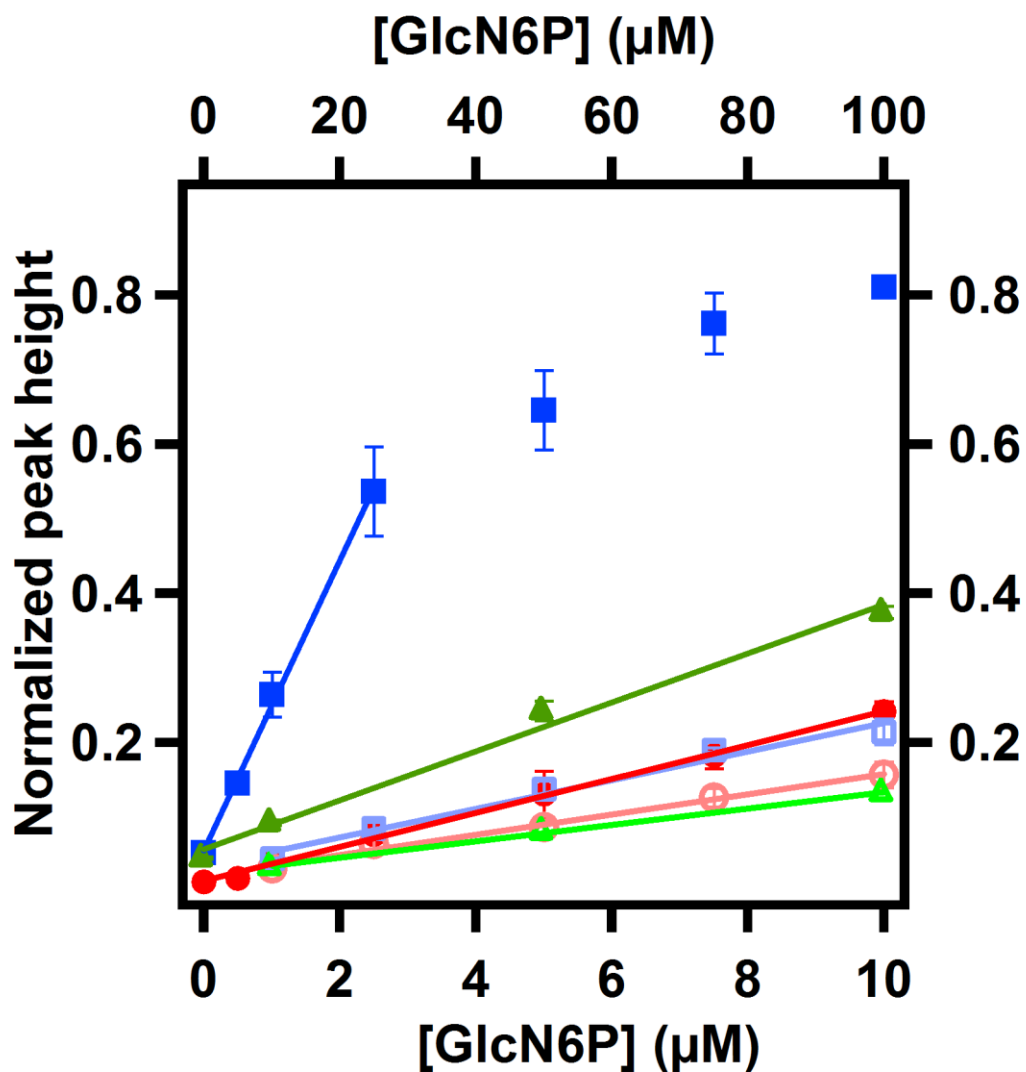


Figure 2-6. CE calibration. Left and bottom axes and closed symbols represent low concentration GlcN6P samples. Right and top axes and open symbols represent high concentration GlcN6P samples. Single-turnover samples are represented by blue squares, multiple-turnover (50 °C) by red circles, and multiple-turnover (cycled) by green triangles.

Both the FRET and CE methods appear to be useful for monitoring the reaction. For kinetic measurements, the FRET reaction achieves a 1 s temporal resolution compared to the 12 s possible by the CE-LIF method. As an assay, the FRET method

has a wider dynamic range; primarily because it is based on the kinetic data rather than a fixed time point like the CE-LIF method. For the same reason, the CE method was much faster, with each sample taking only seconds to analyze after the cleavage reaction, rather than minutes or hours. The CE method offered the advantage of detection of two separate peaks for the cleaved and uncleaved substrate, which allowed for normalization of the signal at a single time point. This kind of normalization is not achievable by FRET. This offers less noise and a lower LOD and is less prone to errors due to non-ribozyme based changes in total fluorescence. The LOD is likely determined by the affinity of the effector for the ribozyme, which has an apparent  $K_d$  of 200  $\mu\text{M}$ ,<sup>38</sup> as well as by the background cleavage observed in the absence of GlcN6P. The CE method uses less analyte with sample volumes as low as 10  $\mu\text{L}$  compared to 150  $\mu\text{L}$  FRET samples. The CE method uses singly-labeled substrate, whereas the substrate for FRET was doubly labeled. The temporal resolution of the FRET method allowed for constant observation of the samples, which was crucial for gaining an understanding of the multiple-turnover reaction. CE could then be used for the single time point, multiple-turnover cleavage assay.

**Multiple-Turnover FRET Assay.** To further improve the sensitivity of GlcN6P detection by the *glmS* ribozyme, multiple-turnover reaction conditions were investigated. Under multiple-turnover conditions, excess substrate is provided, allowing the ribozyme strand to cleave multiple substrate molecules as illustrated in Figure 2-7A (inset). In principle, this approach would allow generation of more signal for a given effector molecule.

In our initial experiments we used 10 nM *glmS* ribozyme and 100 nM substrate and FRET was used to monitor the progress of the reaction. At 25 °C, the increase in donor signal is no greater than the increase observed under single-turnover conditions, indicating that only one set of substrate molecules is cleaved. These results suggested that the 3'-product, which binds the ribozyme with the same number of base pairs as the uncleaved substrate, did not dissociate from the ribozyme rapidly enough to allow efficient multiple-turnover events. We hypothesized that elevated temperatures may accelerate 3'-product dissociation and, thus, substrate turnover. Indeed, as the temperature of the cleavage reaction was increased, the extent of cleavage increased, which is evident from the increase in donor fluorescence (Figure 2-7A). At temperatures up to 50 °C, two phases of cleavage are observed, a slow phase and a fast phase. At 50 °C, the rate of cleavage becomes linear with a slope in between the former slow and fast phases. These observations suggest that the first phase reports on the first turnover where the reaction is rate-limited by substrate cleavage, while the second phase reflects subsequent turnovers where slow 3'-product dissociation becomes rate-limiting. Examining the slope of the linear portion of each the first and second phases further supports this conclusion (Figure 2-7B). In the first phase, the observed rate constant increases with increasing temperature to 37 °C, then decreases to 50 °C. This suggests that the reaction is accelerated with increasing temperature until the rate of substrate association becomes limiting. By contrast, in the second phase the observed rate constant continually increases to its maximum at 50 °C. We think this can be explained by increasing rate of substrate dissociation. At this temperature, a single rate constant is observed over a broader fluorescence signal range, consistent with multiple substrate

turnovers. The ribozyme is inactive at 60 °C. We therefore chose 50 °C, where the ribozyme turns over multiple substrate strands with reasonable efficiency and thus amplifies the signal over that achieved under single-turnover conditions after about ten minutes (Figure 2-7A). The length of time required to achieve such signal amplification is dependent on the concentration of GlcN6P.

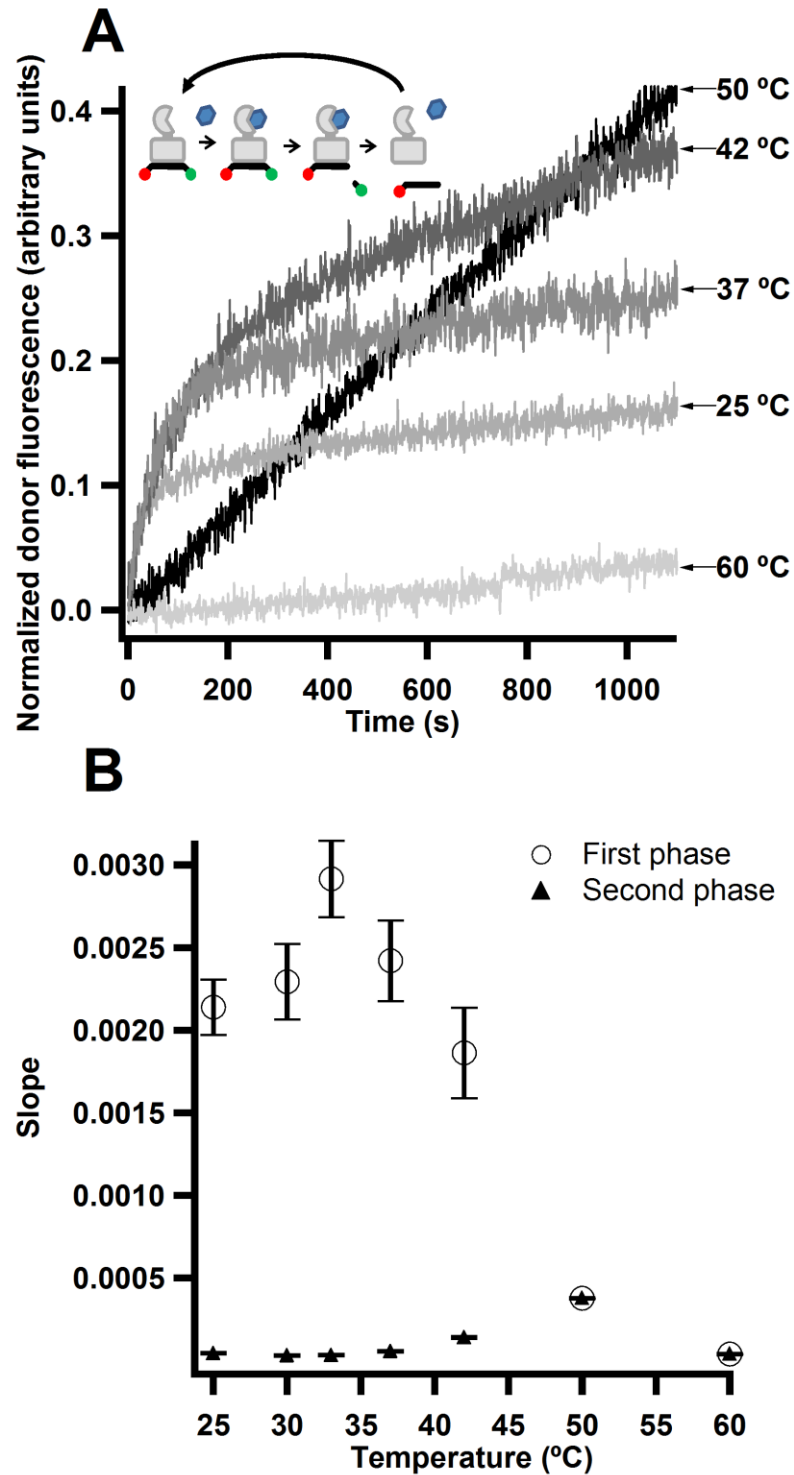
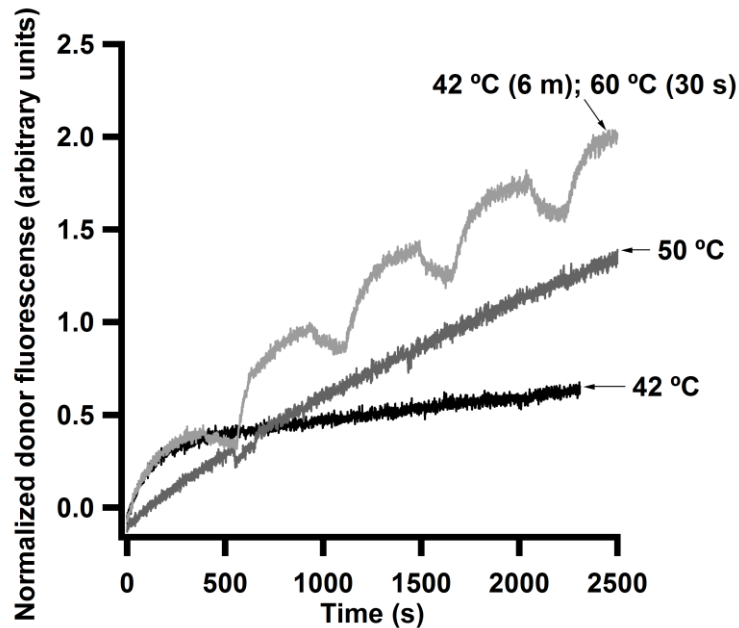


Figure 2-7. Comparison of three constructs of Fyn binding to Fluor-Fyn peptide. Sample contained 500 nM Fyn-SH2-SH3 (trace 1) or GST-Fyn-SH2 (trace 2) or GST-Fyn-SH2-SH3 (trace 3), 200 nM Fluor-Fyn peptide and 10 nM rhodamine 110. Separation conditions were the same as in Figure 3-4.

These results suggested the possibility that a temperature program could be used to achieve better signal amplification. Specifically, we developed a two-temperature program that used an elevated temperature (60 °C) to dissociate the substrate-ribozyme pair, and then lowered the temperature to allow reannealing, reformation of uncleaved substrate-ribozyme-effector complex, and cleavage reaction. We varied the denaturation temperatures from 50 °C to 60 °C (for 30 s) and the reaction time at 42 °C from 3 to 20 min while monitoring the reaction by FRET. The best conditions (i.e., most amplification) were found with 42 °C for 10 min followed by a 30 s pulse to 60 °C. This process of cycling between reaction and dissociation temperatures resulted in about 4-fold signal amplification over fixed temperature at 42 °C and 2-fold at 50 °C after 40 min, as illustrated in Figure 2-8. This method is limited by binding of the 5' cleavage product, which is fully complementary to the ribozyme, and thus competes with uncleaved substrate for binding. An alternate way to achieve multiple turnover events could involve redesign of the substrate to reduce its binding interaction with the ribozyme.



**Figure 2-8. Multiple-turnover FRET with cycling.** Signal amplification is achieved by increasing the temperature to 50 °C. Further amplification is observed when the temperature is cycled between 42 °C and 60 °C. The donor fluorescence increases with cleavage until the temperature is raised to 60 °C, which lowers the quantum yield of the fluorophore. When the temperature is returned to 42 °C, donor fluorescence increases as a new set of substrates bind and are cleaved.

**Multiple-Turnover CE Assay.** The conditions for the multiple-turnover reaction that were optimized by FRET were used in a CE assay. In this assay, ribozyme-substrate samples were either incubated at 50 °C or temperature cycled between 42 °C and 60 °C for 10 min and 30 s, respectively, over a total time of 3.5 hours. High GlcN6P concentration samples were incubated for 5 min either at 50 °C or temperature cycled between 42 °C and 60 °C for 1.5 min and 30 s, respectively. The slopes of the multiple turnover calibration curves are steeper than that of the single-turnover samples by 2-fold for the 50 °C assay and 13-fold for the cycled assay, indicating increased sensitivity (Figure 2-6). The LDR's for these CE based assays are 0.5 to 100  $\mu\text{M}$  ( $R^2$  for 50 °C is 0.995 and 0.999 for cycled), which is the same as the range for the single-



turnover assay, but the detection limit is improved to 0.1  $\mu\text{M}$  for the 50  $^{\circ}\text{C}$  assay and 0.05  $\mu\text{M}$  for the cycled assay.

### Conclusions

This work demonstrates the use of FRET and CE-LIF for detection of the cleavage rate of the *glmS* ribozyme in response to GlcN6P. For kinetic measurements, the FRET reaction achieves a 1 s temporal resolution compared to the 12 s possible by the CE method. The two techniques are in good agreement for determination of the rate constant. We report the use of free-solution CE-LIF for the separation of RNA molecules. These two techniques were used to detect GlcN6P as low as high nanomolar concentrations up to high micromolar concentrations under single-turnover conditions, where FRET has a wider dynamic range, because it is based on kinetic rather than fraction cleaved data. For single turnover assays, the methods have similar detection limits. Using multiple-turnover conditions, CE was used to detect GlcN6P with greater sensitivity over the same range of concentrations. Overall, CE was faster and required smaller sample volumes than FRET. These proof of principle experiments demonstrate the potential of ribozymes for use as recognition elements in FRET and CE based assays.

Future work for these proof-of-principle assays using the *glmS* ribozyme could involve the study of development of insulin resistance in cells. GlcN6P is involved in the hexosamine biosynthetic pathway, whose major end product, UDP-N-acetylglucosamine, serves as a substrate for glycosylation reactions. One to three percent of cellular glucose that is converted to fructose-6-phosphate enters this pathway, and increased flux into this pathway has been shown to result in impaired ability of insulin to

stimulate glucose uptake. The *glmS* ribozyme is also interesting due to its role in the manufacture of GlcN6P, which is a precursor of uridine 5'-diphospho-N-acetyl-D-glucosamine, a molecules that is essential for cell wall biosynthesis in *Bacillus subtilis* and other bacteria.<sup>89</sup> Thus, future work could involve high-throughput screening for potential drug candidates, as repression of the *glmS* gene would reduce the cellular concentration of GlcN6P, ultimately disrupting cell wall biosynthesis. The CE assay is particularly amenable to a high-throughput approach as CE can be performed in parallel. With the current availability of aptazymes that are specific for a variety of target molecules, as well as the ability to engineer or select additional aptazymes, the development of aptazyme-based assays for the detection of many other biologically relevant molecules is an active area of research. The speed and ability to multiplex CE assays either by using multiple capillaries in parallel or by separating the products of multiple reactions in one capillary make CE an attractive mechanism for detecting aptazyme signals.

## CHAPTER 3

### CHARACTERIZATION OF ENGINEERED APTAZYMES FOR USE IN DETECTION OF CAMP AND ATP

#### **Introduction**

Nucleic acids have been demonstrated to function in a variety of different contexts, from storing genetic information to catalyzing biochemical reactions. Relatively recently, they have been demonstrated to be able to catalyze chemical reactions under allosteric control, that is, in response to effector binding.<sup>17, 27, 42, 50</sup> Thus, they can serve as both recognition and transduction elements in bioanalytical assays. In addition, the ease of synthesis and their temperature stability make these aptazymes potentially interesting molecules for affinity assays. There has been some investigation into their analytical potential,<sup>17, 27, 42, 50</sup> but there is still much work to be done. We are interested in developing multiplexed assays using aptazymes for recognition and transduction elements, thus we set out to characterize three known aptazymes for potential use in such an assay.

The potential of aptazymes lies in the ability to design or select them to be responsive to a wide variety of different analytes. To date, they have been demonstrated to cleave in response to oligonucleotides, small molecules, proteins, and metal ions.<sup>17, 27, 42, 50</sup> In addition to developing new aptazymes, a complete characterization of existing ones can lend insight into parameters that will be desirable for precise detection and

quantification of molecules. These parameters can help to inform the selection or design conditions for new aptazymes.

Ideally, aptazymes would be specifically activated by only one analyte and not analogs of that molecule. They would have low background reactivity (typically in RNA backbone cleavage) in the absence of effector. They would be trans-cleaving, so that they could function in a multiple turnover capacity to cleave multiple substrates per aptazyme, thus amplifying the signal. They would have a wide dynamic range. Natural self-cleaving ribozymes catalyze RNA transesterification with rate constants that are near  $1 \text{ min}^{-1}$  under physiological conditions. Aptazymes typically cleave at a much slower rate, especially in their trans-cleaving forms.

Two aptazymes that we will consider herein were developed for ATP and cAMP effectors. The Breaker group designed an aptazyme for ATP by coupling a corresponding RNA aptamer to the hammerhead ribozyme via a variable communication domain.<sup>32</sup> The ATP aptamer has a  $K_d$  of  $0.7 \mu\text{M}$ . The aptamer also binds to adenosine and AMP with similar affinities.<sup>61</sup> The same group used *in vitro* selection to develop aptazymes that respond to cAMP and cGMP.<sup>37</sup> The selection scheme applied selective pressure to a hammerhead ribozyme that was coupled to a 25-nucleotide random sequence domain via a known communication domain and involved both negative and positive selection steps. The apparent dissociation constants for these aptazymes were determined by measuring the half-maximal cleavage activity. For the cGMP aptazyme, the apparent  $K_d$  is  $200 \mu\text{M}$ . The apparent  $K_d$  for the cAMP aptazyme is  $500 \mu\text{M}$ .<sup>38</sup> The high apparent dissociation constants are expected to prevent assays using these aptazymes from rivaling LOD's obtained in current assays.

Assays for ATP as the energy currency of the cell can be used to determine cell viability and to study cellular processes in which it is involved, which include many biosynthetic reactions and signal transduction pathways. Detection of cAMP as a second messenger can be used to study signal transduction and enzyme activity. Commercial kits based on radioactivity, fluorescence, and bioluminescence are available for the detection of ATP, cAMP, and cGMP with detection limits that are in the pM range. With the current stage of development of aptazymes, it is not realistic to assume that they will offer similar LOD's. Perhaps the most interesting characteristic of an aptazyme system is the ability to design or develop aptazymes for a wide range of interesting effectors, which could include analytes that are currently difficult to detect. For now, these serve as proof of principle assays that demonstrate the potential of this interesting group of molecules in analyte detection.

We describe the characterization of two trans-cleaving aptazymes that we have designed from the cis-cleaving aptazymes for cAMP and ATP, described above. We consider their rate of cleavage, pursue optimization of the cleavage conditions, and compatibility for multiplexed detection. These initial studies were done with gel electrophoresis, which has been the workhorse for detection of ribozyme cleavage, and can offer parallel detection by separating many samples on one gel. We use fluorescently labeled RNA substrates, eliminating the need for radiochemicals. Fluorescent labeling is also more practical for real assays by allowing longer storage without the need for relabeling and easier handling and disposal.

## Experimental Section

**Chemicals.** Unless stated otherwise, all chemicals were purchased from Sigma-Aldrich Co. (St. Louis, MO). DNA templates were purchased from Invitrogen (Carlsbad, CA). RNA substrates were purchased from W. M. Keck Foundation (New Haven, CT). See Figure 3-1 for sequences. All solutions were prepared with deionized water from an E-Pure water purification system (Barnstead International Co., Dubuque, IA). T7 RNA polymerase was expressed and purified according to the protocol in Appendix B.

**Preparation of aptazymes.** Complementary DNA strands were annealed at 70 °C for 2 min and cooled to room temperature over 5 min. RNA was transcribed from this DNA template at 37 °C in an overnight reaction using the following reagent concentrations: 100 nM DNA templates; 2 mM NTP mixture; 120 mM HEPES-KOH, pH 7.5; 30 mM MgCl<sub>2</sub>; 2 mM spermidine; 40 mM DTT; 0.04% triton X-100; 0.005 U/μL; 0.1 mg/mL T7 RNA polymerase; and 8% polyethylene glycol. The reaction was purified on a 10 % polyacrylamide gel and eluted overnight in water, then chloroform extracted and ethanol precipitated. RNA substrates were deprotected according to the manufacturer protocol, precipitated with butanol, purified by 15 % PAGE, eluted by tumbling overnight in water, chloroform extracted, ethanol precipitated, and HPLC purified. The concentrations of nucleic acid samples were determined using their absorbance at 260 nm.

**Cleavage reactions.** Cleavage reactions were performed under the following conditions unless otherwise noted: 150 nM aptazyme; 75 nM substrate; 50 mM Tris-HCl, pH 7.5; 50 mM MgCl<sub>2</sub>, and 25 mM DTT. The ribozyme and substrate strands were

annealed at 90 °C for two min, then cooled to room temperature over 5 min. The reaction took place at room temperature for 2 hr, unless otherwise noted. Reactions were separated by 20 % PAGE at 20 W for 2 hr and analyzed on a Typhoon Trio (GE Healthcare, Piscataway, NJ) using fluorescence detection with excitation at 488 nm and detection at 530 nm and the platen focal depth setting, with the gel placed directly on the glass platen. Gel scans were analyzed with ImageQuant, dividing the intensity of the product band by the sum of the intensities of the product and substrate bands.

## **Results and Discussion**

**Design of trans-cleaving aptazymes.** Based on cis-cleaving constructs of aptazymes for cAMP, cGMP, and ATP,<sup>32, 37, 38</sup> we designed trans-cleaving aptazymes by eliminating the loop of stem III (Figure 3-1A and B). We also weakened stem I and thus product (and substrate) binding by replacing two G-C base pairs with A-U pairs to promote product dissociation. Finally, two overhanging (unpaired) G's were added at the 5'-end for efficient transcription. We designed three substrates for these aptazymes, with different 3' ends, for use in possible multiplexed assays, in which the ability to separate 3' cleavage products would be necessary (Chapter 4). All substrates were labeled with fluorescein on the 3' end (Figure 3-1B-D).

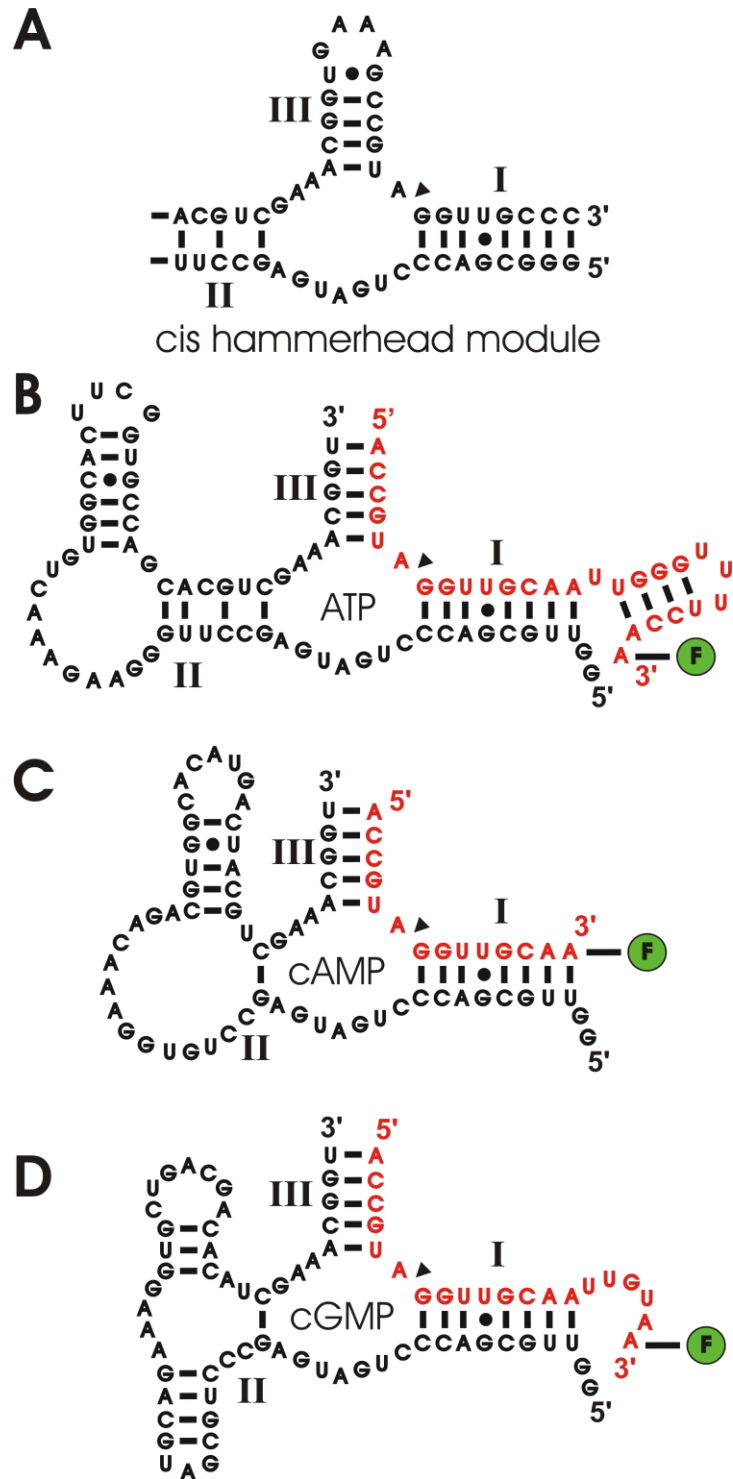
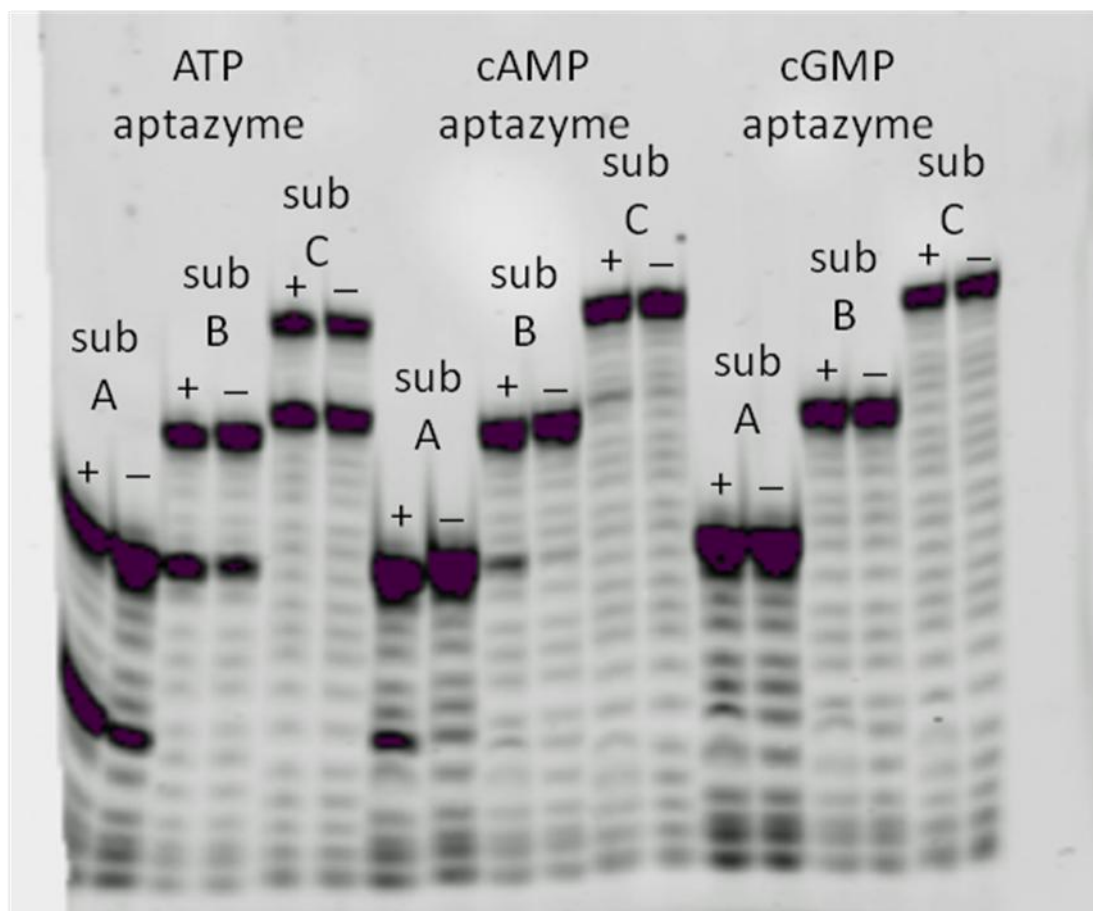


Figure 3-1. Design of trans-cleaving aptazymes. Aptazymes are shown in black and substrates are shown in red. Arrow indicates cleavage site. Substrates are labeled with fluorescein on the 5' end. A. cis-cleaving hammerhead module. B. ATP aptazyme. C. cAMP aptazyme. D. cGMP aptazyme.



**Cleavage of trans-cleaving aptazymes.** In initial experiments, we tested the capability of these constructs to catalyze self-cleavage in response to binding of their respective effector molecules. Due to the method of design of the aptazymes, that is, all used the same hammerhead ribozyme, the binding regions of the substrate molecules were all identical and, thus, interchangeable. As shown in Figure 3-2, the aptazymes for cAMP and ATP cleaved substrates A and B in response to activation by their respective effectors, but the aptazyme for cGMP did not effectively cleave any of the three substrates. None of the aptazymes cleaved substrate C very well, though the ATP aptazyme did show some activation with ATP. The cAMP aptazyme cleaved 26% of substrate A when activated and 11% in the absence of effector, compared to 18% and 7% of substrate B. The ATP ribozyme, on the other hand, activated both substrates equally well. Therefore, we proceeded to characterize the cAMP ribozyme with substrate A and the ATP ribozyme with substrate B. We did not further characterize the cGMP aptazyme.



**Figure 3-2. Cleavage activity of ATP, cAMP, and cGMP aptazymes with each of three substrates. Plus indicates presence of 1 mM effector and minus indicates no effector present.**

**Characterization of trans-cleaving aptazymes.** Aptazyme cleavage is known to be dependent on concentration of divalent and monovalent ions, so we tested cleavage efficiency under a variety of conditions for both aptazymes. Of the conditions tested, the cAMP ribozyme cleaves best at 100 mM MgCl<sub>2</sub> and no KCl, with 28% cleavage in response to effector and 9% in the absence of effector (Figure 3-3A and C). The ATP aptazyme, on the other hand, showed the greatest enhancement in cleavage at 50 mM MgCl<sub>2</sub> and no KCl, with 48% and 30% cleavage with and without effector (Figure 3-3B

and D). At higher concentrations of  $MgCl_2$ , background cleavage is increased while ATP induced cleavage is not. This highlights two important areas that could be addressed in the aptazyme selection process when designing aptazymes to be compatible for a multiplex format. The incompatibility of these aptazymes as a result of their different metal ion dependencies could be addressed by simultaneous selection of aptazymes for use in analytical assays. Additionally, the high background cleavage of the ATP aptazyme might be decreased by adding negative selection steps to remove aptazymes with high background cleavage from the selection pool.

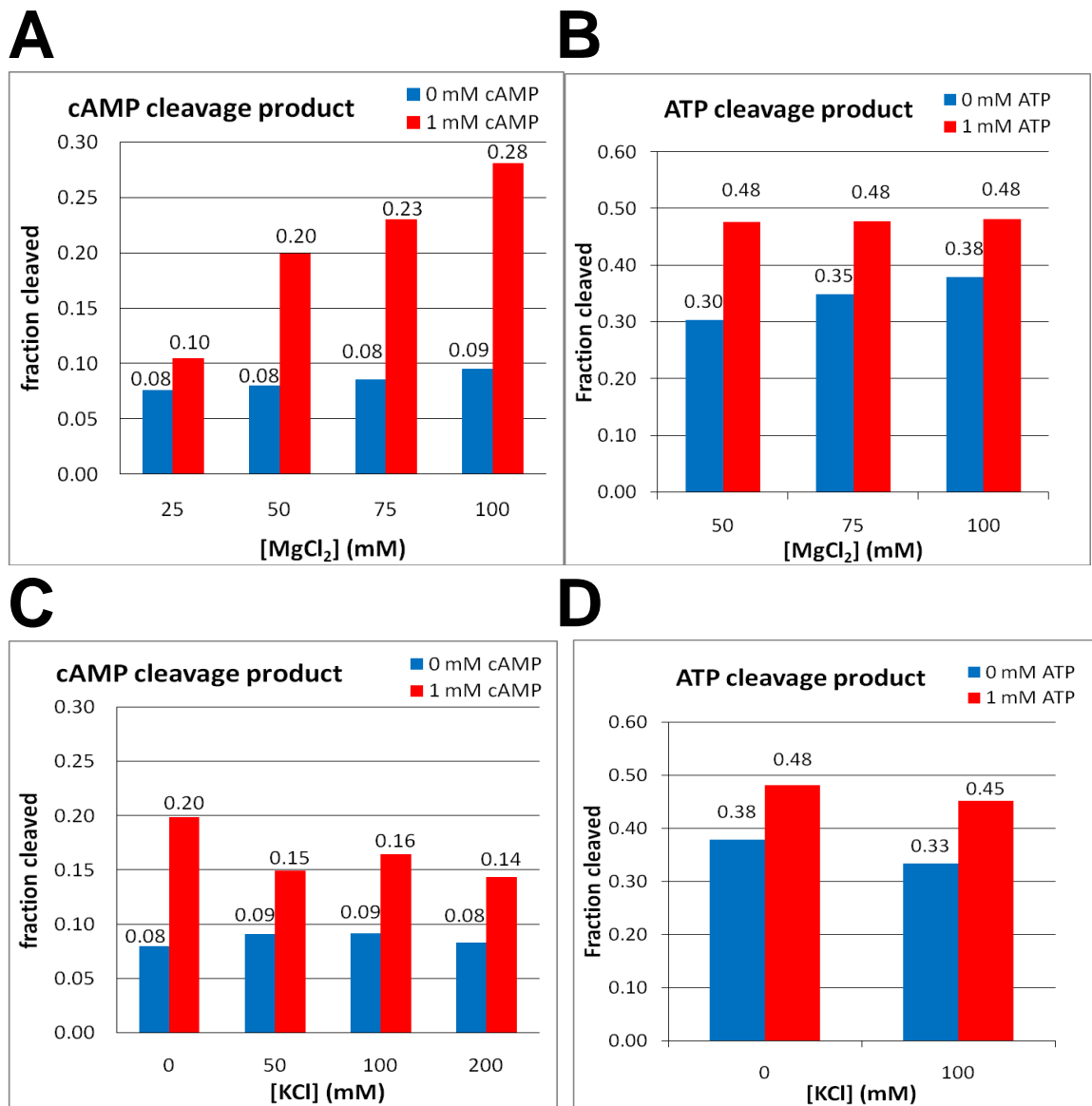


**Figure 3-3. Characterization of ATP and cAMP aptazymes.** A. cAMP aptazyme cleavage at various concentrations of MgCl<sub>2</sub>. B. ATP aptazyme cleavage at various concentrations of MgCl<sub>2</sub>. C. cAMP aptazyme cleavage, KCl characterization. D. ATP aptazyme cleavage, KCl characterization.

With the long-term goal of multiplexing these aptazymes, we considered the compatibility of their reaction conditions. It seemed that the best compromise for both

ribozymes was to use 50 mM MgCl<sub>2</sub> and no KCl, so we tried assays for their respective effectors. The resulting calibration curves demonstrated that while low μM concentrations of effector could be discriminated by the ATP aptazyme, they could not by the cAMP aptazyme. At 100 mM MgCl<sub>2</sub>, however, the cAMP aptazyme could detect low μM concentrations of cAMP (Figure 3-4).

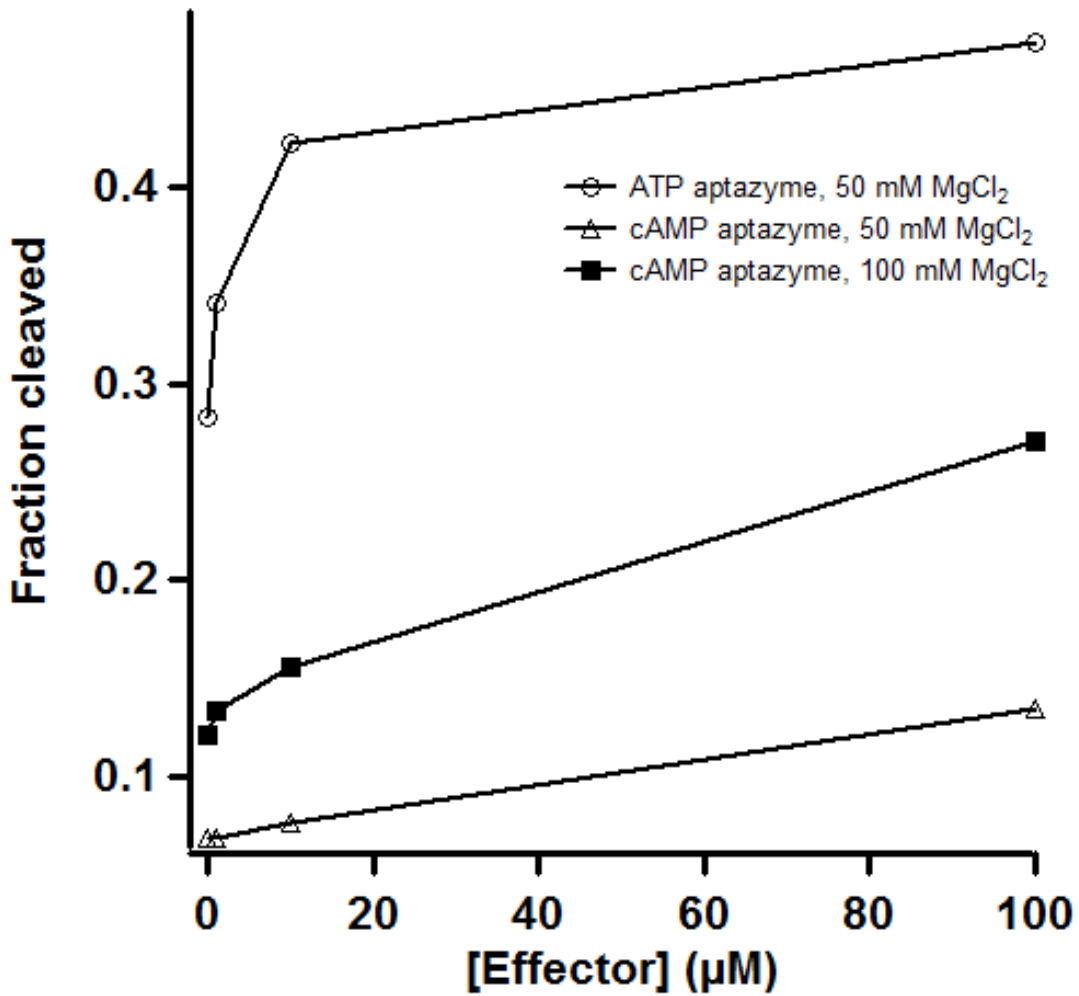


Figure 3-4. Calibration of ATP and cAMP aptazymes. ATP aptazyme cleaves effectively at 50 mM MgCl<sub>2</sub>. cAMP aptazyme is better at 100 mM MgCl<sub>2</sub>.

Another important factor in analyte detection is specificity. We therefore tested the cross-reactivity of the aptazymes with similar compounds. We found that the cAMP aptazyme is not activated by any of the following molecules: ATP, ADP, AMP, or cGMP (Figure 3-5A). In their original aptamer selection, the Breaker group involved many negative selection steps in the evolution of the cAMP aptazyme.<sup>37</sup> The ATP aptazyme, which was generated by a rational design approach with no negative selection steps,<sup>32</sup> is by contrast activated by ADP, AMP, and cAMP, though not by cGMP (Figure 3-5B). These results are consistent with previous work done by the Szostak group, which shows that the ATP aptamer binds to adenosine and AMP with similar affinities as ATP.<sup>61</sup> These results suggest that a careful selection strategy can result in a more specific effector recognition.

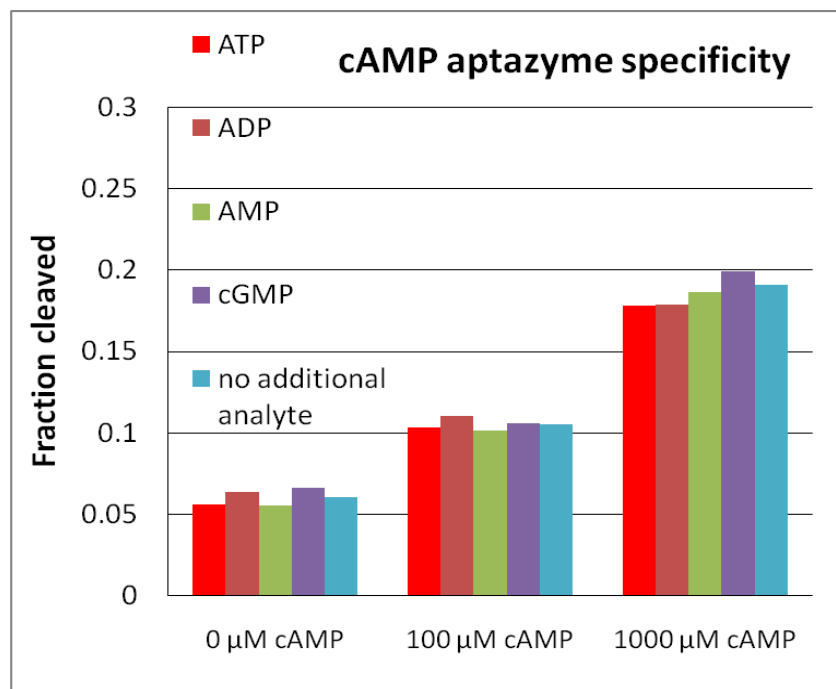
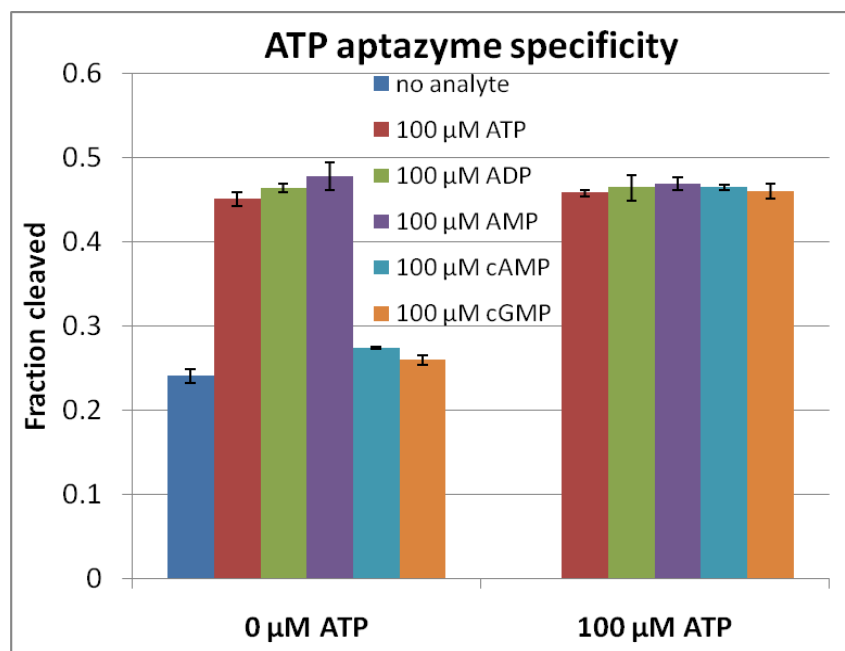
**A****B**

Figure 3-5. Specificity of cAMP and ATP aptazymes. A. cAMP aptazyme is not activated by ATP, ADP, AMP, or cGMP. B. ATP aptazyme is activated by ADP, AMP, and cAMP, but not by cGMP.

To further consider the ATP aptazyme, we compared its activation by ATP and AMP (Figure 3-6). From these data, we can see that the ATP aptazyme is activated by AMP to nearly the same extent as with ATP. A linear regression of the linear portion of the calibration, which is from 0  $\mu\text{M}$  to 10  $\mu\text{M}$  for both effectors ( $R^2$  is 0.999 for ATP and 0.993 for AMP), allows the calculation of the LOD's, which were 3  $\mu\text{M}$  and 2  $\mu\text{M}$  for ATP and AMP, respectively. These results correspond with the demonstrated affinity of the ATP aptamer for other adenosine-containing molecules.<sup>61</sup> Solution structures of the ATP aptamer complexed to AMP reveal that the nucleotide binds in an internal loop. The loop forms a binding pocket which surrounds the AMP molecule, with only the C8 and N7 atoms and the phosphate group exposed to solution. The AMP molecule hydrogen bonds to a G nucleotide.<sup>90, 91</sup> These results suggest that affinity for adenosine is responsible for the broad response of the ATP aptazyme. To develop an aptazyme that would be effective in an analytical assay, the selection conditions for the aptazyme could be improved to include negative selection steps for analytes that are structurally similar, as was done for the cAMP aptazyme.



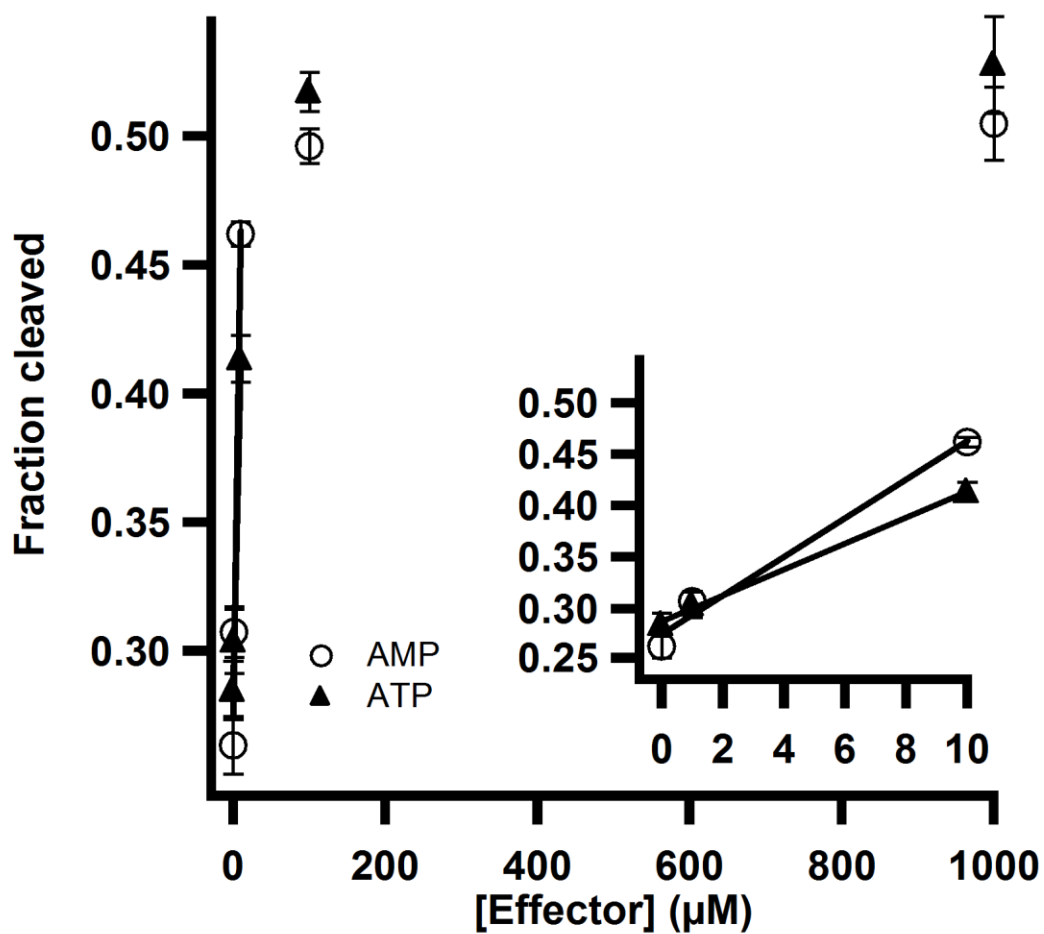


Figure 3-6. ATP aptazyme activation by ATP and AMP. AMP activates aptazyme to nearly the same extent as ATP.

### Conclusions

Aptazymes can be analytically useful molecules as they function both as recognition and transduction elements and can be designed or selected to respond to a wide variety of different molecules. We investigated the cAMP and ATP aptazymes to

evaluate their potential for use in bioanalytical assays. A successful assay will involve aptazymes that are sensitive, specific, and compatible. The cAMP aptazyme is specifically activated by cAMP, is sensitive to low  $\mu\text{M}$  concentrations of cAMP, but is not compatible with the ATP aptazyme, as both buffer conditions and time required for reaction differ. The ATP aptazyme is sensitive to low  $\mu\text{M}$  concentrations of ATP, but activated by a variety of similar molecules including ADP, AMP, and cAMP, which is consistent with data that show that the ATP aptamer binds to adenosine and AMP with similar affinities as ATP.<sup>61</sup> These results suggest that design of selection conditions for an aptazyme intended to be used in bioanalytical assays could be optimized with these desirable characteristics in mind. In particular, aptazymes for use in a multiplex assay could be selected in the same buffer conditions for the same length of time as will be used in the assay. Further, negative selection steps may be necessary to avoid high background cleavage and cross-reactivity.

## CHAPTER 4

### MULTIPLEXED DETECTION OF SMALL MOLECULES BY GEL ELECTROPHORESIS USING APTAZYMES

#### **Introduction**

The ability to simultaneously detect analytes in one assay holds great potential for rapid analysis necessary for detection and characterization of disease states, enzyme function and various high-throughput screening assays. There is potential for use of multiplexed assays in metabolomics and as a clinical panel. Immunoassays have been used for multiplexed detection,<sup>92</sup> as have aptazymes, which are being studied as potential replacements for antibodies in some assay formats. In particular, aptazymes have been arranged into arrays for multiplexed detection.<sup>42, 93</sup> Adding a separation step to an aptzyme assay would eliminate the need for immobilization of the aptazymes to a surface, resulting in an easily transferable assay. Further, it could reduce the sample requirement, because in an array the sample must cover the entire surface, whereas less is required for many separations. In CGE, for example, nL volumes are injected. On the other hand, with a separation, it is necessary to have physically distinguishable cleavage products, which may require redesign of the catalytic domain if the same module is used for multiple aptazymes, whereas in an array format the aptazymes are distinguished spatially. In this chapter, we aimed to develop a multiplexed assay for the aptazymes characterized in Chapters 2 and 3.

The potential of aptazymes lies in the ability to design or select them to be responsive to a wide variety of different analytes. To date, they have been demonstrated to cleave in response to oligonucleotides, small molecules, proteins, and metal ions.<sup>17, 27, 42, 50</sup> For use in a multiplexed assay, each aptazyme would need to be specifically activated by only a single analyte and not related ones. Furthermore, they need to cleave at compatible rates under the same conditions have cleavage products that can be distinguished by the analytical method used. For example, products of different lengths could be used with detection by PAGE, CE, or fluorescence anisotropy or products with different fluorescent labels could be used with fluorescence detection.

Three aptazymes that we will consider herein included one naturally occurring aptazyme, the *glmS* ribozyme; one rationally designed aptazyme, the ATP aptazyme; and one in vitro selected aptazyme, the cAMP aptazyme.<sup>28, 32, 37</sup> Assays for GlcN6P with detection by the *glmS* ribozyme could involve the study of development of insulin resistance in cells, as increased GlcN6P flux into the hexosamine pathway has been shown to result in impaired ability of insulin to stimulate glucose uptake.<sup>56</sup> Assays for ATP can be used to determine cell viability and to study cellular processes in which ATP is involved, which include biosynthetic reactions and signal transduction pathways. Detection of cAMP can be used to study signal transduction and enzyme activity. We set out to pursue proof-of-principle studies to demonstrate the potential of aptazymes in multiplexed analyte detection.

We describe the multiplexing of two pairs of trans-cleaving aptazymes, for ATP and cAMP as well as for GlcN6P and ATP. We consider their rates of cleavage, an optimization of their cleavage conditions, and their compatibility for multiplexed

detection. These initial studies were done with gel electrophoresis, which has been the workhorse for detection of ribozyme cleavage, and can offer parallel detection by separating many samples on one gel. We use fluorescently labeled RNA, eliminating the need for radiochemicals.

### **Experimental Section**

**Chemicals.** Unless stated otherwise, all chemicals were purchased from Sigma-Aldrich Co. (St. Louis, MO). DNA templates were purchased from Invitrogen (Carlsbad, CA). RNA substrates were purchased from W. M. Keck Foundation (New Haven, CT). See Figures 2-1 and 4-1 for sequences. All solutions were prepared with deionized water from an E-Pure water purification system (Barnstead International Co., Dubuque, IA). T7 RNA polymerase was expressed and purified according to the protocol in Appendix B.

**Preparation of aptazymes.** Complementary DNA strands were annealed at 70 °C for 2 min and cooled to room temperature over 5 min. RNA was transcribed from this DNA template at 37 °C in an overnight reaction using the following reagent concentrations: 100 nM DNA templates; 2 mM NTP mixture; 120 mM HEPES-KOH, pH 7.5; 30 mM MgCl<sub>2</sub>; 2 mM spermidine; 40 mM DTT; 0.04% triton X-100; 0.005 U/μL; 0.1 mg/mL T7 RNA polymerase; and 8% polyethylene glycol. The reaction was purified on a 10 % polyacrylamide gel and eluted overnight in water, then chloroform extracted and ethanol precipitated. RNA substrates were deprotected according to the manufacturer protocol, precipitated with butanol, purified by 15 % PAGE, eluted by tumbling overnight in water, chloroform extracted, ethanol precipitated, and HPLC

purified. The concentrations of nucleic acid samples were determined using their absorbance at 260 nm.

**Cleavage reactions.** ATP and cAMP aptazyme cleavage reactions were performed under the following conditions: 150 nM aptazyme; 75 nM substrate; 50 mM Tris-HCl, pH 7.5; 50 mM MgCl<sub>2</sub>, and 25 mM DTT, 1 mM effector. The ribozyme and substrate strands were annealed (each aptazyme separately) at 90 °C for 2 min, then cooled to room temperature over 5 min. The reaction took place at room temperature for 2 h. ATP aptazyme and *glmS* ribozyme cleavage reactions were performed under the following conditions unless otherwise noted: 150 nM aptazyme; 75 nM substrate; 50 mM HEPES-KOH, pH 7.5; 200 mM KCl; 50 mM MgCl<sub>2</sub>; 25 mM DTT; 100 μM ATP; and 10 μM GlcN6P. The ribozyme and substrate strands were annealed (each aptazyme separately), ATP aptazyme at 90 °C and *glmS* ribozyme at 70 °C for 2 min, then cooled to room temperature over 5 min. The reaction took place at room temperature for 20 min. Reactions were separated by 20 % PAGE at 20 W for 2 hr and analyzed on a Typhoon Trio (GE Healthcare, Piscataway, NJ) using fluorescence detection with excitation at 488 nm and detection at 530 nm and the platen focal depth setting, with the gel placed directly on the glass platen. Gel scans were analyzed with ImageQuant, dividing the intensity of the product band by the sum of the intensities of the product and substrate bands.

## Results and Discussion

**Design of trans-cleaving aptazymes.** Based on cis-cleaving constructs of aptazymes for cAMP and ATP, we designed trans-cleaving aptazymes by eliminating the

loop of stem III (Chapter 3, Figure 3-1). We designed three substrates for these aptazymes, with different 3' ends in order to multiplex our assay, so that the ability to separate 3' cleavage products would be necessary. All substrates were labeled with fluorescein on the 3' end (Chapter 3, Figure 3-1B-D).

**Multiplex of cAMP and ATP aptazymes.** We have previously demonstrated that the ATP and cAMP aptazymes have some experimental incompatibility for a multiplexed assay. Namely, the ATP aptazyme cleaves faster than the cAMP aptazyme and at a lower MgCl<sub>2</sub> concentration. Furthermore, though the cAMP aptazyme is not activated by ATP, the ATP aptazyme is activated by cAMP. One further complication is rooted in their design. Because they were both designed with the hammerhead ribozyme as the catalytic portion of the molecule, their substrate is interchangeable. Nevertheless, we tested whether they could serve in a qualitative assay for simultaneous detection of cAMP and ATP. We annealed them separately before mixing them and adding effector in an effort to reduce substrate exchange. After reacting for 2 h, they were separated by PAGE (Figure 4-1).

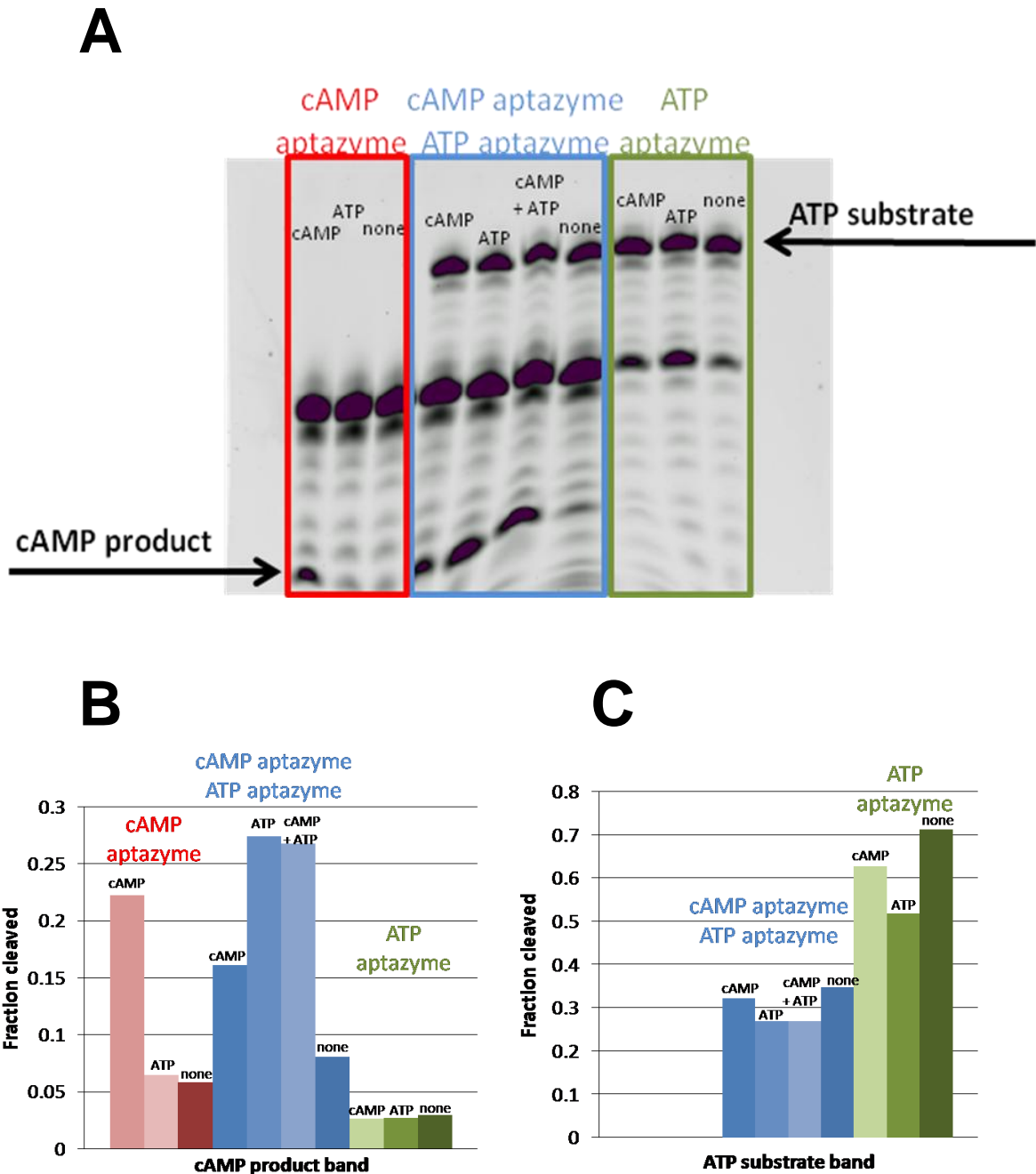


Figure 4-1. Multiplexed detection of ATP and cAMP. A. PAGE of multiplex assay. B. Bar graph representing increase in cAMP aptazyme product band upon effector mediated cleavage. C. Bar graph representing decrease in ATP aptazyme substrate band upon effector mediated cleavage. Effector is listed above bars.



In response to cAMP, the cAMP aptazyme is activated, whereas the ATP aptazyme is not. This can be seen in Figure 4-1B, in which the cAMP aptazyme is represented in shades of red, and the ATP aptazyme in shades of green. The cAMP aptazyme is not activated in response to ATP, as represented by the red bars. When the two aptazymes were mixed for multiplexed detection, addition of cAMP resulted in a product band that was less intense than with cAMP aptazyme alone (Figure 4-1B, blue bars). ATP also results in a cleavage product resulting from cleavage of the cAMP substrate. As the cAMP aptazyme is not activated by ATP, these results suggest that substrate exchange occurs between the aptazymes at room temperature.

Thus, we have developed a multiplexed experiment to qualitatively detect ATP and cAMP with their aptazymes. Due primarily to cross-reactivity and substrate exchange, this assay is not quantitative. These inherent challenges to detection could be addressed at the onset of an aptazyme design experiment by applying appropriate selection conditions for the desired outcome. These preliminary experiments for multiplexing these aptazymes by gel electrophoresis show promise for future assays.

Thus, we have developed a multiplexed experiment to qualitatively detect ATP and cAMP with their aptazymes. Due primarily to cross reactivity and substrate exchange, this assay is not qualitative. These inherent challenges to detection could be addressed at the onset of an aptazyme design experiment by applying appropriate selection conditions for the desired multiplex outcome. Our current preliminary results for multiplexing these aptazymes coupled with analysis by gel electrophoresis show promise for future assays.

**Multiplex of ATP and *glmS* aptazymes.** We decided to investigate a second pair of aptazymes for multiplex potential, which are not expected to suffer from cross reactivity and that cleave under similar reaction conditions. They do not have similar substrate binding regions, therefore, substrate exchange is not expected to be a problem. These aptazymes were annealed separately and mixed before adding effectors and reacting for 20 min. Substrates and products were then separated by PAGE (Figure 4-2).

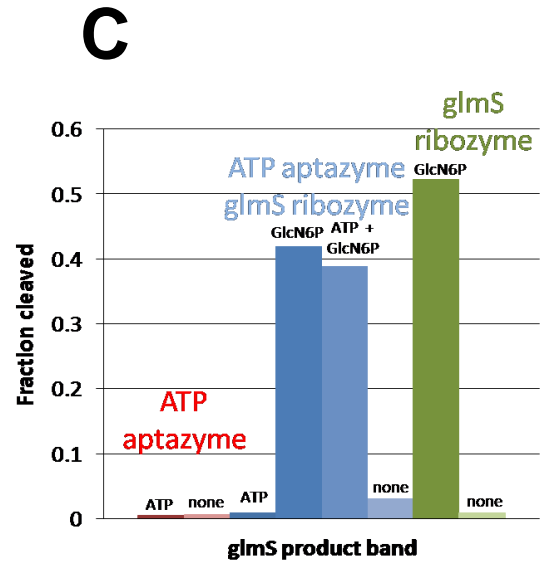
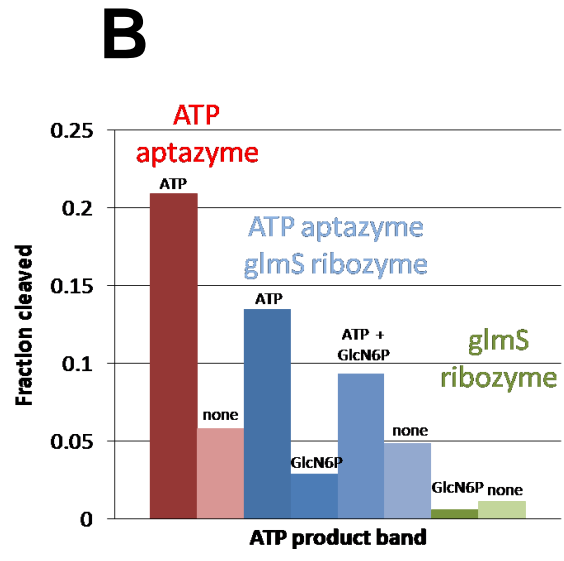
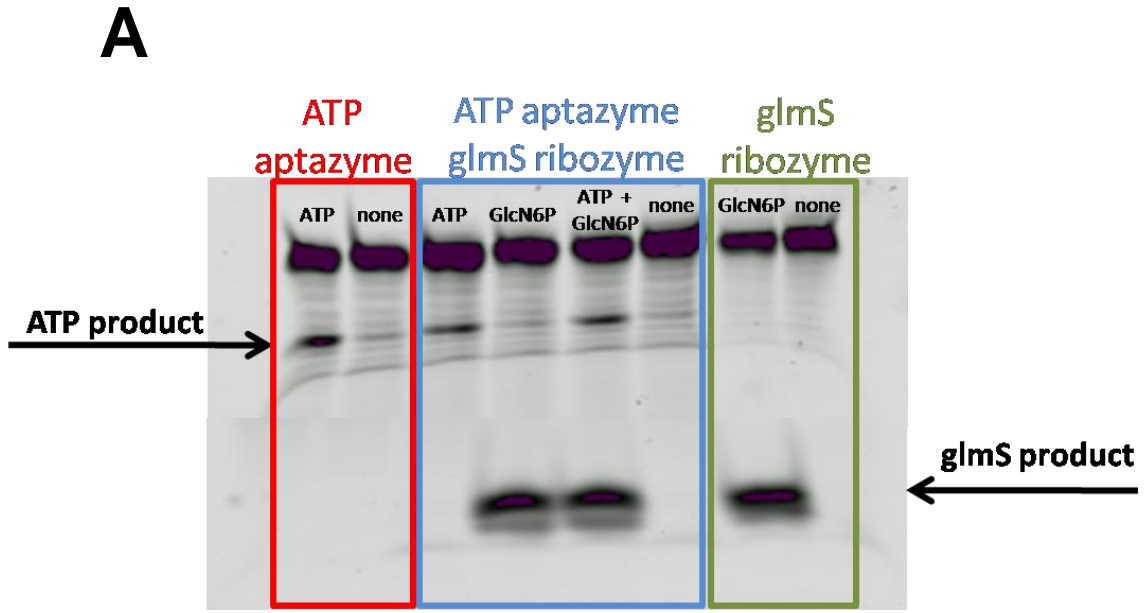


Figure 4-2. Multiplexed detection of ATP and GlcN6P. A. PAGE of multiplex assay. B. Bar graph representing increase in ATP aptazyme product band upon effector mediated cleavage. C. Bar graph representing increase in glmS ribozyme product band upon effector mediated cleavage. Effector is listed above bars.

As illustrated in Figure 4-2, the ATP aptazyme is not activated by GlcN6P (Figure 4-2B, red bars), nor is the *glmS* ribozyme activated by ATP (Figure 4-2C, green bars). There is no evidence for substrate exchange. When the aptazymes are mixed for multiplexed detection (blue bars), both analytes are detected, though the total fraction of aptazyme cleaved is lower than in the single aptazyme experiments. Furthermore, the fraction cleaved is even lower when both analytes are present. Nonetheless, we tried an assay for ATP and GlcN6P (Figure 4-3), in which both analytes were detected simultaneously by both aptazymes. The calibration curves for both analytes are linear at low  $\mu\text{M}$  concentrations of analyte, 0  $\mu\text{M}$  to 10  $\mu\text{M}$  for ATP and 0  $\mu\text{M}$  to 1  $\mu\text{M}$  for GlcN6P. The LOD's are 1  $\mu\text{M}$  for ATP and 40 nM for GlcN6P.

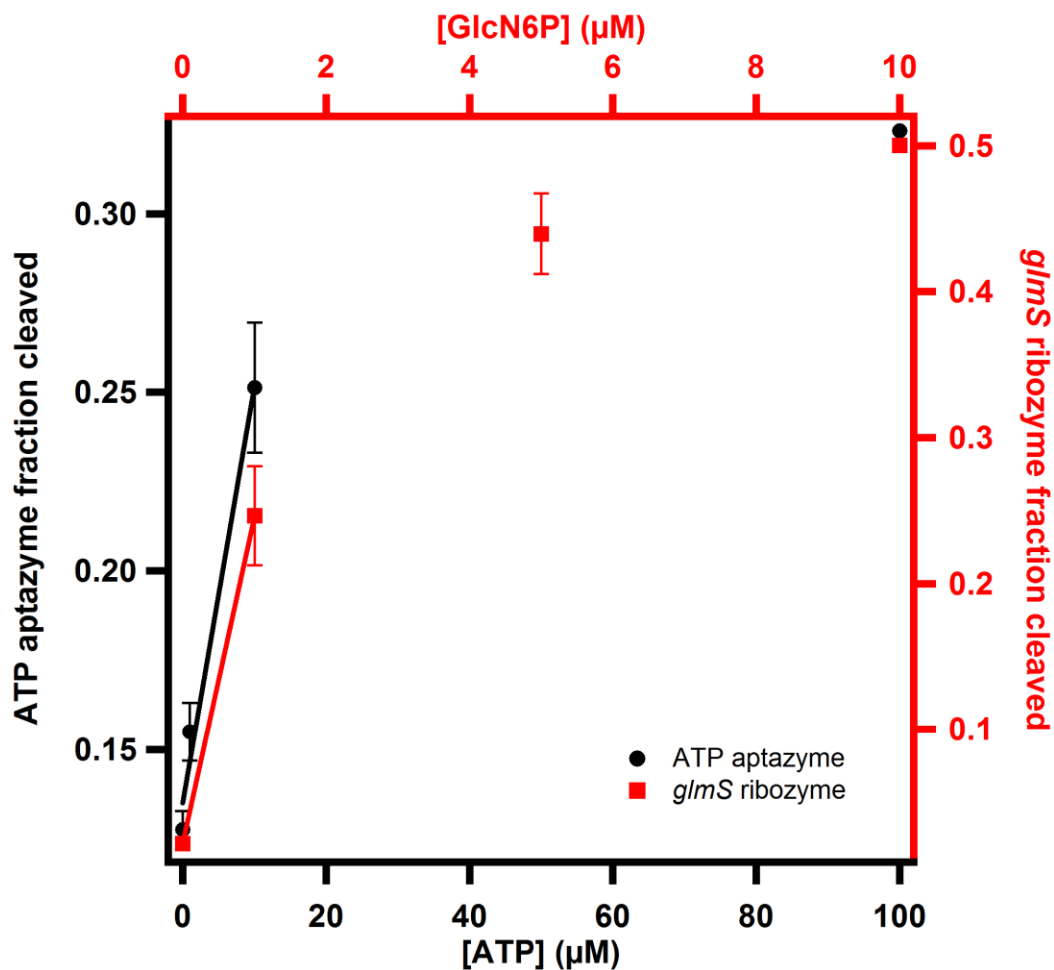


Figure 4-3. Calibration curve for multiplexed assay of ATP (●) and GlcN6P (■).

## Conclusions

We have demonstrated potential for multiplexing aptazymes with PAGE detection. ATP and cAMP can be qualitatively detected using the ATP and cAMP aptazymes. The *glmS* ribozyme and ATP aptazyme are more compatible for a multiplexed format, and can be detected at low  $\mu\text{M}$  concentrations in a multiplexed assay. Design of aptazyme

selection conditions could be changed to design aptazymes that address the potential problems of cross-reactivity and differential reaction conditions and times. The analysis time could be improved by moving to a CGE system, which would also reduce preparation time, buffer and sample consumption, as well as improve peak quantitation and be amenable to parallel analysis.

## CHAPTER 5

### SUMMARY AND FUTURE DIRECTIONS

#### Summary

This thesis has aimed to consider the role of nucleic acids for use in analytical assays. In particular, we have focused on aptazymes for effector detection. We have used three different aptazymes, *glmS*; cAMP; and ATP, and three different methods of detection, FRET; CE; and PAGE. Aptazymes are appealing candidates for analytical assays because they can perform both analyte recognition as well as transduction of analyte binding to a detectable signal. Furthermore, their often modular nature allows for design and selection of aptazymes to a multiplicity of targets, opening their potential to a broad range of molecules. The application of aptazymes in analyte detection is a relatively open field, with much territory available for exploration.

**Assays for GlcN6P using the *glmS* ribozyme.** The *glmS* ribozyme is a natural aptazyme that cleaves in response to the effector molecule GlcN6P, resulting in the degradation of the ensuing mRNA. This aptazyme is unique in its role as a metabolite sensitive genetic regulator, as the only one found in nature to date. In bacteria, GlcN6P is used as a precursor to cell wall biosynthesis; preventing its synthesis could lead to cell death. Thus, the *glmS* ribozyme is a potential target for antibiotic activity, and could be used for high-throughput screening in pharmaceutical development. GlcN6P is also involved in the hexosamine biosynthetic pathway, which is ubiquitous in all organisms.<sup>55</sup>

Increased flux of GlcN6P into this pathway has been shown to result in impaired ability of insulin to stimulate glucose uptake.<sup>56</sup> Detailed characterization of this pathway could lead to insight into a mechanism of development of insulin resistance in cells. Several methods have been developed for monitoring GlcN6P formation in this pathway, and though some are sensitive to pmol concentrations of GlcN6P,<sup>57</sup> they all require multiple derivatization steps and/or radioactivity. Ideally a detection method uses a minimal amount of sample, is fast, can be run in parallel or in array formats, and does not require elaborate design of the reagents.

In this work, we developed several *glmS* ribozyme-based FRET and CE assays for the detection of GlcN6P. In the trans-cleaving model, an external substrate is added to the *glmS* ribozyme and GlcN6P activated cleavage results in three RNA molecules: the cleavage product, a three nucleotide molecule; the cleaved substrate at eight nucleotides; and the unchanged ribozyme molecule, which is twenty three nucleotides in length.<sup>51</sup> We first monitored the kinetics of this single-turnover cleavage reaction by FRET to obtain an assay for GlcN6P based on the rate of the cleavage reaction. As 3' cleavage product (fluorescein labeled) was produced and moved away from the 5' product (tetramethylrhodamine labeled), donor fluorescence increased until the reaction slowed, resulting in a plateau in fluorescence intensity. The rate of the cleavage reaction,  $k_{obs}$ , can be obtained by fitting the increase with a one-component exponential association function. A linear regression of reaction rates versus concentration of GlcN6P results in an LDR of 0.5  $\mu$ M to 500  $\mu$ M and an  $R^2$  of 0.999. The LOD is 800 nM.

We wanted to add a separation step to the *glmS* ribozyme cleavage assay to create an assay for GlcN6P present based on the amount of cleavage product formed. First, we



monitored the ribozyme kinetics by injecting samples every 12.5 s into a high-speed CE-LIF instrument, separating substrate from product in less than 10 s. The product peak heights were normalized and fit with a one-component exponential association function, reporting reaction rates that were comparable to those obtained by FRET. In our free-resolution CE assay, we have an LDR of 0.5  $\mu\text{M}$  to 100  $\mu\text{M}$  ( $R^2$  is 0.998), as the calibration curve plateaus at lower concentrations than the rate-based FRET curve. At higher concentrations of GlcN6P, the reaction has reached completion, thus different concentrations are indistinguishable. This assay has a lower LOD (500 nM) than the FRET assay.

We hoped to further improve the assay by using multiple-turnover kinetics for the aptazyme reaction. In principle, this approach would lead to more signal for each effector molecule as the ribozyme cleaved multiple substrates. In practice, the 5' product is complementary to the ribozyme with as many nucleotide pairs as the uncleaved substrate (19). The data suggest that at temperatures below 50  $^{\circ}\text{C}$ , the 5' product does not dissociate from the ribozyme efficiently but that at 50  $^{\circ}\text{C}$ , the ribozyme-substrate binding reaction reaches equilibrium. At this temperature, the donor fluorescence signal is 2-fold greater after 40 min than the same reaction at 42  $^{\circ}\text{C}$ . The LDR for the multiple-turnover CE assay (at 50  $^{\circ}\text{C}$ ) is the same as the single-turnover CE assay (0.5  $\mu\text{M}$  to 100  $\mu\text{M}$ ,  $R^2$  is 0.995), but the LOD is improved to 100 nM.

The above results suggested that a two temperature cycle designed with one temperature (42  $^{\circ}\text{C}$ ) to allow catalyzation of the cleavage reaction followed by a second temperature for substrate dissociation (60  $^{\circ}\text{C}$ ) may further enhance signal amplification. Indeed, this is what we observed. After 40 m, the signal is 4-fold greater than the same

reaction at 42 °C and 2-fold greater than at 50 °C. The temperature-cycled, multiple-turnover CE assay has the same LDR as the other CE assays (0.5 μM to 100 μM,  $R^2$  is 0.999), with further improvement in LOD, to 50 nM.

Both the FRET and CE methods appear to be useful for monitoring the *glmS* ribozyme cleavage reaction. For kinetic measurements, the FRET reaction achieves a 1 s temporal resolution compared to the 12.5 s possible by the CE-LIF method, which was crucial for gaining an understanding of the multiple-turnover cleavage reaction. As an assay, the FRET method has a wider dynamic range; primarily because it was based on kinetic data rather than a fixed time point like the CE-LIF method. For the same reason, the CE method was much faster, with each sample taking only seconds to analyze after completion of the cleavage reaction, rather than minutes or hours. The CE method uses less analyte with sample volumes as low as 10 μL compared to 150 μL FRET samples. The LOD was improve from 800 nM for single-turnover FRET to 500 nM for single-turnover CE, and improved further by multiple-turnover conditions at 50 °C, 100 nM, and cycled between 42 °C and 60 °C, 50 nM.

**Characterization of the ATP and cAMP aptazymes.** As the *glmS* ribozyme, a natural aptazyme, was effective in assays for GlcN6P, we wanted to investigate the potential of non-natural aptazymes. These are especially appealing because they often have a modular nature, which allows for domain swapping. That is, aptazymes have been broken into three domains, which are binding; communication; and catalytic domains, and they have be separated, swapped, and reassembled into new aptazymes. Aptamers have been used as the binding domains in some cases. Thus, there already is a resource of known potential binding domains that could be tested with known

communication and catalytic domains for aptazyme function, as well as potential for evolving novel domains. Adding a selection step after assembly (or to a random sequence) can lead to aptazymes that possess user-defined characteristics. This research demonstrates the utility of such selection by comparing two aptazymes that were designed differently.

The Breaker group used rational design to design an aptamer for ATP by coupling an RNA aptamer to the hammerhead ribozyme via a variable communication domain.<sup>32</sup> The ATP aptamer has a  $K_d$  of 0.7  $\mu\text{M}$ , and binds to adenosine and AMP with similar affinities.<sup>61</sup> The same group developed an aptazyme that responds to cAMP by applying an allosteric selection scheme to a hammerhead ribozyme that was coupled to a 25 nucleotide random sequence domain via a previously characterized communication domain.<sup>37</sup> The selection involved both positive and negative selection steps, selecting for aptazymes that were specifically activated by cAMP and not other cNMP's and that had low background cleavage. The apparent dissociation constant for this aptazyme was determined to be 500  $\mu\text{M}$  by measuring the half maximal cleavage activity.<sup>38</sup>

We began by designing trans-cleaving aptazymes from the cis-cleaving molecules developed by the Breaker group. We used PAGE with fluorescence detection to characterize the trans-cleaving ATP and cAMP aptazymes. Both aptazymes were developed using the hammerhead ribozyme for the catalytic domain, so the binding regions of the substrate molecules were all identical and, thus, interchangeable. We designed the substrates for these aptazymes with different 3' ends so that they could be separated in multiplexed experiments. All substrates were labeled with fluorescein on the 3' end. Characterizing the cleavage reactions of the aptazymes revealed some

incompatibilities for a multiplexed reaction. They gave the best response to effector at different reaction conditions, and the ATP aptazyme cleaved much faster than the cAMP aptazyme. Furthermore, though the cAMP aptazyme was not activated by ATP, ADP, AMP, or cGMP, the ATP aptazyme was activated by ADP, AMP, and cAMP. During selection, the cAMP aptazyme was put through several negative selection steps, including some to reduce cross-reactivity. These results suggest that development of aptazymes for multiplexed assays could be tailored to meet the specific needs of an assay, like the multiplexed assay that we investigated, by selecting molecules that cleave under the same reaction conditions, reducing cross-reactivity with negative selection steps, and selecting aptazymes that cleave at the same rate.

The ability to simultaneously detect analytes in one assay holds great potential for rapid analysis necessary for detection and characterization of disease states, enzyme function and various high-throughput screening assays. There is potential for use of multiplexed assays in metabolomics and as a clinical panel. Despite the above incompatibilities, we were interested in trying to multiplex the ATP and cAMP aptazymes in a proof-of-principle assay to help inform future aptazyme design for multiplexed assays. With separation by PAGE and fluorescence detection, a qualitative measure of the presence of cAMP and ATP was achieved. Both cross-reactivity and substrate exchange hindered the development of a quantitative assay, but these results encouraged us to try another system.

The *glmS* ribozyme and ATP aptazyme do not have exchangeable substrates and do not show any cross-reactivity. Their optimal reaction conditions are compatible, though the *glmS* ribozyme cleaves somewhat faster than the ATP aptazyme. In the

multiplexed assay, the linear region was from 0  $\mu\text{M}$  to 10  $\mu\text{M}$  for ATP and 0  $\mu\text{M}$  to 1  $\mu\text{M}$  for GlcN6P. The LOD's were 1  $\mu\text{M}$  and 40 nM for ATP and GlcN6P, respectively. These data demonstrate the feasibility of a at least somewhat quantitative multiplexed assay using aptazymes as recognition and transduction elements.

Overall, this thesis demonstrates the utility of aptazymes in a variety of assays for the detection of three small molecules: GlcN6P, ATP, and cAMP. FRET-based detection offered the advantage of 1 s temporal resolution for observing the *glmS* ribozyme cleavage reaction. CE has the advantages of fast separations, low sample and reagent consumption, and good quantitation. Multiple-turnover kinetics resulted in signal amplification and lowered the LOD of the assay. Multiplexed assays demonstrated the potential for simultaneous, multi-analyte detection.

### **Future Directions**

We have demonstrated the potential of aptazymes to serve as recognition and transduction elements in analytical assays. Based on our current results, it seems promising that aptazyme-based assays could be improved and applied to a broad range of molecules.

**Multiple-turnover cleavage reactions of the *glmS* ribozyme.** In our multiple-turnover reactions with the *glmS* ribozyme, we observed that it was necessary to elevate the reaction temperature to achieve multiple substrate turnovers. The results of a temperature titration suggested that the 5' product was not efficiently dissociating from the ribozyme at the reaction temperature. Further evidence came from temperature

cycled experiments, in which the ribozyme was alternately incubated at reaction and dissociation temperatures resulting in substrate turnover and signal amplification.

Another potential method for achieving multiple turnovers with the *glmS* ribozyme could involve redesign of the substrate to reduce the base pairing between substrate and ribozyme. This would reduce the binding interaction between those molecules and lower the temperature at which equilibrium would be expected. As we saw with our cGMP aptazyme, changes in aptazyme structure may interfere with the cleavage reaction, so many *glmS* ribozyme variants may need to be designed in order to achieve reduced binding while retaining catalytic functionality. A successful design could eliminate the need for an elaborate system of temperature cycling in the assay.

**Structure-function relationship of the cAMP and ATP aptazymes: trans versus cis.** In comparison to its cis-cleaving predecessors, the trans-cleaving cAMP aptazyme described in Chapters 3 and 4 requires a higher MgCl<sub>2</sub> concentration and longer incubation times and still does not catalyze effector mediated cleavage reactions as well. Upon activation by 500 μM cAMP, the cis-cleaving aptazyme cleaves to greater than 35% completion after 40 min in buffer containing 20 mM MgCl<sub>2</sub>,<sup>37</sup> whereas our trans-construct cleaves to less than 30% completion upon activation by 1 mM cAMP after 2 h in buffer containing 100 mM MgCl<sub>2</sub>. These results suggest that the change in structure of the aptazyme led to reduced catalytic ability. Perhaps the transition from an intramolecular reaction to an intermolecular reaction leads to reduced catalytic efficiency. The cGMP aptazyme, which we find does not cleave in trans under any conditions that we have tested though its cis-cleaving counterpart cleaves effectively, seems to corroborate this hypothesis

Our trans-cleaving ATP aptazyme, on the other hand, may cleave more rapidly than the cis-cleaving version, though more investigation into this is necessary, as we have not tested comparable cleavage conditions to the original paper. They see a 40-fold activation of the aptazyme by ATP in 20 mM MgCl<sub>2</sub> with 1 mM ATP, from a cleavage rate in the absence of effector of 0.000042 s<sup>-1</sup> to 0.0017 s<sup>-1</sup> when ATP is added. We see a 4-fold activation with 1 mM ATP and 50 mM MgCl<sub>2</sub>, with an increase in rate of cleavage from 0.21 s<sup>-1</sup> to 0.92 s<sup>-1</sup>. Background cleavage of the trans-cleaving construct is higher than the cis-cleaving, and effector activation results in a smaller enhancement in the rate of cleavage. Further study of this aptazyme may reveal that the high background is due to the higher concentration of MgCl<sub>2</sub>, which is known to cause RNA degradation.

Testing several different trans-cleaving versions of the same aptazyme could help elucidate whether the cause of the change in cleavage efficiency can be explained by the separation of the aptazyme into two molecules. Additionally, it may demonstrate what role, if any, the nucleotides removed play in modulating activity in the ATP, cAMP, and cGMP aptazymes. Further investigation into this interesting area may also more generally inform trans-cleaving aptazyme design.

**CGE multiplex assays.** The multiplex assays in Chapter 4 were analyzed by PAGE with fluorescence detection, which was useful for analyzing a large number of samples in parallel. The use of fluorescent labeling was an improvement over radiochemical detection by eliminating the need for radiochemicals, thereby increasing the lifetime of the samples, and simplifying sample handling. Nevertheless, PAGE is a laborious process that consumes a lot of reagents and has relatively poor quantitation.

CGE is widely used for the separation of nucleic acid molecules and has been used to observe ribozyme cleavage.<sup>66</sup> CGE has many advantages over PAGE including higher resolution, higher sensitivity, shorter analysis time, better quantification, less reagent consumption, and ease of automation. Thus, these assays could be simplified by moving to a CGE format for separation and detection.

To maintain (and increase) the parallel nature of the PAGE analysis, the assay could be adapted to capillary array systems,<sup>94, 95</sup> which are commercially available. To miniaturize the instrument and further reduce sample and buffer consumption, microfluidic devices which are capable of parallel separations could be adapted to the assay. Ribozyme cleavage reactions have previously been monitored on a microchip with overlapping, automated capillary injections.<sup>67</sup>

**Application of assays to real samples.** As an analyte, GlcN6P is potentially interesting in at least two different systems. In bacteria, GlcN6P is a precursor in cell wall biosynthesis. Therefore, identification of compounds that could activate *glmS* ribozyme cleavage and potentially inhibit cell wall biosynthesis could be advantageous in drug discovery. The *glmS* ribozyme is highly conserved in genomes of some bacterial pathogens, like *Bacillus anthracis* and *Staphylococcus aureus*, making it a relevant detection target.<sup>54</sup> GlcN6P is involved in the hexosamine biosynthetic pathway and increased flux into this pathway has been shown to result in impaired ability of insulin to stimulate glucose uptake.<sup>56</sup> Detailed characterization of this pathway could lead to insight into a mechanism of development of insulin resistance in cells. Thus, the application of the GlcN6P assays to real samples could be relevant for drug discovery or insulin resistance in cells.



Application of this assay to biological samples may require the use of non-natural bases. RNA can be degraded in nature, so in some cases, non-natural bases have been used to alleviate this problem.<sup>1</sup>

**Design/select new aptazymes for interesting molecules.** After addressing some of the remaining questions surrounding the aptazyme assays we have developed, novel aptazymes could be selected for use in other assays. The power of aptazymes as analytical tools lies in their versatility. In principle, the ability to couple (or evolve) binding to catalyzing function allows the targeting of any molecule. Given the results of Chapters 3 and 4, aptazymes could be designed with a random regions connected to ribozyme domains and put through a series of negative and positive selection steps. In this selection scheme, buffer conditions and time allowed for selection could be chosen to reflect assay conditions. Negative selection steps could be aimed at both reducing background cleavage as well as reducing cross-reactivity with molecules that are structurally similar to the target molecule. It would be interesting to learn whether parallel aptazyme selection aimed at developing aptazymes for multiplex assays would be successful in producing compatible aptazymes.

Further, incorporation of a different ribozyme module in the rational design of new aptazymes may result in faster cleavage, as has recently been demonstrated with a full-length hammerhead ribozyme in an aptazyme for theophylline.<sup>96</sup> One of the selected aptazymes cleaves at a rate of  $8 \text{ min}^{-1}$ . In an assay, this increase in rate of cleavage could lower the LOD and increase the sensitivity.

The assays developed in this thesis demonstrate the potential of aptazymes in analytical assays. Further development is necessary to increase specificity and sensitivity. Additionally, the development of novel aptazymes will enhance their applicability in detecting biologically interesting compounds.

## APPENDIX A

### SELECTIVE EVOLUTION OF LIGANDS BY EXPONENTIAL ENRICHMENT (SELEX)

#### **Introduction**

Advances in understanding the complexity of cellular mechanisms depend upon methods that can quantify affinity interactions between biological molecules. Additionally, fields such as chemical biology and drug discovery require methods for identifying molecules that can probe these affinity interactions. Aptamers or nucleic acids molecules that have been evolved to have non-natural binding interactions with targets of interest can be involved in methods for quantifying affinity interactions and screening for bioactive molecules.

Aptamers are artificial, specific oligonucleotides that bind target molecules. Their sensitive and specific binding characteristics make them useful candidates for diagnostic, therapeutic, and analytical applications. Aptamers are obtained through selective evolution of ligands by exponential enrichment (SELEX), a combinatorial ligand discovery process that evolves large, synthetic libraries of random sequence nucleic acid molecules in order to isolate ligands with high affinity and specificity to molecular targets.<sup>2</sup> An oligonucleotide library is exposed to the target of interest, and subsets of sequences that have affinity are partitioned from those sequences with little or no affinity. The process is iterative, typically involving ten to fifteen rounds of selection with increasing stringency and ending when a set of ligands with the desired binding

characteristics is obtained. This set of ligands is cloned into bacterial plasmids and individual sequences determined by sequencing. The isolated ligands are termed aptamers. SELEX has been used to isolate molecules to a broad range of targets, from small molecules to large proteins.

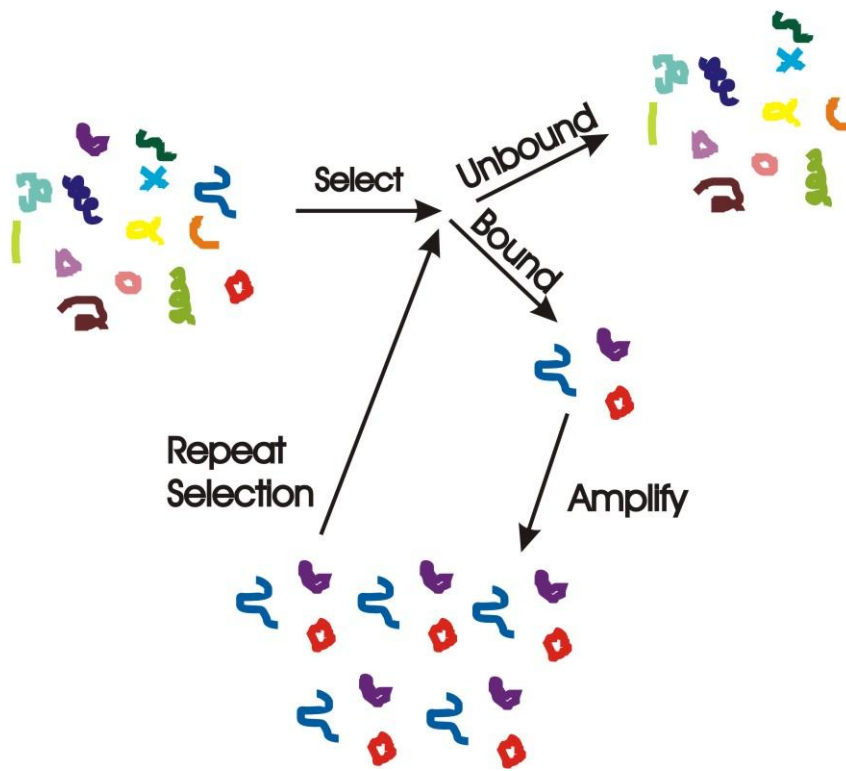


Figure A-1. SELEX.

A typical SELEX library contains  $10^{14}$  to  $10^{16}$  different nucleic acid sequences. Each molecule consists of a segment of random sequence flanked by primer binding sites at each end for enzymatic amplification. Theoretical library size can be determined by  $4^n$  where  $n$  is the number of randomized positions in the molecules. Actual library size is limited by the capability of commercial DNA synthesis instruments, which can

produce about  $10^{16}$  molecules in a single reaction. Base pairing and other sequence dependent intramolecular interactions vary among the molecules, providing a large number of different tertiary structures in the library population. Among these are some commonly recognized motifs: hairpins, bulges within helices, pseudoknots, and G-quartets, among others. Biological function, including binding affinity, is determined by the shape and charge characteristics of each molecule.

Affinities of aptamers for their target molecules can be quite high, with dissociation constants extending down into the picomolar range.<sup>7,8</sup> These affinities rival or exceed the capabilities of antibodies, making aptamers good candidates for analytical assays. The evolution process enables control over kinetic and thermodynamic properties of the aptamer-target binding interaction.

Aptamers have been demonstrated to be viable replacements for antibodies in many immunological experiments. In fact, oligonucleotides provide significant advantages over antibodies in several regards.<sup>9</sup> Many of these come from the evolution process, which allows the *in vitro* development of aptamers as opposed to the *in vivo* development of antibodies. Beyond the advantage of avoiding the need for animals in development, the *in vitro* selection process confers the advantage of a wider range of target molecules by including those that would be toxic *in vivo* as well as those that would not induce an immune response. Due to the reliability of chemical synthesis of aptamers after they have been sequenced, less batch-to-batch variation is expected than is expected for antibodies, which are always produced *in vivo*. Aptamers are more stable for long-term storage than antibodies, and can be restored even after denaturation. Aptamers can be modified after selection to further optimize binding affinities or to add

modified bases to prevent degradation if they will be introduced to biological sample. Further, no immunogenicity is expected from aptamers if they are introduced to the body. Finally, reporter molecules such as fluorescein and linkers such as biotin can often be easily attached to aptamers at precise locations without disrupting their activities.

Thus, aptamers can be used in both diagnostic and therapeutic applications that are based on molecular recognition. Possible uses include affinity purification of proteins, in vitro and in vivo diagnostic work, imaging, drugs, and specific detection and precise quantification of molecules. They have been used in analytical applications including flow cytometry, biosensors, affinity probe capillary electrophoresis, capillary electrochromatography, and affinity chromatography.

Part of this thesis (unsuccessfully) aimed to develop an aptamer for insulin that would be employed in two novel approaches to the direct detection of insulin with a spatially and temporally resolved measurement of secretion by single cells. Diabetes is estimated to affect 6.2% of the population of the United States, or 17 million people. About one third of these cases have not yet been diagnosed. Diabetes carries an increases risk for a wide range of disorders including heart attack, stroke, blindness, damaged kidneys and kidney failure, nerve damage, skin disorders, and gum disease. Ninety to ninety-five percent of diabetics have type II diabetes, which is caused by defective insulin secretion by pancreatic  $\beta$ -cells. High resolution monitoring of insulin secretion can provide insight into the mechanism of secretion.

## Experimental Section

**Chemicals.** DNA library was purchased from Integrated DNA Technologies (Coralville, IA). All solutions were prepared with deionized water from an E-Pure water purification system (Barnstead International Co., Dubuque, IA). Taq DNA polymerase was purchased from Invitrogen (Carlsbad, CA). T7 RNA polymerase was expressed and purified according to the protocol in Appendix B. Bovine insulin and bovine insulin immobilized on 4 % beaded agarose were purchased from Sigma Chemical Company (St. Louis, MO).

**Preparation of RNA library.** DNA was designed with two primer binding regions on either end, flanking a 40 nucleotide region of random sequence. The sequence was as follows: 5'GGG AGT CGA CCG ACC AGA A (N40) T ATG TGC GTC TAC ATC TAG ACT CAT 3'. A T7 promoter sequence was added by polymerase chain reaction (PCR) using 1  $\mu$ M each primer, 5' CAG TAA TAC GAC TCA CTA TAG GAT GAG TCT AGA TGT AGA CGC ACA TA 3' and 5' GGG AGT CGA CCG ACC AGA A 3', 500 nM library, 1 X PCR buffer, 3.0 mM MgCl<sub>2</sub>, 200  $\mu$ M dNTPs, and 0.073 U/ $\mu$ L. The DNA was concentrated with 2-butanol, extracted with phenol/chloroform/isoamyl alcohol followed by chloroform/isoamyl alcohol, and ethanol precipitated. The RNA was transcribed from this DNA template at 37 °C in an overnight reaction using the following optimized reagent concentrations: 2000 nM DNA library; 4 mM NTP mixture; 120 mM HEPES-KOH, pH 7.5; 30 mM MgCl<sub>2</sub>; 2 mM spermidine; 40 mM DTT; 0.04% triton X-100; 0.005 U/ $\mu$ L; 0.1 mg/mL T7 RNA polymerase; and 8% polyethylene glycol. The reaction was quenched with 60 mM EDTA, pH 8.0, and the RNA was extracted with phenol/chloroform/isoamyl alcohol followed by

chloroform/isoamyl alcohol, concentrated with a 3000 kD centricon filter. The RNA was then purified on a 15 % polyacrylamide gel, the band was cut out, crushed and tumbled overnight in crush 'n' soak buffer, chloroform extracted, and concentrated with a 3000 kD centricon filter. The concentrations of all nucleic acid samples were determined using their absorbance at 260 nm.

**Insulin filter binding for selection.** Insulin binding to various membranes was determined by flowing FITC-insulin in binding buffer (118 mM NaCl, 5.4 mM KCl, 1.2 mM MgSO<sub>4</sub>, 1.2 mM KH<sub>2</sub>PO<sub>4</sub>, 20 mM HEPES, pH 7.5) through the membrane with a syringe pump at about 20  $\mu$ L/min. The insulin was eluted from the filter by flowing 60 % acetonitrile in water through the filter. The fluorescence intensities of the original sample, flow through, and eluant were measured on a Perkin Elmer Fusion Universal Microplate Analyzer (Packard Instrument Company, Meriden, CT). Fluorescence was excited at  $485 \pm 10$  nm and emission collected with a  $535 \pm 12$  nm bandpass filter. Insulin filter binding was tried on the following filters: 0.1  $\mu$ M and 0.22  $\mu$ M mixed cellulose esters (Millipore, Billerica, MA), 0.45  $\mu$ M nylon (Fisher Scientific, Waltham, MA), Immobilon-P (0.45  $\mu$ M polyvinylidene fluoride) (Millipore, Billerica, MA), and Immobilon-PSQ (0.2  $\mu$ M polyvinylidene fluoride).

**SELEX experiments.** All SELEX experiments were conducted in binding buffer. Negative selection was performed on 4 % agarose beads (300  $\mu$ m). The beads were washed with binding buffer in a mini column (Pierce, Milwaukee, WI), centrifuging for 30 s at 8,000 x g between washes. The RNA library was annealed by heating to 70 °C for 5 m and cooled to room temperature on the benchtop. The RNA library was then incubated with the beads for 25 m at room temperature with tumbling. The sample was



centrifuged and washed twice with binding buffer. The eluant and washes were collected and concentrated and the RNA was put through rounds of positive selection. Two types of positive selection were carried out in parallel. In both types, insulin immobilized on 4 % beaded agarose was washed 10 times with binding buffer. Annealed RNA was added to the column and incubated at room temperature for 30 m with tumbling. The column was washed 10 times and the RNA was eluted by adding 8.0 mM insulin and incubating at room temperature for either 5 minutes or overnight. The insulin-bound RNA was then eluted from the column, phenol/chloroform extracted, ethanol precipitated, and reverse transcribed. The cDNA was double stranded, extracted, precipitated, and transcribed. The resulting RNA was gel purified and selected in another round of SELEX. Ten total rounds were performed, with a negative selection step before round one.

**Measuring SELEX progress.** The RNA winners from rounds five and ten were radioactively labeled. After annealing, the labeled RNA was incubated with immobilized insulin for 30 m with tumbling. RNA aliquots from various stages of the preparation was transferred onto a nitrocellulose filter and dried. These aliquots included RNA before insulin binding, RNA in flow through, RNA in eluted in wash steps, RNA eluted with 8.0 mM insulin, and RNA eluted with binding buffer at 95 °C. the gel was exposed overnight and quantified using a PhosphorImager Storm 840 with ImageQuant software (Molecular Dynamics, Sunnyvale, CA).

## Results and Discussion

**Library design.** A single stranded DNA library was chemically synthesized (Integrated DNA Technologies, Coralville, IA). Each member of the library had a 19 base amplification region on the 5' end and a 24 base amplification region on the 3' end, as previously described.<sup>97</sup> There was a 40 base variable region of random sequence between the known regions. Thus, the library was theoretically predicted to have  $4^{40}$  or about  $10^{24}$  different sequences, but due to synthesis limitations, only about  $10^{14}$  or  $10^{16}$  are expected. From this template, an RNA library was transcribed and subsequently evolved by SELEX to bind to insulin.

**SELEX.** Insulin is a 6 kD protein, which is relatively small compared to the 26 kD nucleic acids used in our SELEX experiments. We were concerned that its relatively small size may necessitate the use of a free solution selection process so as to avoid having the molecules tethered to a surface or bead. In an effort to conduct the selection this way, we Many ways of separating target-bound nucleic acids from unbound oligonucleotides have been employed, including filtration through nitrocellulose filters, chromatographic fractionation in which the target is immobilized on a solid support, gel electrophoretic and capillary electrophoretic partition in which the target-bound oligonucleotides are physically separated from unbound oligonucleotides on the bases of their electrophoretic mobility.<sup>98</sup> The most widely used partition method is nitrocellulose filtration, which has the benefits of simplicity and convenience as well as the ability to conduct the binding experiment in free solution. We reasoned that the free solution advantage would be particularly appealing for selection of an aptamer that is specific to insulin, because it is a very small protein at only 6 kD.

We first set out to determine the amount of insulin that would bind to various filters by pumping a solution of FITC labeled insulin dissolved in binding buffer through one or more filters with a syringe pump and measuring the relative fluorescence of the flow through. Nitrocellulose is the most common filter material used for protein filter binding assays, but insulin did not bind well except when flowed through three filters. Nylon, Immobilon-P, and Immobilon-PSQ showed similar results. Both of the Immobilon filters are made of polyvinylidene fluoride (Table 1). The best binding was observed with Immobilon PSQ, but with only 70 % efficiency, we were concerned about the potential of losing 30 % of the tight binding nucleic acid molecules. Instead, insulin immobilized on 4 % agarose beads was used.

Filter membrane	Relative fluorescence in flow through (%)
Nylon – 1 filter	71
Nitrocellulose – 1 filter	73
Nitrocellulose – 3 filters	24
Immobilon P – 1 filter	60
Immobilon P – 3 filters	83
Immobilon PSQ – 1 filter	28
Immobilon PSQ – 3 filters	36

**Table A-1. Relative fluorescence detection of FITC-insulin in flow through filter.**

Ten rounds of SELEX experiments were conducted in an effort to obtain an aptamer for insulin. Preceding these was a negative selection step, performed on 4 % agarose beads (300  $\mu$ m) to remove agarose binding nucleic acids from the selection pool. The positive selection steps involved incubation of RNA with immobilized insulin for a short (5 m) and long (12 h) incubation. To add additional selection pressure, we collected winning RNA molecules via a competitive binding assay, where free insulin in binding buffer was added to the binding experiment after the wash steps. Thus, only insulin binders would elute from the column, further reducing the number of non-specific

binders in the pool. We reasoned that tight binders may also have slow off rates, thus we designed two sets of elution conditions. In the first, the competitive binding was conducted for 5 m, whereas the other sample was incubated with free insulin for 12 h. We anticipated finding more binders in the long elution samples.

After five rounds of selection, the progress of the evolution was monitored by incubating radiolabeled RNA with immobilized insulin. After the incubation, RNA was eluted in several steps and small aliquots were transfer to a membrane, which was analyzed for intensity of radioactivity (Figure 2A). Comparing the total RNA bound to the immobilized insulin between the original library and the two evolved pools showed no significant difference in binding affinity. Looking closer at the binding profile by comparing between the pools RNA that washed off with binding buffer, RNA that eluted off in a competition with insulin, and RNA that eluted off of the column with 95 °C binding buffer also showed no difference in affinities between the pools (Figure 2B). Based on these results, we concluded that there was no progress in the evolution up to round 5. We therefore decided not to increase the stringency of the binding reaction, as is typically done in SELEX experiments in later rounds of selection when the pool's affinity for the target molecule is increasing. Instead, the library was subjected to five additional rounds of selection under the same conditions.

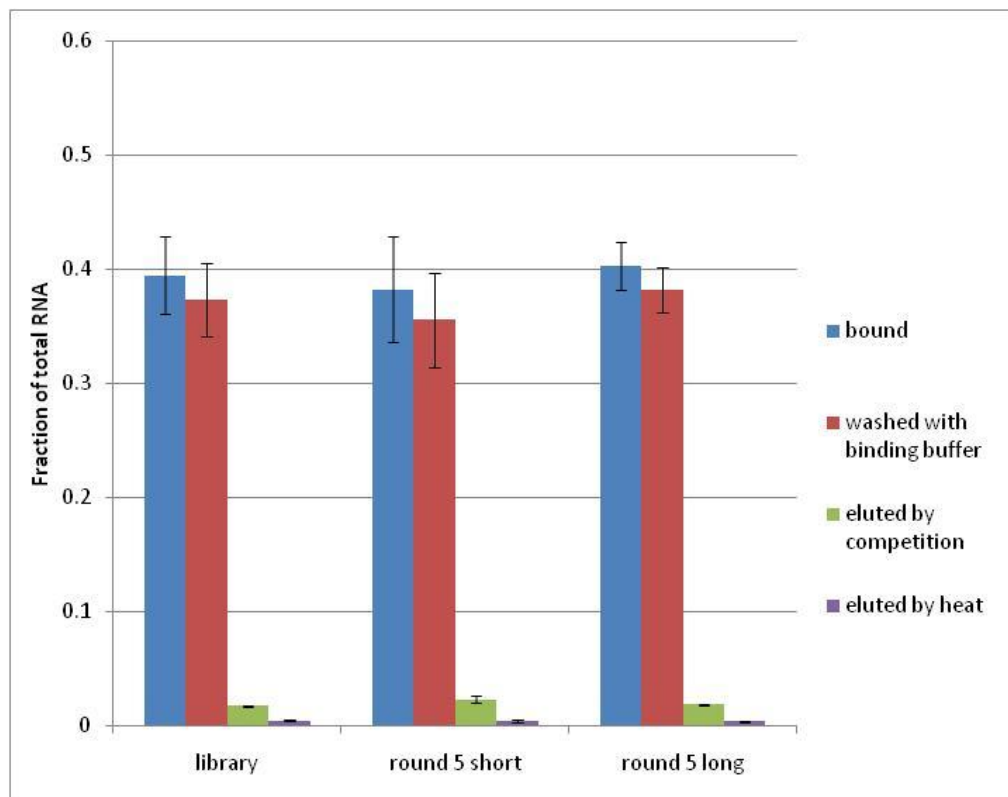


**Figure A-2. Progress of SELEX after five rounds of selection.**

After ten rounds of selection, the progress was monitored in the same way as after five rounds. Similarly, no significant progress was observed in the evolution of the library (Figure 3). In fact, the amount of RNA that eluted with insulin and 95 °C binding buffer was significantly reduced when compared to the elution observed after five rounds.

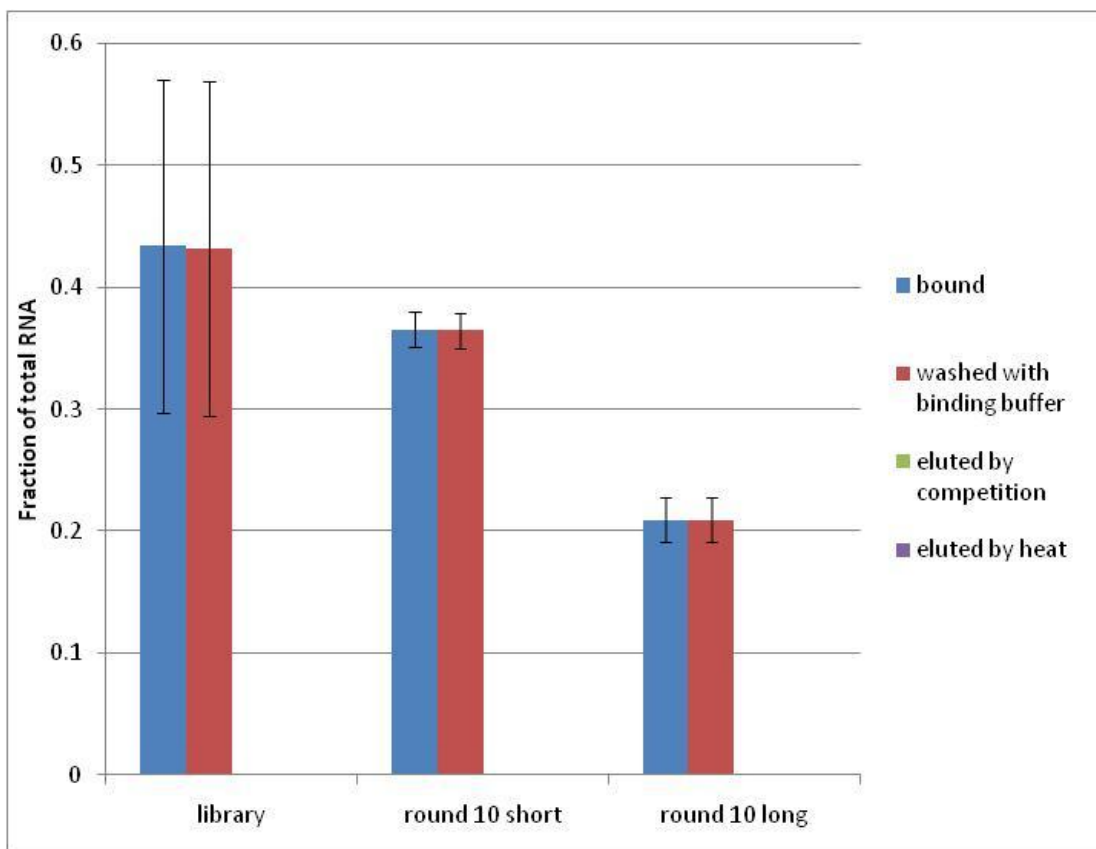


**Figure A-3. Progress of SELEX after ten rounds of selection.**

In SELEX, progress is usually observed before the tenth round of selection. Thus, we decided to end our pursuit of an aptamer for insulin. We hypothesize our failure to select an aptamer could be due to the small size of insulin relative to the nucleic acid molecules as well as insulin's negative charge at the pH used for selection (7.5). Insulin has a pI of 5.5. Given the negative nature of nucleic acids, binding to insulin may have been unfavorable.

It is possible that alterations in the selection protocol may have led to the successful discovery of a high affinity aptamer. For example, bias or hindrance

introduced by immobilization of insulin and poor kinetics of eluting very strong binders could have contributed to the lack of evolution in our experiments. Two free solution selection methods that might be effective are gel mobility shift and capillary electrophoresis. Finally, Larry Gold of SomaLogic, Inc., and one of the developers of the SELEX process has reported only a 60 % success rate in obtaining an aptamer with suitable binding characteristics in the first round of selection, suggesting our findings may not be unusual.

### **Conclusions**

In this work, we investigated the potential of SELEX to obtain an RNA aptamer for insulin. We were unsuccessful in evolving the original library to have increased affinity for insulin. We hypothesize that this could be due to the small size of insulin relative to the aptamers or to insulin's negative charge at the pH used for selection. It is possible that another selection method would be more successful in obtaining a high affinity aptamer.



## APPENDIX B

### T7 HIS TAGGED RNA POLYMERASE PREPARATION

The pRC9 plasmid expresses a His-tagged T7 RNA Polymerase with a mutation that reduces 3' heterogeneity. Purification is BASED on the protocol from [He et al., *Protein Expression and Purification* **9**: 142-151 (1997)].

#### **Materials:**

A gravity flow through column with ~50ml volume  
25ml Chelating Fast Flow Sepharose beads (Amersham cat# 17-0575-01)  
Dialysis tubing ( the T7 Pol is ~100kDa or 100,000g/mol)

#### **Stock solutions (all except NaCl and LB should be sterile filtered):**

##### For the Transformation and Cell Culture (days 1, 2, & 3):

2.5L LB broth (10 g trypton, 5 g yeast extract, 10 g NaCl, 1 L H<sub>2</sub>O, pH to 7.0 with 1M NaOH) – autoclave, add amp<sup>100</sup> after cooled  
3mL SOC broth  
4 LB/Amp<sup>100</sup> agar plates  
50mg/ml ampicillin frozen stock (add to LB right before use)

##### For the IPTG Induction and Cell Wash (day 3):

2mL of 0.4M IPTG either made right before use or from unused frozen stock  
100mL of 1M Tris pH 8.0  
10mL of 0.5M Na<sub>2</sub>EDTA pH~8.0 (to be used again in buffers for cell lysis/wash/elution)

##### For Protein Collection and Column Preparation (day 4):

4ml of 10mg/ml lysozyme either made fresh or from unused frozen stock  
1ml of 20mg/ml (0.115M) PMSF in isopropanol from frozen stock (careful it's toxic)  
10ml of 2M Tris base

100ml of 1.5M Potassium Glutamate (not glutamic acid)  
100ml of 300mM HEPES  
100ml of 0.1% Tween-20  
100ml of 5M NaCl – autoclaved

100ml of 1M imidazole pH 7.5

50ml of 1M Tris pH 7.2

200ml of 1M KCl

100mL 1M DTT

2L glycerol

50ml of 0.1M NiSO<sub>4</sub>

150mL of 0.5M NaCl – autoclaved

100mL of 1M NaOH

Use the above in the preparation of the following:

Lysis Buffer – 150mM K-Glu, 30mM HEPES, 0.05% Tween-20, 250mM NaCl, 5mM Imidazole

Wash Buffer – Lysis Buffer, with 20mM Imidazole

Elution Buffer – Lysis Buffer, with 100mM Imidazole

Storage Buffer – 10mM Tris pH 7.2 (at 25°C), 50mM KCl, 0.1mM EDTA, 1mM DTT, 50% glycerol

### **Induction of Protein Expression (from 2L LB)**

**Day1:** Transform BL21(DE3)pLysS cells (Promega) with pRC9 plasmid and plate on LB plates containing 100µg/ml ampicillin overnight at 37°C.

### Transformation Protocol:

1. Thaw competent cells on ice.
2. Pipet 65µL cells into three microcentrifuge tubes, on ice
3. Add 1-50ng DNA (but no more than 10µL total volume added) per 10µL cells. Flick tube to mix.(ex: 3 x 65µL aliquots to include T7 and controls, as follows:
  - 1.5µL pRC9 (15ng/µL) – T7 plasmid
  - 2.5µL pGEM3Z (0.1ng/µL) – Promega, Amp<sup>R</sup> = positive control
  - 2.5µL H<sub>2</sub>O – negative control)
4. Incubate on ice for 15 minutes
5. Heat shock for 45-50 seconds at 42°C (no shaking)
6. Incubate on ice for 2 minutes
7. Add 900µL cold SOC medium to each tube, incubate at 37°C for 60 minutes (with shaking)
8. Plate onto three LB/Amp<sup>100</sup> (100µg/mL ampicillin) plates

9. Incubate at 37°C overnight

**Day2:** Check for healthy colonies on the T7 and positive control plates (and no growth on the negative control plate). If the colonies look good, pick two fresh colonies from the T7 plate in the morning, and streak them out onto opposite sides of an LB/Amp<sup>100</sup> agar plate. Incubate at 37°C. By evening, healthy single colonies should be on both sides of the plate. Choose one of these colonies to inoculate 50ml LB/Amp<sup>100</sup>. This should be done late at night because it is preferable to use the cell culture when the OD<sub>600</sub> is around 1, which takes roughly ~10-12 hours.

**Day3:** Induce T7 Production with IPTG

Induction Protocol:

1. Add 4 x 10mL of overnight cell culture to 4 x 500mL LB/Amp<sup>100</sup> broth in 4 x 1L sterile erlenmeyers.
2. Incubate at 37°C and ~225rpm until OD<sub>600</sub> is 0.4-0.7 (~ 4 hours).
3. Remove and store 50µL of culture to analyze with PAGE
4. Add 4 x 500µL of 0.4M IPTG to each flask (final conc = 0.4 mM IPTG)
5. Incubate at 37°C and ~225rpm for 4 hours
6. After 4 hours, harvest cells by centrifugation for 15min, 5,000 x g, 4°C (Fierke/Marsh lab centrifuge(s)).
7. Resuspend the 2 pellets with 2 x 100mL cold 50mM Tris pH 8.0+5mM EDTA.
8. Remove and store 50µL of culture to analyze with PAGE
9. Transfer to 4 x 50mL falcon tubes and centrifuge (Walter or Mapp lab) at 9,000rpm, 15min, 4°C and then store at -70°C overnight.
10. Run SDS-PAGE (use a pre-cast gel – Tricine from Invitrogen) on the two 50µL fractions (Can be done on day 4):
  - a. For each fraction: 10µL cells + 10µL dye, heat to 90°C for 3 minutes, cool, load 10µL total into each lane. Run at 150V, until bromophenol blue line is near the bottom of the gel. (dye = denaturing loading buffer (10 mL): 1mL glycerol, 2mL 1M DTT, 3mL 10% SDS, 1.25mL 1M Tris-HCl, pH 6.8, 2.75mL 0.025 % bromophenol blue in H<sub>2</sub>O)
  - b. Stain for 30 minutes (staining solution: 0.5g R250 Coomassie Blue, 100mL methanol, 100mL H<sub>2</sub>O, stir until dye dissolves then stir in 20 mL acetic acid).

- c. Destain until protein bands can be clearly seen, may take overnight, but results will be clear in about one hour (destaining solution: 450mL methanol, 475mL H<sub>2</sub>O, 75mL acetic acid).

#### **Day4: Collect the Protein**

##### Protocol:

##### Cell Lysis:

1. Resuspend each of the 4 pellets in 40mL Lysis buffer.
2. Add 2M Tris base until pH >8 using pH paper.
3. Pool all four pellets into a beaker, add 4mL of 10mg/ml lysozyme and 0.7mL 0.115M (20mg/ml) PMSF, and incubate at room temperature for 15 minutes.
4. Freeze at -70°C (can be done overnight or until frozen), thaw at room temperature in water bath.
5. Sonicate over ice at setting 8, 8 x 15 second pulses with 20 second breaks (Marsh lab, large tip).
6. Spin down the 4 x 40mL at 10,000rpm, 1°C, for 30 minutes. Remove the supernatant and store at 4°C (not overnight, if possible).

##### Column Material Preparation:

1. Centrifuge 10mL of Chelating Fast Flow Sepharose beads stored in 20% ethanol at 500 rpm, room temperature, for 3 to 5 minutes.
2. Pour off supernatant, resuspend in 40mL of autoclaved ddH<sub>2</sub>O, repeat centrifugation.
3. Pour off supernatant, resuspend in 25mL of 50mM NiSO<sub>4</sub>, tumble at 4°C for 30 minutes. Centrifuge as above.
4. Pour off supernatant, resuspend in 40mL of autoclaved ddH<sub>2</sub>O, centrifuge, pour off supernatant. Repeat 2 times.

##### Column Loading and Protein Collection:

1. Resuspend beads in the ~160mL supernatant from the lysed cells into 4 x 50mL falcon tubes and gently tumble at 4°C for 30 minutes.
2. Pack the beads onto the column. Can use 10ml syringe stopper to increase flow rates. The column is run at room temperature
3. Wash beads with wash buffer until OD<sub>280</sub> <0.1 (around 100ml) using pure wash buffer as the blank.
4. Gravity elute the polymerase with ~90mL elution buffer. Collect 1<sup>st</sup> 10mL in falcon tube, then collect 1.5mL fractions in microcentrifuge tubes (~60) until the last of the 90ml reaches the top of the column material. As you collect fractions close the tubes and place them at 4°C or on ice. (Or use fraction collector and ~4mL collection tubes – Fierke lab) The elution can be monitored at OD<sub>280</sub>.

##### Column Material Regeneration:

1. Strip the column of nickel by washing the beads with 10 column volumes of 0.05M EDTA, 0.5M NaCl.
2. Remove residual EDTA by washing with 2 to 3 column volumes of 0.5M NaCl.
3. Remove precipitated proteins and hydrophobically bound proteins and sanitize the column material by soaking it in 100mL of 1M NaOH for 2 hours.
4. Centrifuge the beads at 500 rpm for 5 min at room temperature.
5. Pour off the supernatant, wash twice with autoclaved ddH<sub>2</sub>O.
6. Resuspend in ~75mL of 20% ethanol for storage at 4°C in a pyrex bottle.

Protein Dialysis:

1. Run pre-cast SDS-PAGE gels to look for the polymerase (every third fraction). (as on Day 3, step 10.) (or make your own, recipes follow.)
2. Pool the polymerase-containing fractions in a dialysis bag pre-equilibrated in 2L of Storage Buffer at 4°C. Dialyze overnight at 4°C, with gentle stirring. After ~12 hours change to a fresh 2L of Storage Buffer and dialyze again for ~12 hours at 4°C.
3. Aliquot the dialysate into 1.5mL microcentrifuge tubes and store at -20°C.
4. Measure protein concentration using the dialysis buffer as a blank. The extinction coefficient of the T7 at 280nm is  $1.4 \times 10^5 \text{ Lmol}^{-1}\text{cm}^{-1}$ , the path length of the cuvette is 1cm and the MW is 100 kDa.
5. Run an analytical transcription of the material along with control reactions you know should work to validate functionality.

To Prepare an SDS-PAGE gel:

Make 2 SDS-Page gels (using 1.5 mm spacers)

5 % stacking gel:	Volume
40% polyacrilamide	3.75 mL
1M Tris-HCl, pH 6.8	3.75 mL
ddH <sub>2</sub> O	20.4 mL
10% SDS	0.300 mL
10% APS	0.300 mL
TEMED	0.03 mL
a. 10% running/resolving gel:	
40% polyacrilamide	25 mL
1M Tris-HCl, pH 8.8	37.5 mL
ddH <sub>2</sub> O	35.5 mL
10% SDS	1 mL
10% APS	1 mL
TEMED	0.040 mL
b. 4X Running buffer (1L):	
Tris base	12 g
Glycine	57.6 g
For 1X running buffer (2L)	
4X running buffer	500 mL

10% SDS 20 mL

c. Denaturing loading buffer (10 mL):

Glycerol	1mL
1M DTT	2 mL
10% SDS	3 mL
1M Tris-HCl, pH 6.8	1.25 mL
0.025 % bromophenol blue in H <sub>2</sub> O	2.75 mL

1. After setting up plates, pour the resolving gel about 1-inch below where the comb bottom will be located. Let the solution settle in the vertical position and using a Pasteur pipette, overlay the gel with about 0.5-inch of ddH<sub>2</sub>O. Let gel set and tag the interface between water and gel.
2. After the gel is set (20 minutes), pour off the water and add the stacking gel with the comb (10 lanes) . Allow this gel to set. (Note: stacking gel polymerizes very quickly.).
3. For fractions, remove 20μL from every third fraction and combine with 20μL denaturing loading buffer. In two tubes add 2μl control T7 polymerase.
4. Heat all samples to 90°C for 2 minutes and then ice for 2 minutes. Load 30μL into each well. Run gel at 150V while bromophenol blue is in the stacking gel. Increase the voltage to 250 V when bromophenol blue is in the resolving gel. Run at least, until the bromophenol blue is below the metal plate (about 2.5 hours).
5. Stain gels for 15 minutes in staining solution and then de-stain the gels overnight (you can get a first impression of you results after the first hour).

a. Staining solution (this solution should be reused):

R250 Coomassie Blue	0.5 g
Methanol	100 mL
H <sub>2</sub> O	100 mL

Stir until dye dissolves then stir in:  
20 mL acetic acid

b. De-staining solution (Note: this solution can be reused):

Methanol	450 mL
H <sub>2</sub> O	475 mL
Acetic acid	75 mL

## REFERENCES

- (1) Klussmann, S. *The aptamer handbook : functional oligonucleotides and their applications*; Wiley-VCH: Weinheim, 2006.
- (2) Ellington, A. D.; Szostak, J. W. *Nature* **1990**, *346*, 818-822.
- (3) Robertson, D. L.; Joyce, G. F. *Nature* **1990**, *344*, 467-468.
- (4) Tuerk, C.; Gold, L. *Science* **1990**, *249*, 505-510.
- (5) Ulrich, H.; Trujillo, C. A.; Nery, A. A.; Alves, J. M.; Majumder, P.; Resende, R. R.; Martins, A. H. *Comb Chem High Throughput Screen* **2006**, *9*, 619-632.
- (6) Schwalbe, H.; Buck, J.; Furtig, B.; Noeske, J.; Wohnert, J. *Angew Chem Int Ed Engl* **2007**, *46*, 1212-1219.
- (7) Jenison, R. D.; Gill, S. C.; Pardi, A.; Polisky, B. *Science* **1994**, *263*, 1425-1429.
- (8) Win, M. N.; Klein, J. S.; Smolke, C. D. *Nucleic Acids Res* **2006**, *34*, 5670-5682.
- (9) Mairal, T.; Cengiz Ozalp, V.; Lozano Sanchez, P.; Mir, M.; Katakis, I.; O'Sullivan C, K. *Anal Bioanal Chem* **2007**.
- (10) Jayasena, S. D. *Clin Chem* **1999**, *45*, 1628-1650.
- (11) Deutscher, M. P. *Nucleic Acids Res* **2006**, *34*, 659-666.
- (12) Bock, C.; Coleman, M.; Collins, B.; Davis, J.; Foulds, G.; Gold, L.; Greef, C.; Heil, J.; Heilig, J. S.; Hicke, B.; Hurst, M. N.; Husar, G. M.; Miller, D.; Ostroff, R.; Petach, H.; Schneider, D.; Vant-Hull, B.; Waugh, S.; Weiss, A.; Wilcox, S. K.; Zichi, D. *Proteomics* **2004**, *4*, 609-618.
- (13) Proske, D.; Blank, M.; Buhmann, R.; Resch, A. *Appl Microbiol Biotechnol* **2005**, *69*, 367-374.
- (14) Lucignani, G. *Eur J Nucl Med Mol Imaging* **2006**, *33*, 1095-1097.
- (15) Fichou, Y.; Ferec, C. *Trends Biotechnol* **2006**, *24*, 563-570.
- (16) German, I.; Buchanan, D. D.; Kennedy, R. T. *Anal Chem* **1998**, *70*, 4540-4545.
- (17) Sekella, P. T.; Rueda, D.; Walter, N. G. *Rna* **2002**, *8*, 1242-1252.
- (18) Herr, J. K.; Smith, J. E.; Medley, C. D.; Shangguan, D.; Tan, W. *Anal Chem* **2006**, *78*, 2918-2924.
- (19) Buchanan, D. D.; Jameson, E. E.; Perlette, J.; Malik, A.; Kennedy, R. T. *Electrophoresis* **2003**, *24*, 1375-1382.
- (20) Ravelet, C.; Grosset, C.; Peyrin, E. *J Chromatogr A* **2006**, *1117*, 1-10.
- (21) Deng, Q.; German, I.; Buchanan, D.; Kennedy, R. T. *Anal Chem* **2001**, *73*, 5415-5421.
- (22) Navani, N. K.; Li, Y. *Curr Opin Chem Biol* **2006**, *10*, 272-281.
- (23) Walter, N. G.; Engelke, D. R. *Biologist (London)* **2002**, *49*, 199-203.
- (24) Bartel, D. P. *Cell* **2004**, *116*, 281-297.
- (25) Tucker, B. J.; Breaker, R. R. *Curr Opin Struct Biol* **2005**, *15*, 342-348.
- (26) Cech, T. R. *Biochem Soc Trans* **2002**, *30*, 1162-1166.
- (27) Silverman, S. K. *Rna* **2003**, *9*, 377-383.

- (28) Winkler, W. C.; Nahvi, A.; Roth, A.; Collins, J. A.; Breaker, R. R. *Nature* **2004**, *428*, 281-286.
- (29) Hampel, K. J.; Tinsley, M. M. *Biochemistry* **2006**, *45*, 7861-7871.
- (30) Puerta-Fernandez, E.; Romero-Lopez, C.; Barroso-delJesus, A.; Berzal-Herranz, A. *FEMS Microbiol Rev* **2003**, *27*, 75-97.
- (31) Robertson, M. P.; Ellington, A. D. *Nucleic Acids Res* **2000**, *28*, 1751-1759.
- (32) Soukup, G. A.; Breaker, R. R. *Proc Natl Acad Sci U S A* **1999**, *96*, 3584-3589.
- (33) Soukup, G. A.; Emilsson, G. A.; Breaker, R. R. *J Mol Biol* **2000**, *298*, 623-632.
- (34) Jose, A. M.; Soukup, G. A.; Breaker, R. R. *Nucleic Acids Res* **2001**, *29*, 1631-1637.
- (35) Tang, J.; Breaker, R. R. *Chem Biol* **1997**, *4*, 453-459.
- (36) Koizumi, M.; Kerr, J. N.; Soukup, G. A.; Breaker, R. R. *Nucleic Acids Symp Ser* **1999**, 275-276.
- (37) Koizumi, M.; Soukup, G. A.; Kerr, J. N.; Breaker, R. R. *Nat Struct Biol* **1999**, *6*, 1062-1071.
- (38) Soukup, G. A.; DeRose, E. C.; Koizumi, M.; Breaker, R. R. *Rna* **2001**, *7*, 524-536.
- (39) Araki, M.; Okuno, Y.; Hara, Y.; Sugiura, Y. *Nucleic Acids Res* **1998**, *26*, 3379-3384.
- (40) Piganeau, N.; Jenne, A.; Thuillier, V.; Famulok, M. *Angew Chem. Int. Ed.* **2000**, *39*, 4369-4373.
- (41) Piganeau, N.; Thuillier, V.; Famulok, M. *J Mol Biol* **2001**, *312*, 1177-1190.
- (42) Seetharaman, S.; Zivarts, M.; Sudarsan, N.; Breaker, R. R. *Nat Biotechnol* **2001**, *19*, 336-341.
- (43) Porta, H.; Lizardi, P. M. *Biotechnology (N Y)* **1995**, *13*, 161-164.
- (44) Kuwabara, T.; Warashina, M.; Tanabe, T.; Tani, K.; Asano, S.; Taira, K. *Mol Cell* **1998**, *2*, 617-627.
- (45) Robertson, M. P.; Ellington, A. D. *Nat Biotechnol* **1999**, *17*, 62-66.
- (46) Komatsu, Y.; Yamashita, S.; Kazama, N.; Nobuoka, K.; Ohtsuka, E. *J Mol Biol* **2000**, *299*, 1231-1243.
- (47) Hartig, J. S.; Famulok, M. *Angew Chem Int Ed Engl* **2002**, *41*, 4263-4266.
- (48) Hartig, J. S.; Najafi-Shoushtari, S. H.; Grune, I.; Yan, A.; Ellington, A. D.; Famulok, M. *Nat Biotechnol* **2002**, *20*, 717-722.
- (49) Vaish, N. K.; Dong, F.; Andrews, L.; Schweppe, R. E.; Ahn, N. G.; Blatt, L.; Seiwert, S. D. *Nat Biotechnol* **2002**, *20*, 810-815.
- (50) Frauendorf, C.; Jaschke, A. *Bioorg Med Chem* **2001**, *9*, 2521-2524.
- (51) Tinsley, R. A.; Furchak, J. R.; Walter, N. G. *Rna* **2007**, *13*, 468-477.
- (52) Klein, D. J.; Ferre-D'Amare, A. R. *Science* **2006**, *313*, 1752-1756.
- (53) Cochrane, J. C.; Lipchock, S. V.; Strobel, S. A. *Chem Biol* **2007**, *14*, 97-105.
- (54) Blount, K.; Puskarz, I.; Penchovsky, R.; Breaker, R. *RNA Biol* **2006**, *3*, 77-81.
- (55) Teplyakov, A.; Leriche, C.; Obmolova, G.; Badet, B.; Badet-Denisot, M. A. *Nat Prod Rep* **2002**, *19*, 60-69.
- (56) Buse, M. G. *Am J Physiol Endocrinol Metab* **2006**, *290*, E1-E8.
- (57) Ghosh, S.; Blumenthal, H. J.; Davidson, E.; Roseman, S. *J Biol Chem* **1960**, *235*, 1265-1273.



- (58) Broschat, K. O.; Gorka, C.; Kasten, T. P.; Gulve, E. A.; Kilpatrick, B. *Anal Biochem* **2002**, *305*, 10-15.
- (59) Daniels, M. C.; Ciaraldi, T. P.; Nikoulina, S.; Henry, R. R.; McClain, D. A. *J Clin Invest* **1996**, *97*, 1235-1241.
- (60) Maillard, L. T.; Guerineau, V.; Badet-Denisot, M. A.; Badet, B.; Laprevote, O.; Durand, P. *Rapid Commun Mass Spectrom* **2006**, *20*, 666-672.
- (61) Sassanfar, M.; Szostak, J. W. *Nature* **1993**, *364*, 550-553.
- (62) Bunka, D. H.; Stockley, P. G. *Nat Rev Microbiol* **2006**, *4*, 588-596.
- (63) Vinayak, R.; Andrus, A.; Sinha, N. D.; Hampel, A. *Anal Biochem* **1995**, *232*, 204-209.
- (64) Citti, L.; Boldrini, L.; Nevischi, S.; Mariani, L.; Rainaldi, G. *Biotechniques* **1997**, *23*, 898-900, 902-893.
- (65) Georgopoulos, D. E.; Leibowitz, M. J. *J Chromatogr A* **2000**, *868*, 109-114.
- (66) Saevels, J.; Van Schepdael, A.; Hoogmartens, J. *Anal Biochem* **1999**, *266*, 93-101.
- (67) Paxon, T. L.; Brown, T. S.; Lin, H. Y.; Brancato, S. J.; Roddy, E. S.; Bevilacqua, P. C.; Ewing, A. G. *Anal Chem* **2004**, *76*, 6921-6927.
- (68) Kirk, S. R.; Luedtke, N. W.; Tor, Y. *Bioorg Med Chem* **2001**, *9*, 2295-2301.
- (69) Walter, N. G.; Burke, J. M. *Rna* **1997**, *3*, 392-404.
- (70) Singh, K. K.; Rucker, T.; Hanne, A.; Parwaresch, R.; Krupp, G. *Biotechniques* **2000**, *29*, 344-348, 350-341.
- (71) Walter, N. G.; Harris, D. A.; Pereira, M. J.; Rueda, D. *Biopolymers* **2001**, *61*, 224-242.
- (72) Klostermeier, D.; Millar, D. P. *Methods* **2001**, *23*, 240-254.
- (73) Walter, N. G. *Methods* **2001**, *25*, 19-30.
- (74) Gaits, F.; Hahn, K. *Sci STKE* **2003**, *2003*, PE3.
- (75) Klostermeier, D.; Millar, D. P. *Biopolymers* **2001**, *61*, 159-179.
- (76) Kraly, J.; Fazal, M. A.; Schoenherr, R. M.; Bonn, R.; Harwood, M. M.; Turner, E.; Jones, M.; Dovichi, N. J. *Anal Chem* **2006**, *78*, 4097-4110.
- (77) Schou, C.; Heegaard, N. H. *Electrophoresis* **2006**, *27*, 44-59.
- (78) Pavski, V.; Le, X. C. *Anal Chem* **2001**, *73*, 6070-6076.
- (79) Fu, H.; Guthrie, J. W.; Le, X. C. *Electrophoresis* **2006**, *27*, 433-441.
- (80) Berezovski, M.; Nutiu, R.; Li, Y.; Krylov, S. N. *Anal Chem* **2003**, *75*, 1382-1386.
- (81) Cunliffe, J. M.; Sunahara, R. K.; Kennedy, R. T. *Anal Chem* **2006**, *78*, 1731-1738.
- (82) Cunliffe, J. M.; Sunahara, R. K.; Kennedy, R. T. *Anal Chem* **2007**.
- (83) Winkler, W. C.; Breaker, R. R. *Annu Rev Microbiol* **2005**, *59*, 487-517.
- (84) Mayer, G.; Famulok, M. *ChemBiochem* **2006**, *7*, 602-604.
- (85) Harris, D. A.; Rueda, D.; Walter, N. G. *Biochemistry* **2002**, *41*, 12051-12061.
- (86) Pereira, M. J.; Harris, D. A.; Rueda, D.; Walter, N. G. *Biochemistry* **2002**, *41*, 730-740.
- (87) Yang, P. *Development of Analytical Techniques for Protein Binding Kinetics and Drug Screening*, 2007.
- (88) Shackman, J. G.; Watson, C. J.; Kennedy, R. T. *J Chromatogr A* **2004**, *1040*, 273-282.
- (89) Milewski, S. *Biochim Biophys Acta* **2002**, *1597*, 173-192.
- (90) Dieckmann, T.; Suzuki, E.; Nakamura, G. K.; Feigon, J. *Rna* **1996**, *2*, 628-640.
- (91) Jiang, F.; Kumar, R. A.; Jones, R. A.; Patel, D. J. *Nature* **1996**, *382*, 183-186.

- (92) Nielsen, U. B.; Geierstanger, B. H. *J Immunol Methods* **2004**, *290*, 107-120.
- (93) Hesselberth, J. R.; Robertson, M. P.; Knudsen, S. M.; Ellington, A. D. *Anal Biochem* **2003**, *312*, 106-112.
- (94) Kheterpal, I.; Mathies, R. A. *Anal Chem* **1999**, *71*, 31A-37A.
- (95) Dovichi, N. J.; Zhang, J. *Methods Mol Biol* **2001**, *167*, 225-239.
- (96) Link, K. H.; Guo, L.; Ames, T. D.; Yen, L.; Mulligan, R. C.; Breaker, R. R. *Biol Chem* **2007**, *388*, 779-786.
- (97) Srisawat, C.; Engelke, D. R. *Rna* **2001**, *7*, 632-641.
- (98) Gopinath, S. C. *Anal Bioanal Chem* **2007**, *387*, 171-182.